



3 4456 0379846 0

ORNL/TM-12660

ornl

**OAK RIDGE
NATIONAL
LABORATORY**

MARTIN MARIETTA

Fluid Dynamic Demonstrations for Waste Retrieval and Treatment

E. L. Youngblood, Jr.
T. D. Hylton
J. B. Berry
R. L. Cummins
F. R. Ruppel
R. W. Hanks

OAK RIDGE NATIONAL LABORATORY

CENTRAL RESEARCH LIBRARY

CIRCULATION SECTION
4500N ROOM 175

LIBRARY LOAN COPY

DO NOT TRANSFER TO ANOTHER PERSON

If you wish someone else to see this
report, send in name with report and
the library will arrange a loan.

UCN-7969 (3 9-77)

MANAGED BY
MARTIN MARIETTA ENERGY SYSTEMS, INC.
FOR THE UNITED STATES
DEPARTMENT OF ENERGY

This report has been reproduced directly from the best available copy.

Available to DOE and DOE contractors from the Office of Scientific and Technical Information, P.O. Box 62, Oak Ridge, TN 37831; prices available from (615) 576-8401, FTS 626-8401.

Available to the public from the National Technical Information Service, U.S. Department of Commerce, 5285 Port Royal Rd., Springfield, VA 22161.

This report was prepared as an account of work sponsored by an agency of the United States Government. Neither the United States Government nor any agency thereof, nor any of their employees, makes any warranty, express or implied, or assumes any legal liability or responsibility for the accuracy, completeness, or usefulness of any information, apparatus, product, or process disclosed, or represents that its use would not infringe privately owned rights. Reference herein to any specific commercial product, process, or service by trade name, trademark, manufacturer, or otherwise, does not necessarily constitute or imply its endorsement, recommendation, or favoring by the United States Government or any agency thereof. The views and opinions of authors expressed herein do not necessarily state or reflect those of the United States Government or any agency thereof.

Chemical Technology Division

**FLUID DYNAMIC DEMONSTRATIONS FOR WASTE RETRIEVAL
AND TREATMENT**

E. L. Youngblood, Jr.
T. D. Hylton
J. B. Berry
R. L. Cummins
F. R. Ruppel*
R. W. Hanks†

* Instrumentation & Controls Division

† Richard W. Hanks Associates, Inc., Slurry Transport Consultant

Date Published: February 1994

NOTICE This document contains information of a preliminary nature.
It is subject to revision or correction and therefore does not represent a
final report.

Prepared for the
OAK RIDGE NATIONAL LABORATORY
Oak Ridge, Tennessee 37831-6330
managed by
MARTIN MARIETTA ENERGY SYSTEMS, INC.
for the
U.S. DEPARTMENT OF ENERGY
under contract DE-AC05-84OR21400



3 4456 0379846 0

CONTENTS

LIST OF FIGURES	v
LIST OF TABLES	vi
1. INTRODUCTION	2
2. DESCRIPTION OF EQUIPMENT	3
3. PROCESS PARAMETERS AND PROCEDURES	6
4. NON-NEWTONIAN MODELS AND FLOW CORRELATIONS	8
4.1 Rheological Models	8
4.2 Viscometry and Data Analysis	11
4.2.1 Experimental Data	12
4.2.2 Data Reduction and Analysis	12
4.3 Pipeline Flow Correlations	13
4.3.1 Newtonian Fluids	13
4.3.2 Bingham Plastic Fluids	14
4.3.3 Power Law Fluids	15
4.3.4 Yield Power Law Fluids	16
4.4 IBM PC Programs	16
4.4.1 Commercially Available Programs	17
4.4.2 Software Development Projects Required	19
5. WASTE CHARACTERIZATION AND SIMULANT DEVELOPMENT	21
5.1 Melton Valley Storage Tank Waste	21
5.2 Hanford Single-Shell Tanks	27
6. SUPERNATE RHEOLOGY MEASUREMENTS	30
7. CALIBRATION OF PIPELINE VISCOMETERS IN SLURRY TEST LOOP ...	30
8. RESULTS OF RHEOLOGICAL MEASUREMENTS FOR SIMULATED WASTE	34
8.1 Rheological Measurements for Simulated MVST Slurry	34
8.1.1 Run MVST 1	38
8.1.2. Run MVST 2	42
8.1.3 Runs MVST 3, 3A, 3B, and 3C	42

8.2	Rheological Measurements of Simulated Hanford Single Shell Tank Waste	43
9.	PERFORMANCE OF EQUIPMENT AND INSTRUMENTATION	49
10.	SUMMARY AND CONCLUSIONS	49
	ACKNOWLEDGMENTS	50
	REFERENCES	51
	APPENDIX A	53
	APPENDIX B	74

FIGURES

<u>Figure</u>	<u>Page</u>
1. Flow diagram of slurry test loop	4
2. Typical pipeline viscometer	5
3. Shear stress vs shear rate curves for typical Newtonian and non-Newtonian fluids .	9
4. Apparent viscosity vs shear rate for Hanford single-shell waste and simulant	29
5. Pipeline viscometer (0.18-in. ID) calibration curves	32
6. Rheograms for simulated Melton Valley Storage Tank (MVST) supernate and Hanford salt cake	32
7. Rheogram from calibration of pipeline viscometers with sucrose solutions	35
8. Pipeline viscometer calibration curves with water	36
9. Pipeline viscometer calibration curves with 50 wt % sucrose solution	36
10. Plot of $\Delta p/Q$ versus flow rate for calibration of pipeline viscometers for 50 wt % sucrose solution	37
11. Pressure drop vs flow rate for MVST 1 simulated sludge through pipeline viscometers	39
12. Flow curve for simulated MVST 1 slurry	40
13. Rheogram for MVST 1 simulated slurry	41
14. Pressure drop vs flow rate curves for run H-2.	47
15. Rheograms for run H-2	47
16. Measured and calculated friction factors and critical Reynolds numbers for run H-2.	48

TABLES

<u>Table</u>	<u>Page</u>
1. Instruments and equipment used in the slurry test loop	7
2. Range of compositions of major components and properties of Melton Valley Storage Tank waste	22
3. Physical properties of Melton Valley Storage Tanks W26 and W28 and evaporator waste tanks W21 and W23	23
4. Melton Valley Storage Tank surrogate composition	25
5. Viscosity measurements for Melton Valley Storage Tank waste and simulated waste mixtures	26
6. Composition of synthetic single-shell tank salt cake	28
7. Composition of synthetic sludge	28
8. Composition of mixtures used for supernatant viscosity measurements	31
9. Viscosity measurements for simulated supernatant liquids and calibration fluids	33
10. Summary of rheological measurements with Melton Valley Storage Tank simulant in the slurry test loop.	44
11. Summary of rheological measurements with Hanford simulated waste	46

FLUID DYNAMIC DEMONSTRATIONS FOR WASTE RETRIEVAL AND TREATMENT

E. L. Youngblood, Jr., T. D. Hylton, J. B. Berry
R. L. Cummins, F. R. Ruppel, R. W. Hanks

EXECUTIVE SUMMARY

A large quantity of radioactive waste is stored as a two-phase mixture of sludge and supernatant liquid in underground storage tanks at U.S. Department of Energy facilities. There is a need to transport the waste from the tanks to other locations for processing or for improved storage. One method used in the past and expected to be used in the future is transport by pipeline. Past experience has shown that the slurry behaves as a non-Newtonian fluid and that the use of correlation for Newtonian fluids for the design and operation of slurry pipelines could result in considerable error. The objective of this study was to develop or identify flow correlations for predicting the flow parameters needed for the design and operation of slurry pipeline systems for transporting radioactive waste of the type stored in the Hanford single-shell tanks and the type stored at the Oak Ridge National Laboratory (ORNL). This was done by studying the flow characteristics of simulated waste with rheological properties similar to those of the actual waste.

Chemical simulants with rheological properties similar to those of the waste stored in the Hanford single-shell tanks were developed by Pacific Northwest Laboratories, and simulated waste with properties similar to those of ORNL waste was developed at ORNL for use in the tests. Rheological properties and flow characteristics of the simulated slurry were studied in a test loop in which the slurry was circulated through three pipeline viscometers (constructed of 1/2-, 3/4-, and 1-in. schedule 40 pipe) at flow rates up to 35 gal/min. Runs were made with ORNL simulated waste at 54 wt % to 65 wt % total solids and temperatures of 25°C and 55°C. Grinding was done prior to one run to study the effect of reduced particle size. Runs were made with simulated Hanford single-shell tank waste at approximately 43 wt % total solids and at temperatures of 25°C and 50°C. The rheology of simulated Hanford and ORNL waste supernatant liquid was also measured.

The results indicated that both the ORNL and Hanford wastes were non-Newtonian and could be represented by the Bingham plastic model under the conditions studied. Mathematical models and commercially available computer programs for calculating pressure drop, critical Reynolds numbers, and minimum transport velocities were identified and described by a slurry transport consultant for the project. Comparison of measured values of pressure drop and critical Reynolds numbers with calculated values using a commercially available computer program (YPLPIPE) showed good agreement. The simulated waste used behaved as a homogeneous slurry (i.e., did not settle); minimum transport velocities were not studied.

Additional studies using slurries with a wider range of composition, particle size, and suspended solids concentration are recommended. Additional work needed to develop computer programs for analysis of data from pipeline viscometers and to modify existing programs for calculating deposition velocity for non-Newtonian fluids and fluids that contain particles of more than one density is described.

1. INTRODUCTION

Waste management and environmental restoration programs have identified a need for the development, demonstration, testing, and evaluation of methods to retrieve and transport radioactive waste that is stored in underground tanks at U.S. Department of Energy (DOE) facilities. A large quantity of the waste is stored as two-phase mixtures of sludge and supernatant. The Hanford Site has 149 single-shell waste tanks with capacities up to 1 million gallons each, the Oak Ridge National Laboratory (ORNL) has eight primary waste storage tanks (50,000 gal each) filled with waste, and additional waste is stored at other DOE facilities.

One method of removal and transport of radioactive waste used in the past and planned for future use is mixing the liquid and sludge phases to produce a slurry that is transported by pipelines. Past experience has shown that the slurry behaves as a non-Newtonian fluid. The use of Newtonian correlations for the design and operation of slurry transport systems could result in considerable error in calculating design parameters and operating conditions.

The primary objective of the fluid dynamic demonstration project is to identify or develop mathematical models for predicting the flow parameters needed for the design and operation of slurry pipeline transport systems for the type of waste stored in the Hanford single-shell tanks and the ORNL Melton Valley Storage Tanks (MVSTs). The chemical composition and concentration of the waste contained in the tanks vary considerably. Because of the radioactive environment and limited accessibility, only small amounts of waste material are available for chemical analysis and rheological measurements on a laboratory scale. In this study, nonradioactive simulated waste with chemical and rheological properties similar to the actual waste is studied in a slurry test loop to provide engineering-scale data for the evaluation of flow correlations. Evaluation and testing of flow correlations that cover a range of waste compositions may enable predictions of the conditions for pipeline transfer of the waste based on future laboratory rheology measurements of the actual waste.

Simulated waste compositions with rheological properties similar to those of the single-shell tanks at Hanford were developed by Pacific Northwest Laboratories (PNL). Simulants with rheological properties similar to those of the MVSTs were developed at ORNL for use in this study. Data from the operation of a slurry test loop using simulated waste were analyzed to determine the rheological properties of the slurry over a range of conditions. The rheological data were used to identify flow correlations (for pressure drop and transition from laminar to turbulent flow) needed for the design and operation of slurry transport pipelines. A slurry transport consultant (Richard W. Hanks Associates, Inc.) assisted in the analysis of the data and the evaluation of flow correlations. In addition, Dr. Hanks wrote Sect. 4 of this report, which describes non-Newtonian flow correlations and the computer programs available for non-Newtonian flow calculations.

The project was sponsored by the DOE Office of Technology Development as a part of the Underground Storage Tank Integrated Demonstration program (TTP No. OR-1112-02). Work done for this project includes modification of an existing slurry test loop

for use for the fluid dynamics tests, testing and calibration of instruments and equipment in the slurry loop, development of simulants for the Hanford single-shell tanks and the ORNL waste storage tanks, operation of the slurry test loop with the simulated wastes, and evaluation of the flow data obtained. Also as part of the project, a data base was prepared of the equipment and methods used in previous pipeline waste transfers at DOE facilities,¹ and an evaluation was made of instruments for measuring suspended solids concentrations in slurries.² This report describes the slurry test loop and the approach used for data analysis and correlation, provides information on simulant development, and gives rheological data obtained from operation of the test loop.

2. DESCRIPTION OF EQUIPMENT

The slurry test loop was used to circulate the simulated waste slurry through pipeline viscometers to determine rheological properties and flow characteristics. A flow diagram of the system is presented in Fig. 1. Simulated waste slurry is made up in either feed tank F-100 or F-200 by mixing the chemical components with water in approximately 50-gal batches. During mixing and operation, slurry can be circulated from the bottom to the top of the feed tank with centrifugal pump J-300 to assist the agitators in keeping the slurry in suspension. Size reduction of solid particles in the slurry can be accomplished by recirculating slurry from the feed tanks through mixer/grinder J-350. After the simulated waste slurry has been prepared, it is circulated through the test loop at predetermined flow rates by progressive cavity pumps J-110 (0 to 5 gal/min) and J-120 (4 to 35 gal/min). The flow rate is controlled by varying the pump speed. The level and density in the feed tank are measured by pressure differential instruments LT-100 and DT-100.

The slurry flow rate through the test loop is measured and recorded by flow instruments FE-125 (magnetic flowmeter) and by pumping from tank F-100 into tank F-200, which is located on weigh table WT-205. Mass flowmeter FE-130 is used to measure the density of the slurry in the recirculating loop. The pumping rate is verified by measuring the change in weight vs time using weigh table WT-205. Ports are located at the feed tank and in circulation lines for taking samples to determining particle size and density measurements, for composition analysis, and for laboratory viscosity measurements. The viscosity of the slurry is measured at different shear rates (flow rates) using pipeline viscometers in the circulating loop. The loop has three horizontal pipeline viscometers (PLV-1, PLV-2, and PLV-3) of different diameters (1.049-, 0.824- and 0.622-in. ID. A sketch of the pipeline viscometers is shown in Fig. 2. Shear stress vs shear rate data for the fluid are determined by accurately measuring the pressure drop across a known length of pipe at known flow rates. Pressure-differential transmitters (PdT-155, PdT-165, and PdT-175) are used to measure the pressure drop across the pipeline viscometers. The pressure at the discharge of the pumps is measured using pressure gage PI-135 and pressure transmitter PT-125. The temperature of the slurry is measured by chromel-alumel thermocouples located in the feed tanks, in thermowells, and on the surface of the circulation loop. The temperature of the slurry is controlled (either heated or cooled) by use of heat exchanger HE-500 in the circulating loop.

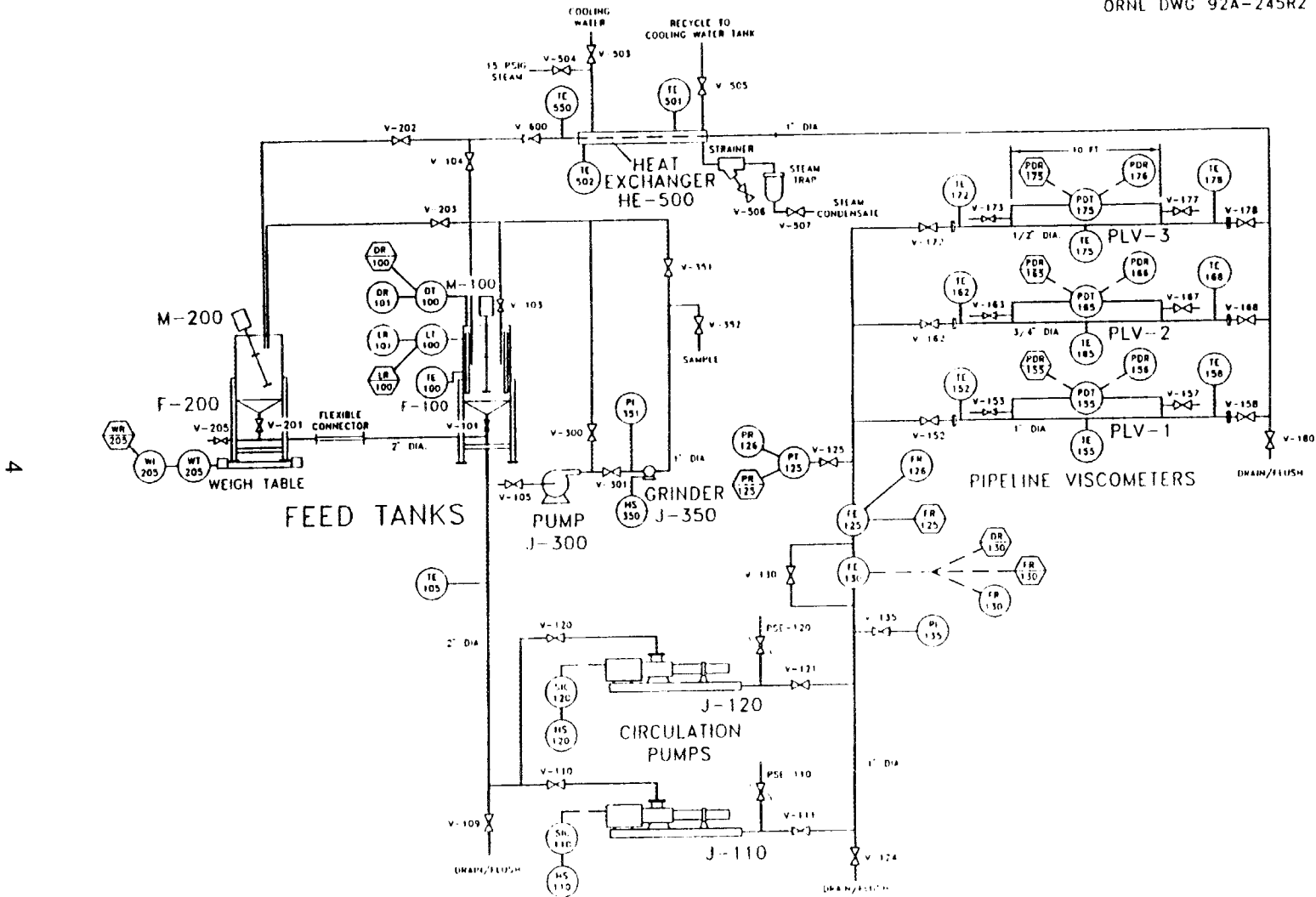


Fig. 1. Flow diagram of slurry test loop.

Viscometer sizes : 1', 3/4' and 1/2' diameter
Schedule 40 pipe

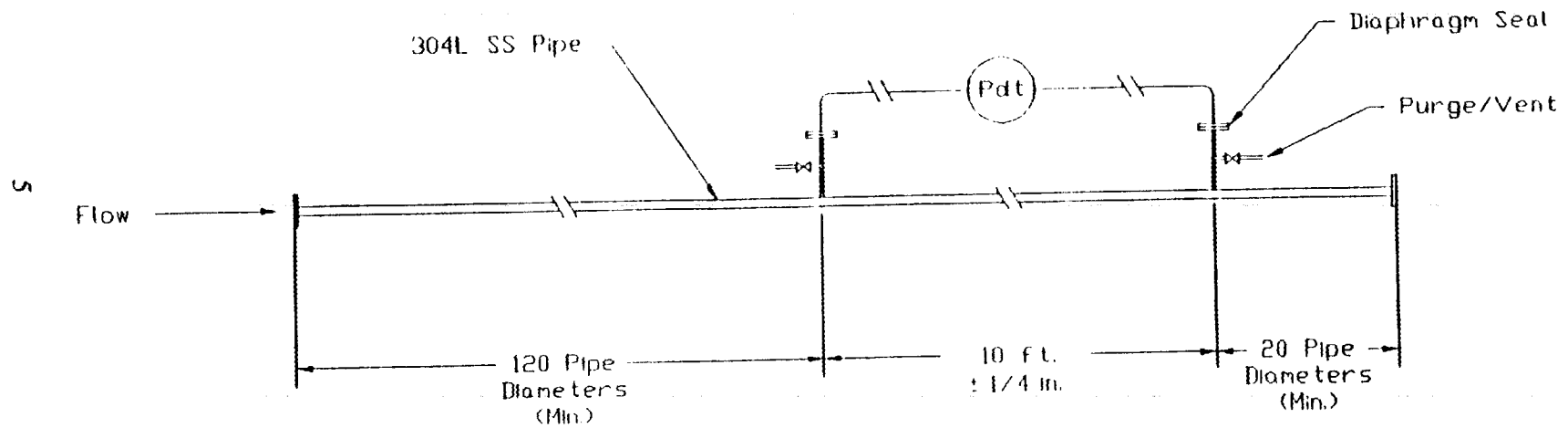


Fig. 2. Typical pipeline viscometer.

Signals from the flow instruments (FE-125 and FE-130), viscometer pressure-differential instruments (PdT-155, PdT-165, and PdT-175), weigh table WT-205, and the thermocouples are recorded by a data-logging system (386 PC with Genesis™ software and an MT-1000™ interface board).

In addition to using the instrumentation for process measurements, the instruments and equipment are being evaluated to determine reliability and suitability for use in radioactive waste transfer systems. A description of the major equipment items is given in Table 1.

3. PROCESS PARAMETERS AND PROCEDURES

A primary objective of the studies in the slurry test loop was to determine the flow behavior of simulated waste and to provide the rheological data required to select or develop flow correlations that can be used to predict conditions under which waste can be satisfactorily transported. Primary flow correlations needed for the design and operation of slurry transport systems are

- pressure drop vs flow rate,
- region of transition from laminar to turbulent flow, and
- minimum deposition velocity (minimum velocity at which a layer of sliding or stationary particles appear).

Rheological data needed for selection or development of flow correlations are obtained by circulating slurry through pipeline viscometers and other instrumentation in the slurry test loop. The following parameters are measured or determined:

- pipeline viscometer diameter and length;
- slurry flow rate through viscometer;
- pressure drop across viscometer;
- slurry density, concentration, composition, and particle size; and
- temperature.

Rheograms (shear stress vs shear rate diagrams) were prepared from pipeline viscometer data taken in laminar flow. Three sizes of pipeline viscometers are used to provide a wider range of shear rates and to permit evaluation of slippage of the slurry at the wall. Data from the rheograms were analyzed to select a rheological model representative of the slurry. Flow correlations available for determining pressure drop, critical Reynolds number, and minimum transport velocity were identified.

Mathematical models for use in the design and operation of pipeline slurry transport systems were evaluated by comparing calculated results using the models with measured values. The stability of the slurry and time-dependent properties were evaluated by observing changes in the rheological properties over a period of time.

Table 1. Instruments and equipment used in the slurry test loop

Process instruments

1. *Magnetic flowmeter* — Endress & Houser, Inc.; Discomag, Size 1.0-in., full-scale flow rate 75 gpm; T max 300°F, P max 600 psig; PIPO 1060 Cal F1.165; Electrode 316 ss, liner PTFE, S/N1942-001423786. *Readout* — Variomag, full-scale 75 gpm; 4-20 ma output; 115 V, Model FTI1942-1-01-TF-SS-A1-N4-GP3-00-SP, Serial No.1942-001423785.
2. *Mass flowmeter* — Micromotion Model D S1005126, SN113294.
3. *Rosemount Model 1151 DP/GP pressure and differential pressure transmitters* — Model 1199 Remote Diaphragm Seals.
4. *Honeywell ST3000 Smart Transmitter* — Model STD624-A1A.
5. *Pressure gages* — Ashcroft, filled with diaphragm seal (type 301; Teflon diaphragm, 316 ss housing; halocarbon filled fluid).
6. *Fairbanks scales* — Model H90-3051, Serial No. H110288CT, Range 0-1000 lb.

Equipment

1. *Moyno progressive cavity pump* — Model 2L8, type SSB; trim AAA Robbins & Myers Moyno Industrial Pump, 316 ss suction casing, ss internals, chrome-plated ss rotor turning in a EPDM stator, braided Teflon water flush packing, 30 gal/min at 60 psig discharge pressure.
 2. *Model 3L3 Moyno progressive cavity pump*, — Type SSGD, Trim AAA, Form GJ with C5303B stator.
 3. *Centrifugal Pump* — Durco Mark III 1/2 × 1-6 with 1/2 hp 1750-rpm motor (rated at 65 gal/min at 11-ft head).
 4. *IKA in-line three-stage disperser* — Model DR 3- 6/6A.
 5. *Whitey ball valve* — 316 ss with INCO X750 seats with coned disc springs and chevron design packing.
 6. *Worcester high-per mizer ball valve* — 1/2 inch, Series PT-51, Body of 316 ss, Metal A seat with lever handle operator.
 7. *Stainless steel ball valve* — Watts, UHMW polyethylene seat material.
-

Rheological properties were measured for one simulated waste composition for the ORNL MVSTs and one simulated waste composition for the Hanford single-shell tanks over a range of solids concentrations and temperatures. The effect of reduced particle size was studied in one MVST run; however, under the conditions studied, all of the slurries appeared to behave as homogeneous slurries, and no minimum transport velocity measurements were made. Rheological measurements were also made of simulated supernatant solution without solids present. Additional work is recommended to study the rheological properties of both the MVST and Hanford single-shell tank waste over a larger range of compositions, concentrations, and particle sizes.

4. NON-NEWTONIAN MODELS AND FLOW CORRELATIONS

4.1 Rheological Models

Rheology is the science of determining the functional dependence of shear stress upon shear strain rate for fluid and semisolid materials. The mathematical expression that describes this dependence is called a "constitutive relation" and is truly characteristic of the nature or constitution of the material. The constitutive relation is independent of the stress environment into which the fluid is placed and hence is independent of the equipment used to measure rheological phenomena.

Constitutive relations are developed by mathematically modeling experimentally determined curves of shear stress vs shear rate, or rheograms. Certain "classical" models (Newtonian, Bingham plastic, power law, and yield power law or Herschel-Bulkley), described by common curve shapes on a rheogram and illustrated schematically in Fig. 3, have been developed. These classical models are³

Newtonian. A simple proportionality,

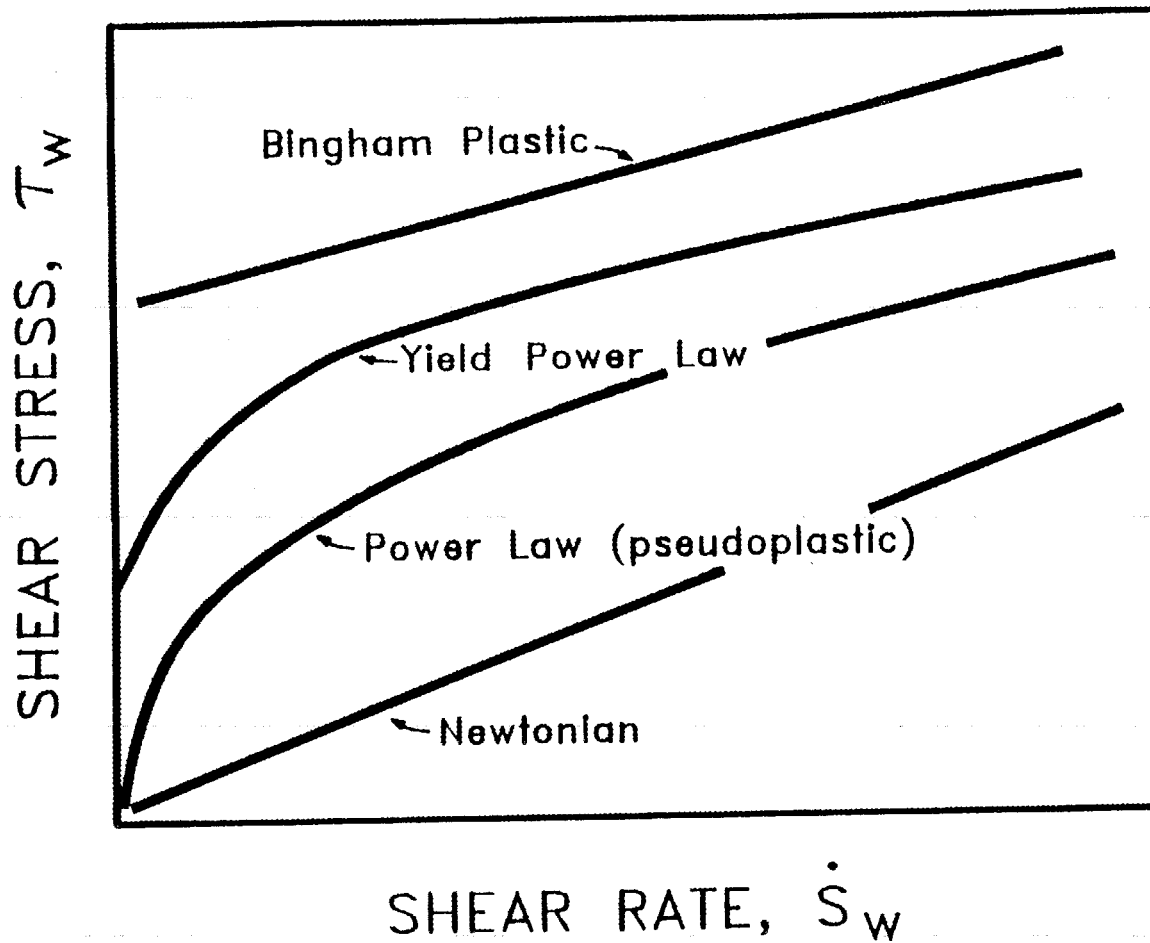
$$\tau = \mu \dot{S}, \quad (1)$$

where τ is the shear stress, μ is the "viscosity" (more correctly the viscosity function), and \dot{S} is the shear rate, describes the straight line through the origin labeled "Newtonian" in Fig. 3. The unique characteristic of the Newtonian fluid is that the viscosity function is a constant, independent of shear rate. This is called the viscosity of the fluid.

Bingham Plastic. A simple linear relation,

$$\tau = \tau_0 + \eta \dot{S}, \quad (2)$$

where τ_0 is yield stress and η is the "plastic viscosity" or "coefficient of rigidity," describes a straight line with an intercept labeled "Bingham plastic" in Fig. 3. The significance of the yield stress is that this amount of stress must be overcome before any motion is initiated. Many slurries tend to exhibit yield stresses.



6

Fig. 3. Shear stress vs shear rate curves for typical Newtonian and non-Newtonian fluids.

If Eq. (2) is rearranged into the form of Eq. (1), the viscosity function (which is no longer a constant as in the Newtonian fluid case) is given by

$$\mu = \frac{\tau_o}{\dot{S}} + \eta. \quad (3)$$

The characteristic of this variable viscosity fluid is that its viscosity function approaches infinity as shear rate becomes very small (corresponding to the presence of a finite yield stress). It also approaches η in the limit of large shear rate. Thus, η is also called the "high shear limiting viscosity."

Power Law. If the Fig. 3 rheogram were replotted on logarithmic coordinates, one would see that many shear-thinning fluids (fluids whose viscosity function decreases with increasing shear rate) exhibit curves with substantial portions that are linear corresponding to

$$\log(\tau) = \log(K) + n\log(\dot{S}). \quad (4)$$

This logarithmically linear equation when translated to the linear coordinates of the rheogram becomes

$$\tau = K\dot{S}^n, \quad (5)$$

which is the well-known Power Law relation. The parameter K is called the "consistency factor," and the parameter n is called the "flow behavior index." The viscosity function for the Power Law model is

$$\mu = K\dot{S}^{(n-1)}. \quad (6)$$

If $n < 1$, this viscosity function decreases with increasing shear rate, and the fluid is said to be "pseudoplastic." If $n > 1$, this viscosity function increases with increasing shear rate, and the fluid is said to be "dilatant" or shear thickening. In the special case where $n = 1$, the viscosity function reduces to the constant value K , which is equivalent to the viscosity of a Newtonian fluid. This role of the parameter n gives rise to its name of flow behavior index.

Note that for pseudoplastic fluids, Eq. (6) has a limiting value of zero as shear rate increases indefinitely. This is clearly not physically realistic as all real materials have some residual limiting high shear-rate viscosity. For this reason, the Power Law can safely be used only for interpolation between existing measured values of shear rate but not for extrapolation to higher values. The Power Law has become popular because of its mathematical simplicity.

Yield Power Law. If one adds a yield stress to Eq. (5), obtaining

$$\tau = \tau_o + KS^n, \quad (7)$$

one characterizes a curve similar to that labeled "yield power law" in Fig. 3, which is a Power Law model with a yield stress. The viscosity function for this model is given by

$$\mu = \frac{\tau_o}{\dot{S}} + K\dot{S}^{n-1}. \quad (8)$$

Note that for the special case $n > 1$, this viscosity function is shear thinning for small values of shear rate but shear thickening for large values of shear rate: that is, the viscosity of such a material first decreases, reaches a minimum value, and then increases as shear rate increases. This very complex behavior is often exhibited by high-concentration slurries of finely divided solids.

The rheological constitutive behavior of a great many slurries is almost always described by one of the above models.

4.2 Viscometry and Data Analysis

Viscometers are mechanical devices that create stress fields in fluid samples. They are always instrumented to measure two macroparameters, one functionally related to (but not equal to) the shear stress, and the other functionally related to (but not equal to) the shear rate. Thus, raw viscometer data, regardless of the type or make of the device used for their collection, must be converted into shear stress and shear rate values before any meaningful evaluation of the constitutive behavior of the fluid can be made. In the case of Newtonian fluids, this is a simple matter of multiplying each measured variable by an appropriate instrument constant. This is a direct consequence of the mathematical form of Eq. (1). For all other constitutive relations, however, this simple conversion is not possible; a more complex type of data reduction must be employed.

If one knew the correct constitutive relation for the fluid being tested, one could solve the basic differential field equations for momentum transport in the geometrical configuration corresponding to the viscometer used and obtain the functional relation between the measured variables appropriate to that constitutive relation. However, the very purpose for constructing and using a viscometer is to discover the constitutive relation of the fluid. Hence, one cannot resort to the direct comparison of data with theoretical solutions as described above. An alternative procedure is needed. For the tube or capillary or pipeline viscometer, this alternative is the method of Rabinowitsch and Mooney.^{4,5}

4.2.1 Experimental Data

In a pipeline viscometer, the primary measured variables are the pipe diameter, D ; the length between two pressure taps, L ; the pressure differential across that length, Δp ; and the volume rate of flow of fluid through the pipe, Q (alternatively, one may measure the mass flow rate, m , and the fluid density, ρ , from which Q may be calculated as m/ρ).

4.2.2 Data Reduction and Analysis

For all fluids, regardless of constitutive relation, it can be very simply shown that the shear stress at the wall of the tube or pipe is related to measured variables by

$$\tau_w = \frac{D\Delta p}{4L} . \quad (9)$$

A second variable, related to Q and called a "pseudo-shear rate," is

$$\Gamma = \frac{32Q}{\pi D^3} = \frac{8V}{D} . \quad (10)$$

In the method of Rabinowitsch and Mooney, a logarithmic plot of the calculated variables τ_w and Γ is prepared. The raw data are then smoothed by fitting a curve to them. This curve is then graphically (or numerically if computer fitting is used) differentiated at points corresponding to each experimental value of Γ . The derivative thus obtained is

$$n' = \frac{d \ln \tau_w}{d \ln \Gamma} . \quad (11)$$

It can easily be mathematically proved that, independent of the constitutive relation of the fluid, the shear rate at the wall may be calculated from Γ by

$$\dot{S}_w = \Gamma \frac{3n' + 1}{4n'} . \quad (12)$$

Thus, by using the procedure outlined above, the measured variables D , L , Δp , and Q may be converted into the required rheogram variables τ_w and \dot{S}_w . Once these variables have been calculated, a rheogram is prepared, and one of the constitutive relations is curve fitted to the data to obtain the equation parameters.

4.3 Pipeline Flow Correlations

Once the appropriate constitutive relation is known, one can determine the proper relation between Δp and Q for laminar, transitional, and turbulent flow in a pipeline. It is also possible to determine the conditions for transition from laminar to turbulent flow and for the deposition of heterogeneously suspended solids from turbulent flows as well as the Q - Δp relation for heterogeneously suspended solids in turbulent flow. There are no generically applicable relations for these flow conditions, and separate results are required for each constitutive relation. We give below a brief summary of the appropriate relations for each of the constitutive relations described above, which are useful for most slurries.

4.3.1 Newtonian Fluids

Friction factors for Newtonian fluids are given by the well-known Moody chart. In laminar flow, the familiar result

$$f = \frac{16}{N_{Re}} \quad (13)$$

where

$$f = \frac{2\tau_w}{\rho V^2} \quad (14)$$

is the Fanning friction factor, and

$$N_{Re} = \frac{DV\rho}{\mu} \quad (15)$$

is the Reynolds number. The above are the dimensionless equivalent of the Poiseuille equation

$$Q = \frac{\pi D^4}{128\mu} \left(-\frac{\Delta p}{L} \right) \quad (16)$$

Transition from laminar to turbulent flow is determined by the condition $N_{Re} = 2100$. The turbulent flow relation is given graphically by the Moody chart or numerically by a number of empirical curve-fit correlations. One that is useful for the computer is the Colebrook relation⁶

$$4f = a + bN_{Re}^{-c} \quad (17)$$

with $k = \epsilon/D$ being the relative pipe-wall roughness and

$$a = 0.094k^{0.225} + 0.53k, \quad (18)$$

$$b = 88k^{0.44}, \quad (19)$$

and

$$c = 1.62k^{0.134}. \quad (20)$$

The prediction of V_{DC} , the velocity of deposition of heterogeneously suspended solids from a turbulent flow, is best accomplished by using the model of Hanks and Sloan.⁷ This model is mathematically complex; its details are not included here. However, an IBM PC-compatible program is commercially available that permits calculation of V_{DC} using this method.

The calculation of the Q - Δp relation for heterogeneous turbulent transport of solids is accomplished by the method of Wasp.⁸ This method has been used successfully in numerous commercial pipeline designs. An IBM PC program is commercially available that performs the necessary calculations using this method.

4.3.2 Bingham Plastic Fluids

The Bingham plastic equivalent of the Poiseuille relation for laminar flow is the Buckingham equation³

$$Q = \frac{\pi R^4}{8\eta} \left(-\frac{\Delta p}{L} \right) \left[\frac{1}{3} \left(\frac{2\tau_o}{R} \right)^4 \left(-\frac{L}{\Delta p} \right)^4 + 1 - \frac{4}{3} \left(\frac{2\tau_o}{R} \right) \left(-\frac{L}{\Delta p} \right) \right]. \quad (21)$$

Note that even though the Bingham plastic constitutive relation is linear, this flow equation is nonlinear. It is generally true for non-Newtonian fluid models that the integration of the constitutive relation for pipe flow produces a nonlinear flow relation.

The condition of transition from laminar to turbulent flow may be determined by using the method of Hanks.⁹ This is mathematically complex, and the equations are not presented here. However, IBM PC programs are commercially available that make this calculation.

Friction factors for the turbulent flow of Bingham plastic fluids must be calculated by the method of Hanks and Dadia.¹⁰ IBM PC programs for using this method are also commercially available.

In some of the early studies of turbulent flow of Bingham plastic fluids, it was erroneously concluded¹¹ that one could use the conventional Moody diagram of Newtonian flow with μ replaced by η in the Reynolds number to calculate friction factors if $\tau_o < 24 \text{ N/m}^2$ (240 d/cm^2). While there are some combinations of flow and rheological parameters for which this procedure fortuitously works, there are also many combinations of flow and rheological parameters for which this procedure will produce significantly erroneous results. Therefore, only the method of Hanks and Dadia should be used.

No direct computational model is available for predicting V_{DC} for non-Newtonian fluids of any type. The method of Hanks and Sloan could be modified to include non-Newtonian constitutive relations, but this would require a special development effort. This same situation exists for the calculations of the $Q-\Delta p$ relation for solids suspended heterogeneously in non-Newtonian fluids.

A combination experimental-computational method modifying Wasp's method has been developed by Hanks for calculating heterogeneous turbulent head losses in non-Newtonian fluids.¹² However, this method involves extensive, detailed experimental evaluation of the dependence of constitutive model parameters on both solid concentration and particle-size distribution.

4.3.3 Power Law Fluids

For the power law constitutive relation, the equivalent of the Poiseuille equation for laminar flow is

$$Q = \pi R^3 \left(\frac{n}{1+3n} \right) \left(\frac{D}{4K} \right)^{\frac{1}{n}} \left(-\frac{\Delta p}{L} \right)^{\frac{1}{n}}. \quad (22)$$

This equation can be expressed in dimensionless form identical to the Newtonian result as

$$f = \frac{16}{N_{RE,PL}} \quad (23)$$

where $N_{RE,PL}$ is a power law "Reynolds number" defined by

$$N_{RE,PL} = 2^{3-n} \left(\frac{n}{1+3n} \right)^n \frac{D^n V^{2-n} \rho}{K}. \quad (24)$$

Because of the simple form of the power law model and the form of Eq. (23), Metzner and Reed sought to develop a generalized method of data representation that would make Eq. (23) applicable for all fluids.¹³ They succeeded in manipulating the method of Rabinowitsch and Mooney, described earlier, into the form

$$f = \frac{16}{N_{Re,MR}} \quad (25)$$

where $N_{Re,MR}$ is a "generalized" Reynolds number defined by

$$N_{Re,MR} = \frac{D^{n'} V^{2-n'} \rho}{8^{n'-1} K'} \quad (26)$$

with n' being the Rabinowitsch-Mooney parameter defined earlier and K' being the intercept value of the straight line of slope n' tangent to the curve of $\log \tau_w$ vs $\log(8V/D)$ at the point where n' is determined. In the special case where the Rabinowitsch-Mooney plot is a straight line (i.e, the fluid is truly a power law in the range of the data), we have $n = n'$ and $K' = K$ so that Eqs. (24) and (26) reduce to the identity $N_{Re,PL} = N_{Re,MR}$.

Because of the generality of the Rabinowitsch-Mooney relation in laminar flow, Eqs. (25) and (26) correlate laminar flow data for any fluid, regardless of its true constitutive relation. This generality was erroneously assumed to extend to transitional and turbulent flow.¹³ Thus, Metzner and Reed proposed that Newtonian turbulent flow correlations could be used to predict non-Newtonian flow behavior if N_{Re} were replaced by $N_{Re,MR}$. Unfortunately, this is not true; more complex results are required. Hanks has shown¹⁴ that since the Rabinowitsch-Mooney relation is not valid in turbulent flow, it is impossible to correlate turbulent flow data using $N_{Re,MR}$. Rather, one must develop separate models for each constitutive relation.

The prediction of conditions of transition from laminar to turbulent flow for power law fluids may be accomplished by using the method of Ryan and Johnson¹⁵ or Hanks.¹⁶ The prediction of turbulent-flow friction factors may be accomplished by using the method of Hanks and Ricks.¹⁷ An IBM PC program to accomplish these calculations is commercially available.

4.3.4 Yield Power Law Fluids

Because of the presence of a third parameter in the yield power law constitutive relation, the mathematical expressions for laminar and turbulent flow $Q-\Delta p$ relations and the conditions for transition from laminar to turbulent flow are quite complicated and are not presented here. However, they are known,^{3,18} and IBM PC programs are commercially available for performing calculations for all three conditions.

4.4 IBM PC Programs

Mention was made several times of commercially available IBM PC programs to perform the various model calculations described. Here is a brief overview of what these programs contain and how they work. All the programs described below are available

from Richard W. Hanks Associates, Inc. They were developed and written by Dr. Hanks, the slurry consultant on this project.

Also presented is an outline of the development efforts that will be required to create currently unavailable programs needed to successfully carry out all of the studies proposed in this project.

4.4.1 Commercially Available Programs

4.4.1.1 YPLPIPE

The program code named YPLPIPE is an interactive, menu-driven program that allows the operator to select a variety of different calculations. Based upon the turbulent pipe-flow model of Hanks¹⁸ for Yield Power Law PIPEflow, it allows the operator to input values of τ_o , K , n , and ρ , together with various combinations of D , Q , or $-\Delta p$. The last three are entered in pairs, and the third variable is calculated. If $\tau_o = 0$ is entered, the model of Hanks and Ricks¹⁷ is used to compute power law behavior. If $n = 1$, $K = \eta$ is entered, the model of Hanks and Dadia¹⁰ is used to compute Bingham plastic behavior. If $\tau_o = 0$, $K = \mu$, and $n = 1$ is entered, the Newtonian flow models are used.

Thus, this one program handles all four rheological constitutive models with equal ease. In addition to the computation of either laminar or turbulent friction factors, pressure losses, or flows, this program also computes all pertinent variables corresponding to the transition from laminar to turbulent flow for any of the four constitutive models.

In addition to the above features, the program also permits the operator to select from any of the commonly used systems of units for each of the appropriate input variables and output results. All unit conversions are automatically handled internal to the program. The selections of units, types of variables to be input or output, whether laminar or turbulent flow is desired, and whether a single point or an entire friction factor curve is desired are all made by simple menu-selection key strokes.

For laminar flow calculations, the appropriate equivalent of the Poiseuille equation (listed above for the various models) is solved to give $Q(D, -\Delta p/L)$, $-\Delta p/L(Q,D)$, or $D(Q, -\Delta p/L)$, depending on the choice of input variables selected. For the transition from laminar to turbulent flow, the various equations that have been developed for the four models are solved. Some of these are direct calculations while others require iterative computation.

The turbulent flow calculations all require evaluation of systems of equations from the various models. All of these involve the numerical evaluation of complicated integrals. This is accomplished by means of a 20-point Gaussian quadrature routine that is extremely accurate. All calculations require iterative solution of one or more equations that in most cases are coupled. The iterations use combinations of Newton's method and quadratic interpolation for root-finding. These iterative methods converge quite rapidly and are very stable numerically.

4.4.1.2 SLOANVDC

A program code named SLOANVDC uses the method of Hanks and Sloan to compute V_{DC} for heterogeneously suspended solids in Newtonian liquids. The program allows the operator to input complete particle-size distribution (PSD) data, particle and fluid densities, fluid viscosity, pipe diameter, and solids concentration. The program also can accommodate the situation where the solid absorbs a certain percentage of the liquid (the inherent moisture problem).

In this model, two coupled, nonlinear differential equations must be solved simultaneously. This is performed in an iterative fashion with all integrations made by the same 20-point Gaussian quadrature routine used in YPLPIPE.

The PSD data are analyzed to determine a portion that is presumed to be uniformly and homogeneously suspended. This portion of the PSD, together with the suspending liquid, is treated as a single-phase, Newtonian fluid called the "vehicle." A density and viscosity are computed for the vehicle using well-known correlations. The remainder of the particles are presumed to be heterogeneously suspended in this vehicle. The heterogeneously suspended portion of the PSD is then analyzed to determine for it a value of d_{85} (the diameter for which 85% of the particles are smaller). In the model, all particles are treated as if they were uniform spheres of this diameter. The value of V_{DC} computed by this program is the sliding-bed deposition velocity (the minimum velocity at which a layer of sliding particles appears) for spheres of diameter d_{85} heterogeneously suspended in the vehicle in the pipe of diameter D (which was input).

4.4.1.3 WASP

A program code WASP solves the model equations of Wasp to calculate the head loss (either single velocity value or complete velocity curve between input limits) for heterogeneously suspended particles in a Newtonian fluid. The program permits the operator to input a complete PSD, pipe diameter, solid and fluid densities, fluid viscosity, particle fluid absorbtivity, and operating velocity or a range of velocities if a full curve is desired.

In the method of Wasp, a portion of the solids is presumed to be uniformly and homogeneously suspended in the liquid, creating a Newtonian "vehicle" (like in SLOANVDC). The remainder of the solid particles are presumed to be heterogeneously suspended in this vehicle and to obey Durand's correlation.¹⁹

The vehicle is determined by an iterative process in which a fraction is assumed, density and viscosity are calculated, and a concentration distribution is calculated from a model chosen by Wasp. When the fraction determined from the calculated concentration distribution equals the assumed fraction, the iteration is converged. This process usually converges quite rapidly. The remainder of the particles are then assumed to be heterogeneously suspended. All iterations are converged to four digits of agreement.

4.4.1.4 LOOPFLOW

An IBM PC program LOOPFLOW is available that permits analysis of slurry pressure-drop data obtained in a recirculating flow loop. The extremely useful feature of this program is its ability to analyze time-dependent changes in slurry properties caused by particle attrition. This phenomenon can be very important if particles break up either due to physical fracturing or chemical dissolution (a distinct possibility with the slurry systems to be studied in the present projects). When particle attrition or chemical dissolution occurs, the $Q-\Delta p$ relation observed in a recirculating flow loop is not the same as would be observed in a single-pass-through pumping system. Consequently, the data are not useful unless the effect of the time-dependent properties can be correctly accounted for. LOOPFLOW is capable of doing this. Details of the program and its computational methods are very complicated and extensive and will not be presented here.

4.4.2 Software Development Projects Required

4.4.2.1 Viscometer Data Reduction and Analysis

The only proper method of viscometer data reduction is the method of Rabinowitsch and Mooney described above. However, this method is very laborious and slow when performed graphically by hand. Therefore, it is important that a user-friendly, menu-driven, interactive IBM PC graphics program be developed that can accomplish this method quickly. This same program should also have the capability of curve-fitting any of the four rheological constitutive models to the derived rheograms and determining appropriate model parameters.

Several years ago, Dr. Hanks developed a program for Battelle PNL to perform similar types of operations for data obtained with their Haake rotational viscometer.²⁰ Because of the fundamental differences between the rotational viscometer and the pipeline viscometer used by ORNL, the details of the data-reduction and computational models used are quite different, and the PNL programs cannot be used for the ORNL data. However, many of the basic data-handling procedures, curve-fitting procedures, and graphics display methods used in the PNL programs can be readily adapted to the Rabinowitsch-Mooney procedure required for the ORNL data.

As a part of the ongoing work of this project, Dr. Hanks will develop a menu-driven program similar to the PNL program but adapted to the ORNL needs. The program will permit input of raw data from the ORNL data-collection system and will convert the raw data to τ_w and $8V/D$ equivalents. The program will use the smoothed Rabinowitsch-Mooney curves in the calculation of n' values and reduction of $8V/D$ values to equivalent shear rate values to create the rheogram. Once the rheogram is calculated, the program will use nonlinear regression and interactive parameter variation methods, together with graphics display of the data, fitted curves, and distributions of deviations between data and calculated values to allow the operator to curve fit any of the four constitutive models to the rheogram data. Finally, it will output raw data, converted data, rheogram data, and model parameters in any set of units desired. All internal calculations will be performed using SI units as the standard. All unit conversions will be handled internally in the program. No hand computations or graphical procedures will be required.

4.4.2.2 Extension of SLOANVDC to Include Non-Newtonian Constitutive Relations

At present, SLOANVDC is restricted to Newtonian fluid behavior. While it is possible to extend this model to include various non-Newtonian constitutive models, this extension is not trivial because it requires the separate solution of the calculation of particle concentration distributions in the non-Newtonian fluid. In the case of the yield power law model, and perhaps also the power law model, this may require simultaneous numerical integration of coupled differential equations because of the nonlinearity of the fundamental constitutive relations.

As a part of the ongoing work of this project, Dr. Hanks will develop the appropriate mathematical solutions and computer programs to perform this extension. This extension is very important because the presence of a yield stress (as in both the Bingham plastic and yield power law models) will greatly influence the suspending power of the fluid in the slurry.

The computer program to be developed will be patterned rather closely after the present SLOANVDC with the addition of menu selections for choice of constitutive model to be used. It will be written in the following two versions:

- a stand-alone version that may be used to compute V_{DC} for given input conditions, and
- a subroutine version that may be coupled with other programs that may require V_{DC} as part of a more extensive computation.

4.4.2.3 Extension of WASP to Include Multicomponent Mixtures of Solids Having More Than One Density and Non-Newtonian Vehicle Rheology

All of the simulant slurries to be studied in this project will be composed of multicomponent mixtures of different materials. The real slurries at Hanford and other sites also contain numerous materials. Any slurring process used in the real system will undoubtedly create a slurry with a number of different-density heterogeneously suspended solids. It is also quite likely that the real slurries will have non-Newtonian rheological behavior under some conditions. The current versions of WASP are based upon Wasp's original model,⁸ which presumed that only a single-density solid was present and that the vehicle portion of the mixture behaved as a Newtonian fluid.

As part of the ongoing work of this project, Dr. Hanks will develop the necessary mathematical and computer models to extend the current method of Wasp to include a multicomponent mixture of solids of differing densities. Each different-density solid will be presumed to have its own PSD to permit complete flexibility in specification of slurry properties. Two versions of the method will be developed:

- a program presuming the vehicle to be Newtonian, and
- a more expanded version presuming the vehicle to be non-Newtonian with choice of constitutive relations.

The second version will require the inclusion as a subroutine of the upgraded non-Newtonian version of SLOANVDC as well as models for concentration dependence of constitutive relation parameters.

5. WASTE CHARACTERIZATION AND SIMULANT DEVELOPMENT

Because of the difficulty in working with radioactive waste, nonradioactive simulants that have rheological and physical properties (viscosity, density, and particle size) similar to those of samples taken of actual waste were used for the fluid dynamics tests in the slurry test loop. Because rheological properties of many of the waste tanks have not been measured, it is desirable to have simulants based on formulations that can be extrapolated to simulate the properties of the wide ranging waste compositions contained in the Hanford and ORNL tanks. This can best be accomplished by the use of simulants with chemical compositions similar to those of the actual waste, although the mechanism by which the chemical compounds were formed in the waste tanks and changes that result from exposure to heat and radiation cannot be duplicated.

5.1 Melton Valley Storage Tank Waste

MVSTs contain a two-phase waste material. The supernatant is an aqueous solution composed primarily of sodium and potassium nitrate; the major radionuclides present are strontium and cesium.²¹ There is a 2- to 5-ft-deep sludge accumulation on the bottom of the tanks, composed primarily of particles of calcium and magnesium hydroxides and carbonates with smaller amounts of aluminum and iron compounds. Sodium and potassium nitrate are present as dissolved salts in the interstitial area between particles. The sludge also contains uranium, thorium, radionuclides, and transuranic elements. Settling tests indicate that the sludge particles have an agglomerate radius of about 20 μm .²² The consistency of the sludge in the tanks ranges from soft sludge to hard mud.

The method proposed for removal and disposal of the waste in the MVST is by sluicing with supernatant and transporting by pipeline to a proposed Waste Handling and Packaging Plant where the material will be solidified, packaged, and sent to the Waste Isolation Pilot Plant in Carlsbad, New Mexico, for disposal.²³ A similar method of mobilization and transport was used to transfer slurry from the ORNL Gunitite tanks to the MVSTs in 1983.²⁴

Analytical measurements have not been made to identify the specific chemical compounds (only anion and cation species) present in the MVSTs. The simulated waste composition for the MVST is based on the cation and anion analysis of the sludge and supernatant liquid. A chemical simulant composition was initially formulated by Mattus²⁵ based on the composition of MVST waste tanks W26 and W28. The simulant composition was modified for this study to include sample information taken from other tanks and chemically characterized by Sears et al.²¹ from samples taken between September 19 and December 5, 1989, and physical characterization of the sludge samples by Ceo et al.²² Major components in the sludge and supernatant liquid phases are summarized in Table 2, and the physical properties of selected waste tank samples are given in Table 3.

Table 2. Range of compositions of major component and properties of Melton Valley Storage Tanks waste

Supernatant liquid

Dissolved solids content: 334 g/L to 478 g/L

Density: 1.21 g/mL to 1.28 g/mL

pH range: 11 to 13

Nitrate concentration: 3 M to 5 M with average of 4 M

Sodium concentration: 61 g/L to 110 g/L

Potassium concentration: 8 g/L to 78 g/L

Potassium/sodium mass ratio: 0.1:0.3, except tanks W26 and W23 at 0.8:1.0

Chloride concentration: about 0.08 M

Sludge phase

Total solids (dissolved plus undissolved): 400 to 500 g/kg

Density: 1.3 to 1.5 g/mL

Sodium plus potassium concentration: 40 to 60 wt % of the total metal concentration

Calcium plus magnesium concentration: 30 to 40 wt % of the total metal concentration

Uranium plus thorium concentration: 4 to 20 wt % of the total metal concentration

Aluminum concentration: 0.1 to 0.8 wt % of total metal concentration

Iron concentration: 0.1 to 0.25 wt % of total metal concentration

*Includes some of the evaporator facility waste tanks.

Source: M. B. Sears, et al., *Sampling and Analysis of Radioactive Liquid and Waste Sludges in the Melton Valley and Evaporator Facility Storage Tanks at ORNL*, ORNL/TM-11652, Oak Ridge National Laboratory, Oak Ridge, Tenn., September 1990.

Table 3. Physical properties of Melton Valley Storage Tanks W26 and W28 and evaporator waste tanks W21 and W23

Physical property	W21	W23	W26	W28
Density (g/mL)				
Bulk liquid	1.24	1.24	1.22	1.29
Bulk sludge	1.34	1.44	1.36	1.40
Interstitial liquid	1.26	1.27	1.23	1.29
Undissolved solids	1.68	2.44	2.16	2.00
Sludge solids (wt %)				
Total solids	51.9	52.4	46.0	51.4
Dissolved solids	28.2	27.5	23.6	29.4
Undissolved solids	23.7	24.9	22.4	22.0
Viscosity^a				
Bulk liquid (cP)	1.82	2.12	1.67	2.22
<i>Neat sludge</i>				
Plastic viscosity (cP)	56	<i>b</i>	<i>c</i>	7700 ^d
Yield stress (dyn/cm ²)	57	-	-	22
<i>Sludge diluted 1:1^e</i>				
Plastic viscosity (cP)	5.5 ^d	95	70	130
Yield stress (dyn/cm ²)	2.2	44	105	66
<i>Sludge diluted 1:3</i>				
Plastic viscosity (cP)	<i>f</i>	<i>f</i>	<i>f</i>	55
Yield stress (dyn/cm ²)	<i>f</i>	<i>f</i>	<i>f</i>	20
<i>Agglomeration radius (μm)</i>	18	23	20	26
<i>Floc sedimentation rate</i>				
Terminal velocity (cm/min)	1.0	3.9	2.9	2.9

^a Sludge viscosity is characterized as Bingham plastics. Measured at 21 ± 2°C.

^b Radiation field from undiluted sludge was too intense to permit viscosity measurement.

^c Rheological data are too scattered to determine plastic viscosity or yield stress.

^d Coagulation during test; not a true viscosity.

^e Sludge diluted 1:1 by volume with bulk liquid taken from same tank as the sludge.

^f Not measured.

Source: R. N. Ceo, M. B. Sears, and J. T. Shor, *Physical Characterization of Radioactive Waste Tank Sludges*, ORNL/TM-11653, Oak Ridge National Laboratory, Oak Ridge, Tenn., October 1990.

Viscosity measurements for the MVST sludge were limited to relatively low shear rates (16 s^{-1}) by the radioactive sample size that could be handled and the viscometer used. Measurements at higher shear rates that are closer to the operating shear rates (on the order of 500 s^{-1}) are needed for accurate modeling. Also, no information is available on whether the viscosity of the slurry is time dependent.

The simulant developed for the MVSTs was based on the major chemical components in the waste given in Table 2. The composition of the initial soluble and insoluble components of the simulated sludge is given in Table 4. Other mixtures were made by adding higher concentrations of insoluble components in the same proportions as given in Table 4. The simulant was made by mixing bulk chemicals as purchased from the manufacturer. Laboratory viscosity measurements were made using a Fann Model 35A viscometer for comparison with viscometer data from the actual waste to determine the composition ranges for use in the slurry test loop. The results, shown in Table 5, indicate that the simulant has a yield stress and exhibits a non-Newtonian behavior that can be represented as a Bingham plastic (as does the actual waste). However, the simulated waste composition required a considerably higher total solids concentration to achieve yield stresses and plastic viscosities similar to those of the actual waste. The sludges from the different tanks have considerably different plastic viscosities for similar solids concentrations. The rheological properties of the simulant are in the same general range as expected for the actual waste after dilution for mobilization.

The particle size of the simulated waste is somewhat similar to that of the actual waste; however, the same methods of size determination were not used. As shown in Table 3, the agglomeration radius of the sludge from four of the waste tanks is in the range of $20 \mu\text{m}$. Particle size measurements were made for the simulant mixture given in Table 4 using a Leeds and Northrup Microtrac laser scanner and by optical image analysis. Results from the Microtrac indicate that 99 wt % of the particles are less than $30 \mu\text{m}$ in diameter and have a volume mean diameter of $10 \mu\text{m}$. Results from image analysis indicate that the particles have a maximum and minimum area equivalent diameter of 22.06 and $0.58 \mu\text{m}$ and an average area equivalent diameter of $1.82 \mu\text{m}$.

To determine the effect of grinding and particle size reduction on the rheology of the sludge, the simulant composition given in Table 4 was homogenized for 1 h with an IKA Labortechnik Ultra-Turrax T25 homogenizer. Grinding resulted in an obvious change in the appearance and settling rate of the sludge. Optical image analysis indicated a reduction in the maximum particle diameter from $22.06 \mu\text{m}$ to $10.94 \mu\text{m}$ and a reduction in the average diameter from $1.82 \mu\text{m}$ to $1.23 \mu\text{m}$. A slight increase in particle size (a mean volume diameter increase from $10 \mu\text{m}$ to $11 \mu\text{m}$) was indicated by the Microtrac measurement. As shown in Table 5, grinding of the simulant resulted in an increase of the yield stress from 20 dyn/cm^2 to 36 dyn/cm^2 ; however, the plastic viscosity remained essentially the same at about 4 cP to 5 cP .

The simulant composition discussed above was considered acceptable for the initial studies in the slurry test loop; however, additional work is recommended to identify other factors that may be important in determining the properties of the sludge.

Table 4. Melton Valley Storage Tank surrogate composition^a

Component	Concentration (g/L)
Soluble components	
NaOH	0.4
NaCl	4.7
NaNO ₃	185.0
KNO ₃	185.0
Na ₂ CO ₃	21.2
Insoluble components	
CaCO ₃	115.4
H ₂ SiO ₃	4.7
Mg(OH) ₂	58.3
Al(OH) ₃	25.0
Fe ₂ O ₃	7.1
Ca(OH) ₂	<u>93.2</u>
Total	700.0

^aProperties: density = 1.41 g/mL; pH = 13.4; total solids = 46.9 wt %; insoluble = 21.5 wt %.

Table 5. Viscosity measurements for Melton Valley Storage Tank waste and simulated waste mixtures

Total solids (wt %)	Insoluble ^a (wt %)	Plastic viscosity (cP)	Yield stress (dyn/cm ²)
Simulated waste^b			
46.9	21.5	4	20
46.9	21.5	5 ^c	36 ^c
62.7	37.7	14	15
66.2	41.9	55	152
70.8	48.0	130	101
Sludge samples^d			
<i>Tank W21^e</i>			
51.9	23.7	56	57
<i>Tank W26 sludge diluted 1:1 with supernatant</i>			
45.4	13.6	70	105
<i>Tank W28 sludge diluted 1:1 with supernatant</i>			
44.8	11.5	130	66

^a Calculated based on insoluble components.

^b Viscosity measurements made with a Fann viscometer at shear rates up to 1021 s⁻¹.

^c After homogenization.

^d Viscosity measurements made a low shear rate (up to 16 s⁻¹).

^e W21 is an evaporator service tank.

5.2 Simulant Development for Hanford Single-Shell Tanks

Simulated waste compositions for Hanford waste tanks have been developed by PNL for many applications²⁶; however, chemical simulants needed for the rheological studies in the slurry test loop had not been previously developed for the single-shell waste tanks. Development of simulants by PNL specifically for use in the slurry test loop was initiated under a subcontract between PNL and ORNL as a part of this project.

A program is under way to obtain samples from all of the single-shell tanks at Hanford. However, only about 18 of the 149 single-shell tanks at Hanford had been sampled at the time this study was done, and rheological characterization has been completed on only a few of the tanks that have been sampled.²⁶ The waste composition varies widely among the tanks but generally consists of a soluble phase (salt cake) and a sludge phase. Compositions for synthetic salt cake and sludge are given in Tables 6 and 7.²⁶ Typically, the single-shell tanks contain a sludge phase on the bottom, a salt-cake phase in the middle, and a liquid phase on top; however, tanks may contain essentially all salt cake, or all sludge, or mixtures of the two. The waste in many of the tanks has been allowed to dry to a consistency of a moist solid and crust with possibly considerable crystal growth. Dissolution of the soluble components and resuspension and possibly grinding of the insoluble components will be required for pipeline transport of the waste as a slurry. The concentration at which the slurry is transported will likely be dependent to a certain extent on the method used for mobilization but must be within the range that can be transported effectively.

Rheological characterization of the waste samples is being done by PNL using a Haake RV 100 viscometer. A rheogram for one of the samples that has been characterized (homogenized 241-B-110 Core 1 composite) is shown in Fig. 4. The sample (which contains 21.1 wt % undissolved solids and 41.6 % centrifuged solids) has been characterized (at 31°C) as a yield-power-law fluid described by the following equation:²⁷

$$\tau_w = 4.83 + 0.0448 (\dot{\gamma})^{0.8817} \quad (27)$$

where

$$\begin{aligned} \tau_w &= \text{shear stress, (Pa)} \\ \dot{\gamma} &= \text{shear rate (s}^{-1}\text{)}. \end{aligned}$$

For purposes of comparison with the MVST data, 110-B Core 1 composite has a yield stress of 48 dyn/cm², and if a power law coefficient of 1 is assumed, the plastic viscosity would be 45 cP.

Four simulants that exhibit rheological properties similar those of 110-B core samples were developed by PNL (recipes F3, F4, F5, and G) for possible use in the slurry test loop.²⁸ The recipes for preparing the simulants and the properties of the simulants are given in Appendix A. All of the recipes used aluminum hydroxide (gibbsite), sodium

Table 6. Composition of synthetic single-shell tank salt cake

Component	Dry weight percent
NaNO ₃	75.2
NaNO ₂	4.8
Na ₂ SO ₄	2.4
Na ₂ CO ₃	4.3
NaAlO ₂	4.3
Na ₃ PO ₄	4.6
NaOH	4.4
	100.0

Source: M. R. Elmore, E. D. Jones and N. G. Colton, *Underground Storage Tank-Integrated Demonstration; 1st Quarter FY92 Status Report for Tank Waste Simulant Development Task* TTP#RL-8529-PT, Pacific Northwest Laboratories, January 1992.

Table 7. Composition of synthetic sludge

Component	Dry weight percent
Al ₂ O ₃ , Al(OH) ₃	38
BiPO ₄	10
FeOOH, Fe ₂ O ₃ , FePO ₄	15
SiO ₂	17
Organic salts	2
Na ₂ SO ₄	2
Ce ₂ O ₃ (for U)	2
CaO	1
Cr ₂ O ₃	1
Na ₂ O, NaOH	1
La ₂ O ₃	1
Oxides, hydroxides, phosphates (<1% each of Pb, Mg, Ag, Zn, Mn, Zr, Sr) and water of hydration	10
	100

Source: M. R. Elmore, E. D. Jones and N. G. Colton, *Underground Storage Tank-Integrated Demonstration; 1st Quarter FY92 Status Report for Tank Waste Simulant Development Task* TTP#RL-8529-PT, Pacific Northwest Laboratories, January 1992.

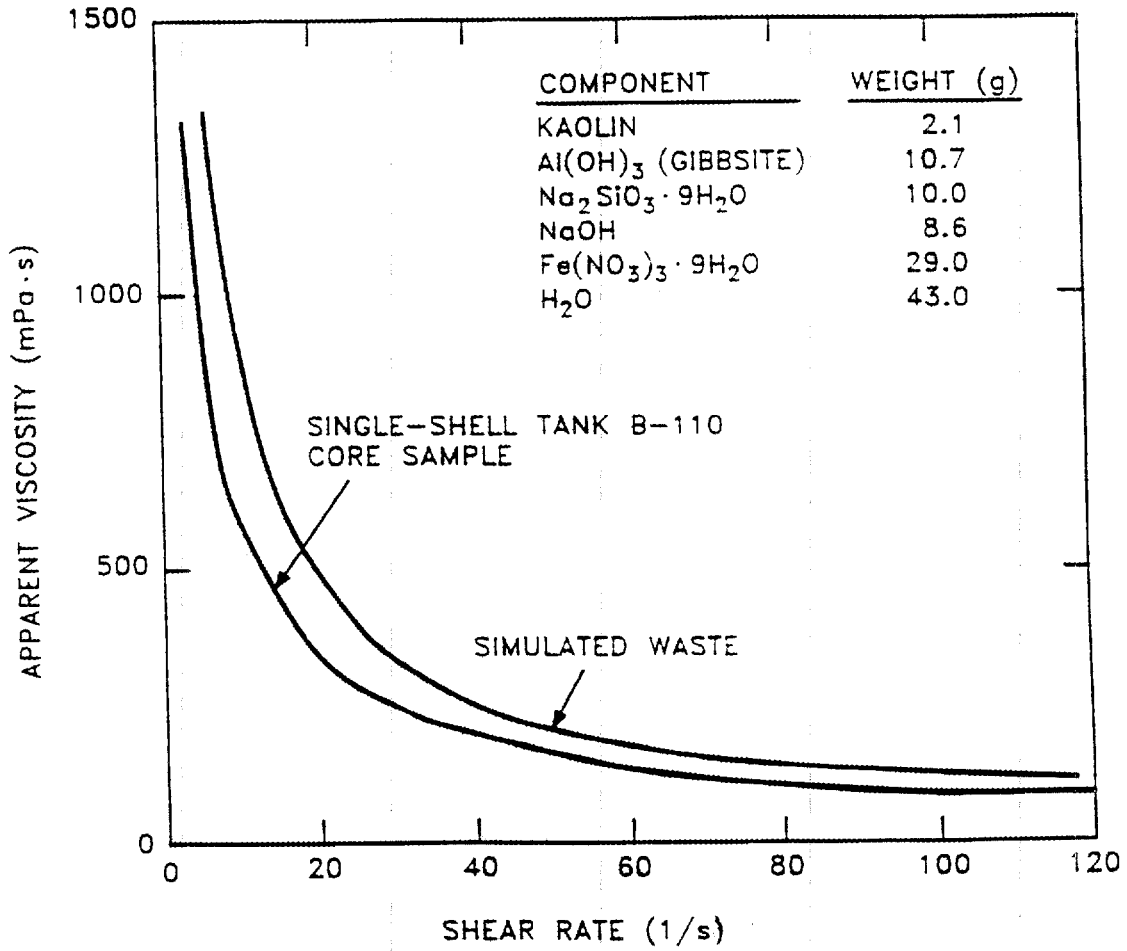


Fig. 4. Apparent viscosity vs shear rate for Hanford single-shell waste and simulant.

silicate, sodium hydroxide, ferric nitrate, and water. Recipe G included bismuth phosphate, while kaolin was used as a stand-in for bismuth phosphate in the F series recipes because of the expense and difficulty in obtaining large quantities of bismuth phosphate. The quantity of kaolin and water was varied in the F series simulants. The mean particle sizes of recipes G and F5 were 42.6 μm and 36.9 μm respectively, as determined by a Brinkmann Particle Size Analyzer. The mean particle size ranged from 10.0 μm to 33.6 μm in four segments of the 110-B core sample as shown in Appendix A. PNL suggested that recipe F5 be used as a base simulant and that the quantity of the components be varied to simulate a range of compositions. As shown in Fig. 4, the rheogram for simulant F5 is similar to that of core sample 110-B.

6. SUPERNATANT RHEOLOGY MEASUREMENTS

The major dissolved material in the supernatant liquid in the MVST and the soluble components (salt cake) in the Hanford single-shell tanks is sodium nitrate. The MVST also contains potassium nitrate and smaller amounts of carbonates, hydroxides, and chlorides. The Hanford salt cake contains sulfates, phosphates, nitrites, and aluminates. The supernatant in the MVSTs is approximately 4 *M* in sodium and potassium nitrates. Efforts are under way to reduce the volume in the tanks by evaporation, which will increase the concentration of dissolved salts in the supernatant liquid.

Rheology measurements of simulated MVST supernatant and Hanford salt cake were made using a pipeline viscometer constructed of 1/4-in. (0.180-in.-ID) tubing that was 10 ft long and by using the simulated supernatant compositions shown in Table 8. The results of calibration of the pipeline viscometer with water and sucrose solutions are shown in Fig. 5 and in Table 9. Viscosity measurements made using Brookfield and Fann viscometers are given in Table 9 for comparison with the pipeline viscometer measurements. Measurements were for MVST supernatant at sodium and potassium nitrate concentrations (combined) of 4 *M* to simulate material presently in the tanks and at a concentration of 6 *M* to simulate conditions after the supernatant has been concentrated by evaporation. The rheology of the Hanford salt cake was also measured at 4 *M* and 6 *M* sodium nitrate concentrations. For comparison, the rheology of 4 *M* sodium nitrate was measured. The rheograms shown in Fig. 6 indicate that the simulated supernatant liquids for both the MVST and the Hanford salt cake are Newtonian (as expected) at the concentrations measured. The viscosity of the MVST 4 *M* simulant of 1.4 cP is somewhat less than those measured for actual supernatants that range from 1.7 to 2.2 cP. However, this may be within the range of the accuracy of the measurements.

7. CALIBRATION OF PIPELINE VISCOMETERS IN SLURRY TEST LOOP

To ensure proper operation of the pipeline viscometers in the slurry test loop, the viscometers were dimensionally measured and calibrated with Newtonian fluids for which the viscosity was known or could be verified by the use of laboratory viscometers (Brookfield and Fann). The pressure differential instruments used for pipeline viscometer

Table 8. Composition of mixtures used for supernatant viscosity measurements

Component	4 M ^a (g/L)	6 M ^a (g/L)
Melton Valley Storage Tank supernatant surrogate		
NaOH	0.4	0.6
NaCl	4.7	7.1
NaNO ₃	185.0	278.0
KNO ₃	185.0	278.0
Na ₂ CO ₃	21.2	30.9
Ca(OH) ₂	14.1	21.1
Mg(OH) ₂	4.1	6.2
Hanford salt cake surrogate		
NaNO ₃	341.8	512.7
NaNO ₂	21.8	32.7
Na ₂ SO ₄	10.9	16.4
Na ₂ CO ₃	19.6	29.3
NaAlO ₂	19.6	29.3
Na ₃ PO ₄	20.9	31.4
NaOH	20.0	30.0

^a Nitrate molarity.

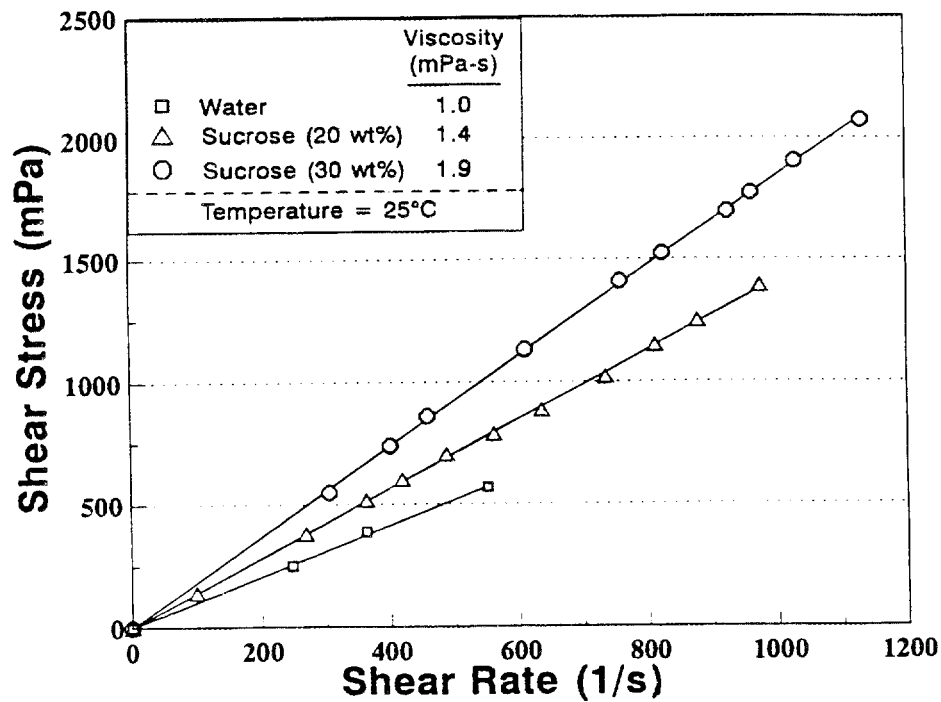


Fig. 5. Pipeline viscometer (0.18-in. ID) calibration curves.

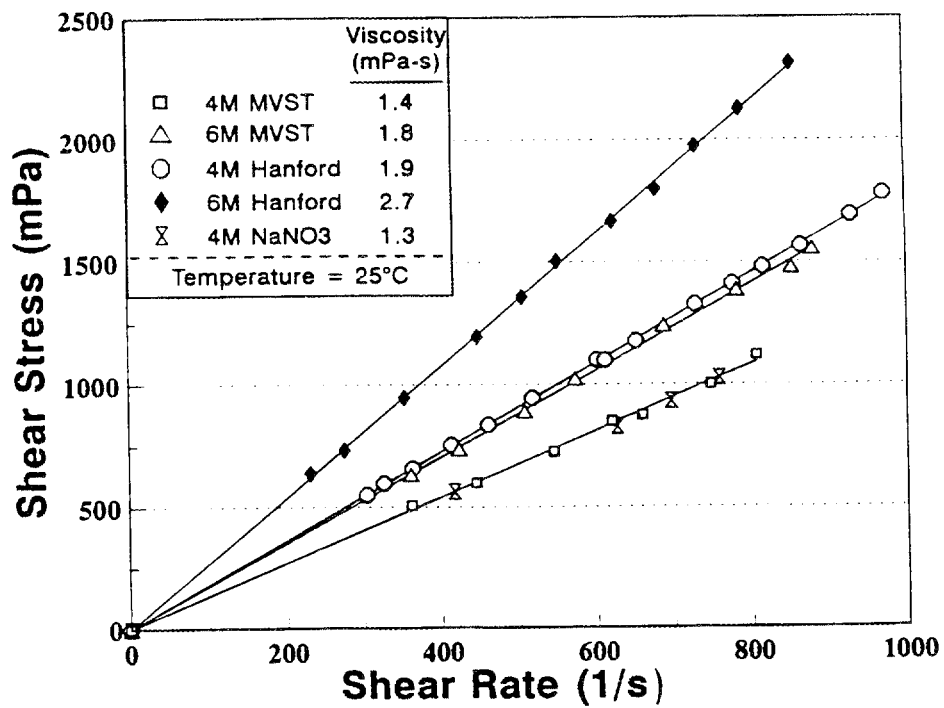


Fig. 6. Rheograms for simulated Melton Valley Storage Tank (MVST) supernate and Hanford salt cake.

Table 9. Viscosity measurements for simulated supernatant liquids and calibration fluids

Fluid	Temperature (°C)	Viscometer	
		PLV ^a (cP)	Brookfield (cP)
PLV calibration fluid			
Water	22	1.0	---
20 wt % sucrose	23	1.4	1.8
30 wt % sucrose	25	1.9	2.1
Simulated supernatant liquid			
4 M MVST	25	1.4	1.5
6 M MVST	25	1.8	1.7
4 M Hanford	27	1.9	2.0
6 M Hanford	25	2.7	---
4 M NaNO ₃	25	1.3	---

^a Pipeline viscometer (0.018-in. ID).

measurements, the level and density instruments, the weigh table and scales used to measure chemicals, and the thermocouples were periodically calibrated by ORNL Instrumentation and Control Division or Quality Division using standard Martin Marietta Energy Systems approved procedures. Calibration of the pipeline viscometers in the laminar flow region was done by operation of the slurry test loop with 50 wt % and 60 wt % sucrose in water. A shear stress vs shear rate rheogram of the results from the three viscometers (PLV-1, PLV-2, and PLV-3) is shown in Fig. 7. The data shown are the results of several sets of measurements. The results from all three of the horizontal viscometers are generally consistent. The viscosity of the 50 wt % sucrose as indicated by the slope of the line on the rheogram is 11 cP (mP · s) and that of the 60 wt % sucrose solution is 35 cP at 27°C. The pipeline viscometer value of 11 cP for the 50 wt % sucrose compares with 13 cP measured with a Brookfield viscometer. The pipeline viscometer value of 35 cP for 60 wt % solution compares with 34 cP measured with a Brookfield viscometer and a value of 34 cP from Perry's Handbook²⁹ (at 30°C).

The 50 wt % sucrose solution and tap water were used for determining the roughness factors for the viscometers in the turbulent flow region. The data for water were not used in the laminar flow region because turbulent flow began at a low flow rate (below 1 gal/min for all three viscometers) and 60 wt % sucrose solution did not become turbulent at the flow rates used in the slurry test loop. The pressure drop vs flow rate curves for water in turbulent flow for the three viscometers are shown in Fig. 8. The pressure drop vs flow rate curves for 50 wt % sucrose are shown in Fig. 9. Also shown is the pressure drop calculated by the Colebrook friction factor equation with a zero roughness. The results indicate that the pipes for all three viscometers are smooth. The region of transition from laminar to turbulent flow, as determined by the change in slope of the pressure drop curves, is also in general agreement with the calculated value. Poiseuille's equation (16) indicates that in the laminar region $\Delta p/Q$ should be constant for a Newtonian fluid. The $\Delta p/Q$ vs flow rate for calibration of pipeline viscometers with 50 wt % sucrose solution is shown in Fig. 10.

All of the viscometers frequently had small zero off-sets (approximately 1 to 2 in. of water) at the start of a run as a result of difficulties in balancing the liquid head in lines to the pressure differential instruments. The data were corrected by the zero shift present at no flow.

8. RESULTS OF RHEOLOGICAL MEASUREMENTS FOR SIMULATED WASTE

8.1 Rheological Measurements for Simulated MVST Slurry

Rheological measurements were made in the slurry test loop using simulated waste based on the composition given in Table 4. The simulant development test results given in Table 5 indicated that a higher solids concentration is required for the simulated waste

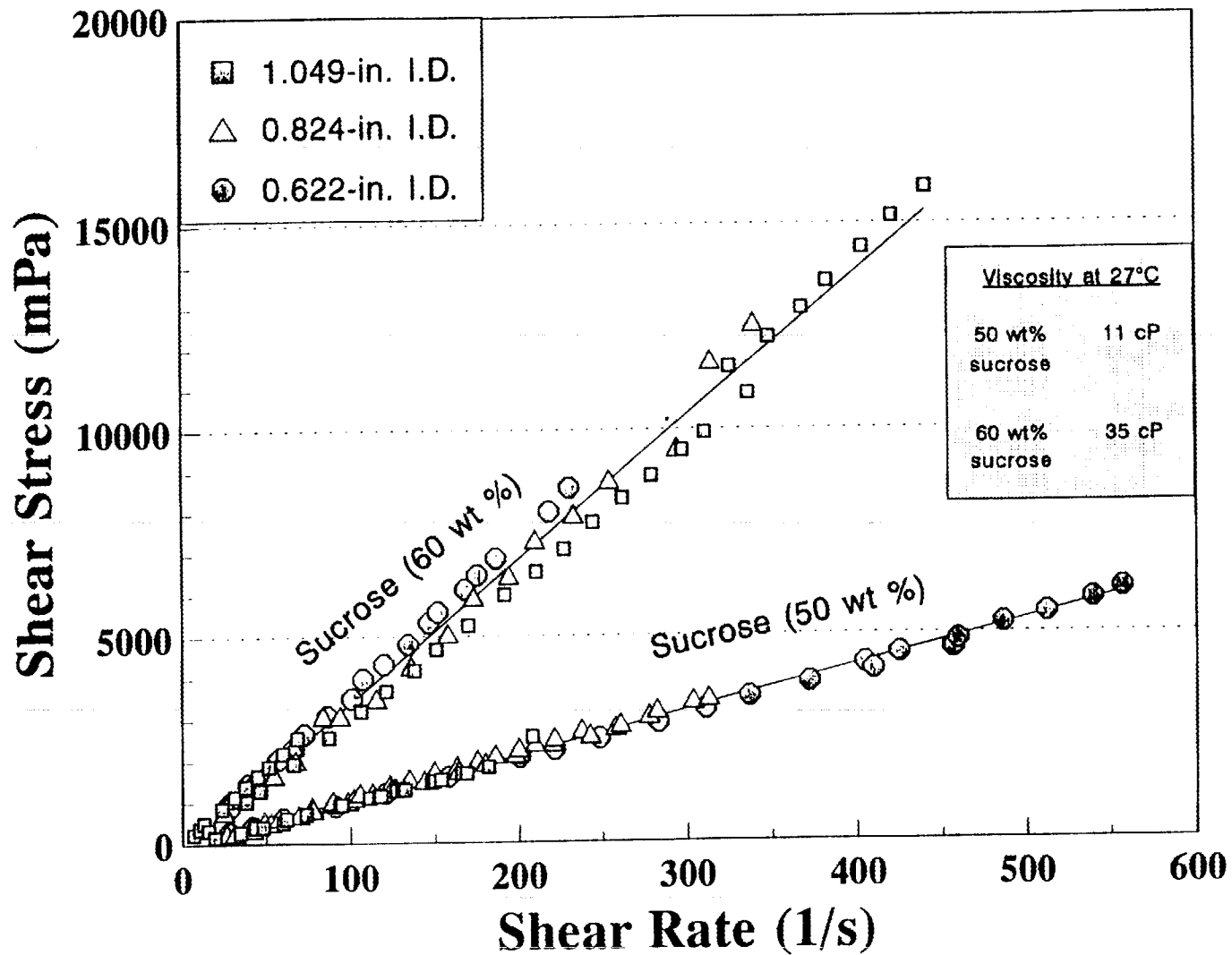
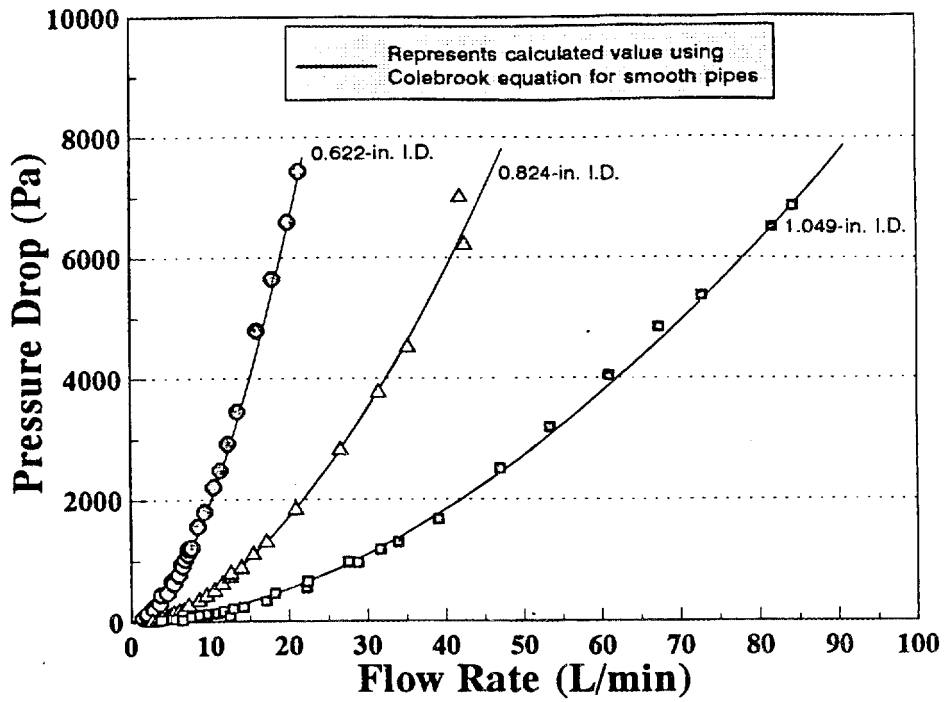
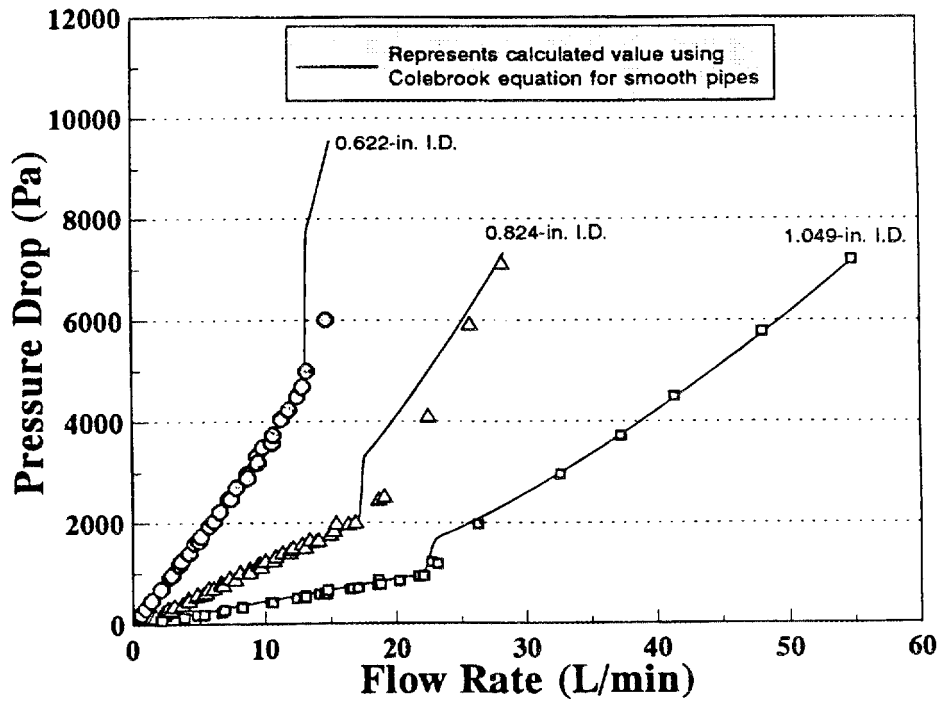


Fig. 7. Rheogram from calibration of pipeline viscometers with sucrose solutions.



Water

Figure 8. Pipeline viscometer calibration curves with water.



Sucrose 50%

Figure 9. Pipeline viscometer calibration curves with 50 wt% sucrose solution.

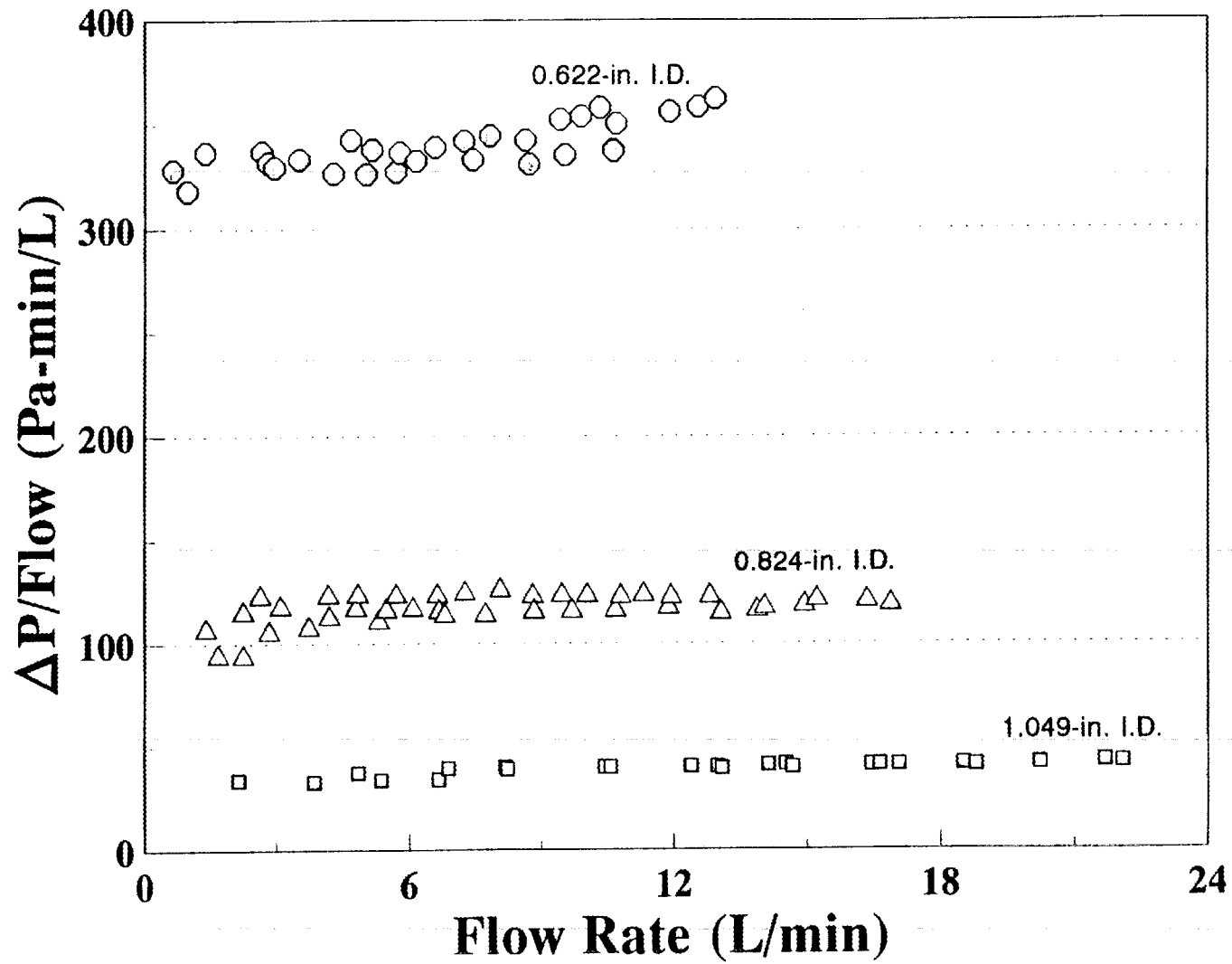


Fig. 10. Plot of $\Delta p/Q$ vs flow rate for calibration of pipeline viscometers with 50 wt % sucrose solution.

to give rheological properties similar to those of the sludge in the MVST. The first run in the test loop (MVST 1) was done with simulant containing a 65 wt % total solids (39 wt % undissolved solids). Run MVST 2 was done with the same batch of simulant but with the solids content reduced to 54 wt % total solids and 26 wt % undissolved solids by adding supernatant and removing sludge. A series of runs (MVST 3, 3A, 3B, and 3C) was made with the same simulant that had been adjusted to 57 wt % total solids (29 wt % undissolved) by adding sludge that had been previously removed. The temperature of the waste in the MVSTs varies with outside temperature from about 7°C to 21°C (45°F to 70°F). All of the tests except MVST 3A were made at room temperature (25°C). Run MVST 3A was made at 55°C to evaluate the effect of temperature on the rheology of the slurry. Also, for the final test the MVST simulated waste was passed through the IKA grinder to reduce the particle size of the slurry. Rheograms for the runs indicate that the slurry in all of the runs can be characterized as Bingham plastics. Pressure drop vs flow rate plots and rheograms for the runs are given in Appendix B.

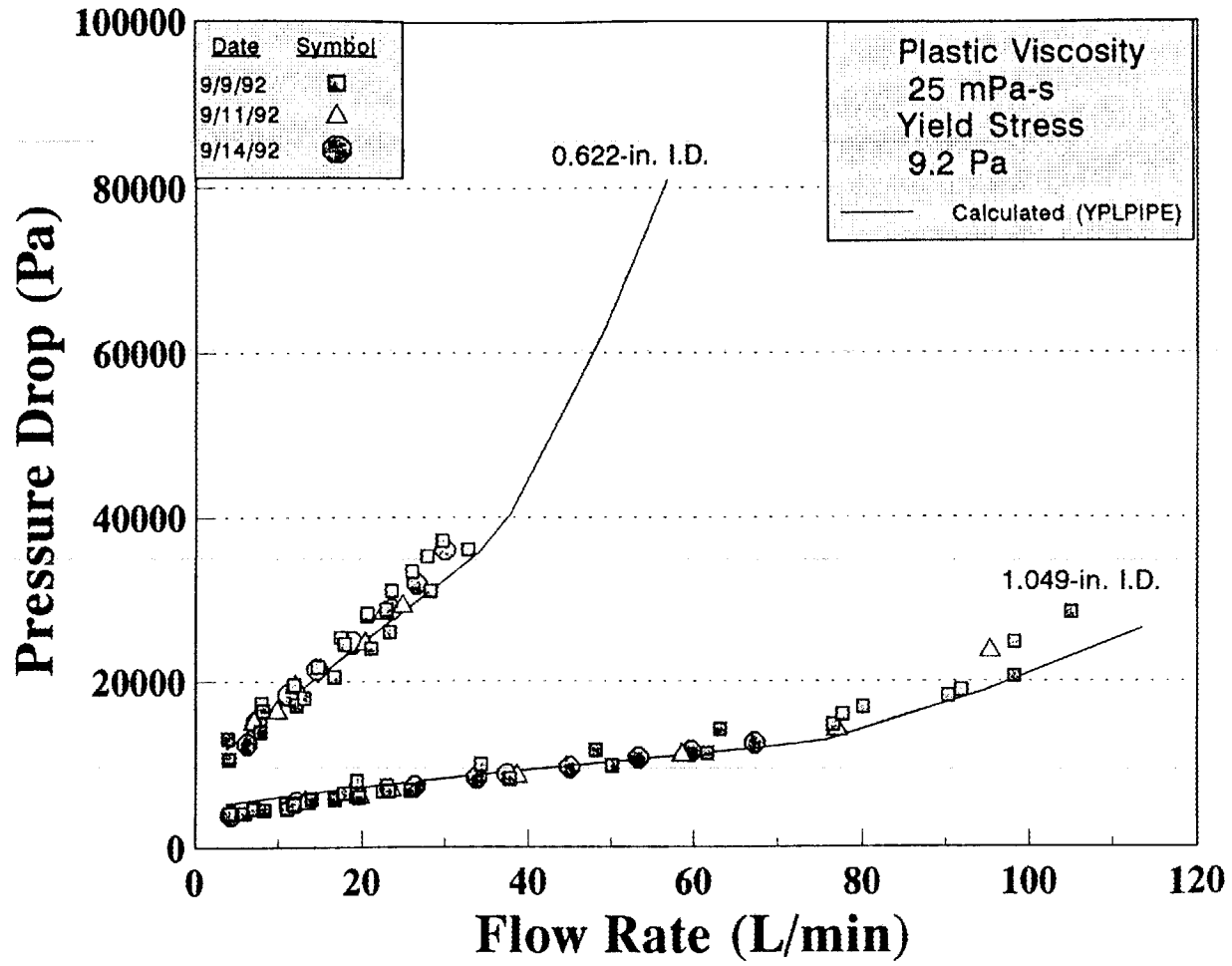
8.1.1 Run MVST 1

Initially, approximately 40 gal of simulant containing 65 wt % total solids and 39 wt % undissolved solids was prepared for use in the test loop. Runs with MVST 1 slurry were made over a 5-d period to collect data, to test the equipment and instrumentation, and to evaluate the stability of the slurry. Rheological measurements were made by circulating the slurry sequentially through the pipeline viscometers at varying flow rates while recording flow rate, temperature, density, and pressure drop across the pipeline viscometers. At the concentrations, particle size, and temperatures studied, the slurry appeared to behave as a homogeneous fluid; therefore, no minimum transport velocity measurements were made. However, the waste tanks may contain larger particles that will require higher velocities for pipeline transport. During operation, data from the instruments were recorded on the computer disk at 5-s intervals. Flow rate vs pressure drop data for the pipeline viscometers in run MVST 1 are shown in Fig. 11.

Data from the pipeline viscometers were analyzed by the Rabinowitsch-Mooney method described in Sect. 4 of this report. A logarithmic plot of the shear stress at the wall ($D\Delta p/4L$) vs the pseudo-shear rate ($8V/D$) for the MVST 1 slurry is given in Fig. 12 for the 1.049-in. ID and the 0.622-in. ID horizontal viscometers. The flow rate covered by PLV-2 (0.824-in. ID) was limited to a relatively low rate by the range of the pressure transmitter available for the first run, and the data were not included. For this analysis, the plot was considered to be a straight line. The slope of the line on the logarithmic plot (n') was determined by linear regression using the Lotus 123 computer program. Occasional outlying points (usually at low flow rates) were disregarded for a better fit of the data. The value of n' was then used to determine the shear rate by the following Rabinowitsch-Mooney relationship:

$$\dot{\gamma}_w = \frac{8V}{D} \frac{3n' + 1}{4n'} . \quad (28)$$

The shear stress vs shear rate rheogram for the data shown in Fig. 13 (average from the two viscometers) indicates that the slurry has a yield stress of 9.2 Pa (92 dyn/cm²) and



M-1

Fig. 11. Pressure drop vs flow rate for MVST 1 simulated sludge through pipeline viscometers.

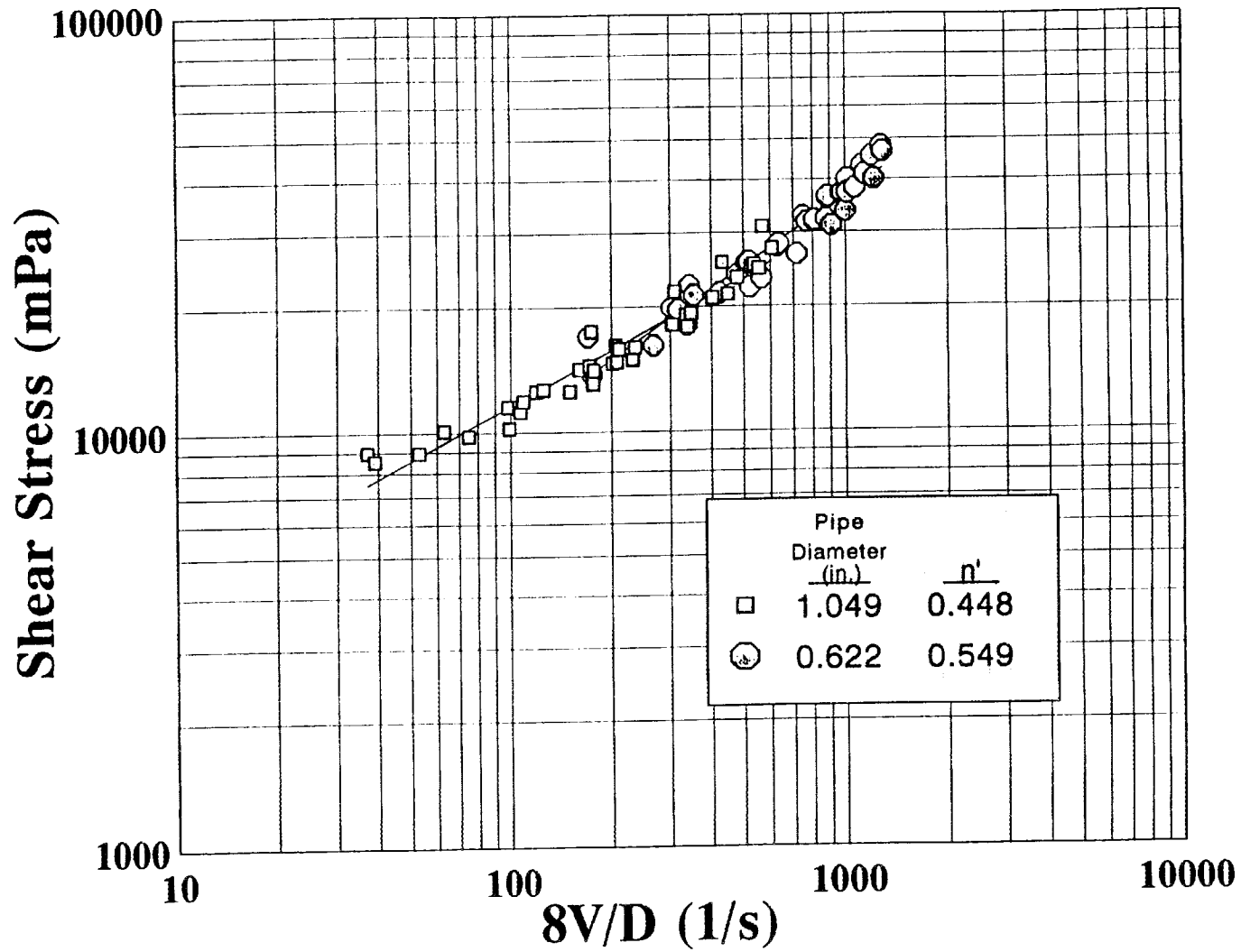
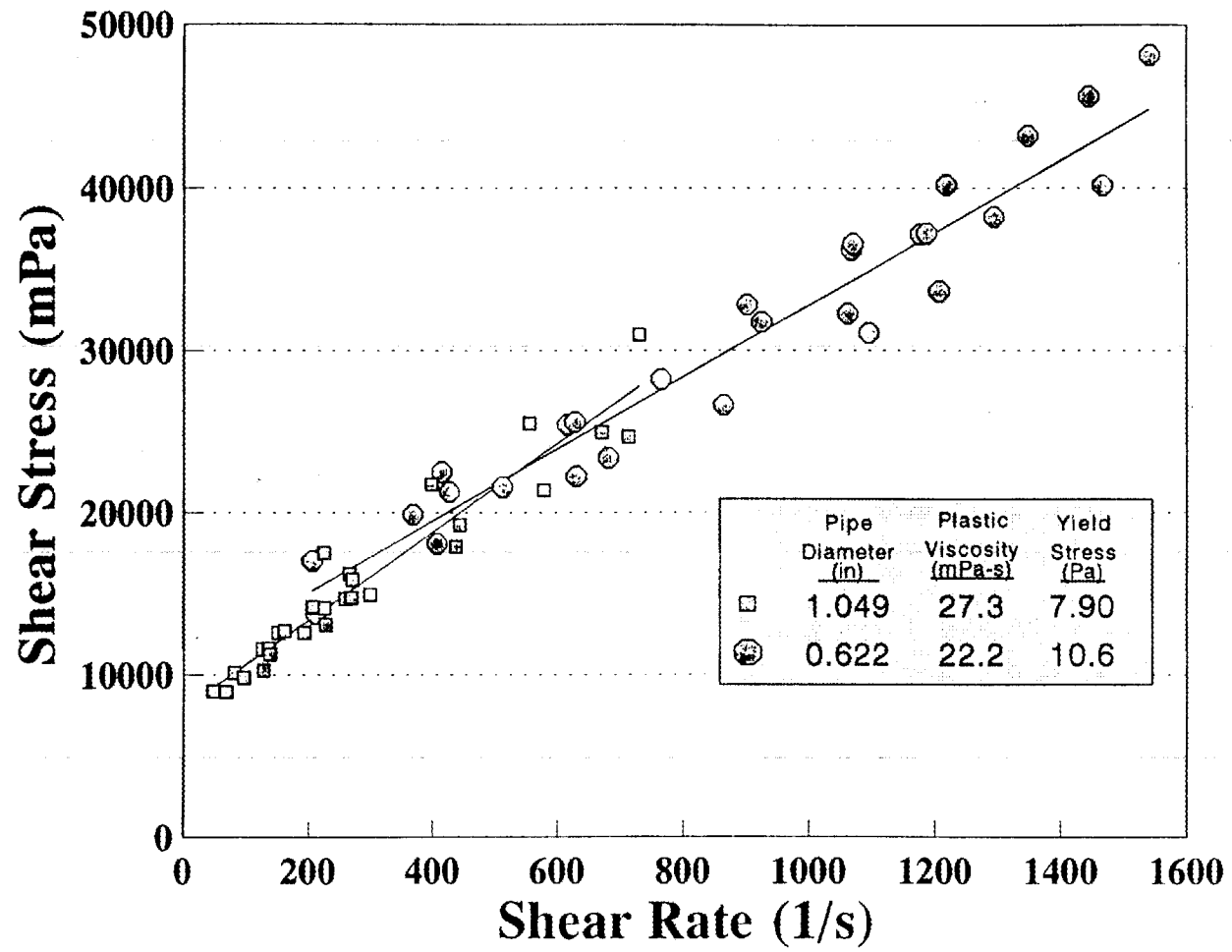


Fig. 12. Flow curve for MVST 1 slurry.



M-1

Figure 13. Rheogram for MVST-1 simulated sludge.

can be characterized as a Bingham plastic with a plastic viscosity of $25 \text{ mPa} \cdot \text{s}$ (25 cP). Although some of the settled sludge in the MVSTs has a considerably higher viscosity than that of the simulant, viscosity of the simulant is in the range that may be expected for pipeline transport of the slurry because up to three times as much supernatant as sludge may be used for mobilization (see Table 3). The pipeline transfer of the same general type of slurry from the Gunit tanks to the MVSTs was done at an apparent viscosity of about 16 cP (at a shear rate of 510 s^{-1}).²⁴ In tests with Hanford double-shell tank slurry in 1984, it was determined that the effective pipeline viscosity of the most concentrated evaporator fluid was less than 56 cP.³⁰

8.1.2 Run MVST 2

To study the effect of a slurry with lower solids content, a simulant was made from MVST 1 with a portion of the sludge removed and additional supernatant added. Run MVST 2 was made at a slurry concentration of 54 wt % total solids and 26 wt % undissolved solids. The pressure drop curves and rheograms obtained with the 0.622-in. ID and the 0.0824-in. ID viscometers are shown in Figs. B.3 and B.4 in Appendix B. The results from the 1.049-in. ID viscometer were not used because of excessive zero shift of the pressure transmitter. Rheograms for run MVST 2 indicate that the slurry can be characterized as a Bingham plastic fluid having plastic viscosity of $7.8 \text{ mPa} \cdot \text{s}$ and a yield stress of 0.9 Pa.

8.1.3 Runs MVST 3, 3A, 3B, and 3C

For the third series of runs (MVST 3, 3A, 3B, and 3C), the solids concentration in the slurry was increased to 57 wt % total solids and 29 wt % undissolved by adding concentrated sludge from run MVST 1. The density of the slurry was 1.5 g/cm^3 . Runs were made in the slurry test loop at room temperature 25°C (run MVST 3) and at 55°C (run MVST 3A). After heating the slurry (in run MVST 3A), a second run was made at 25°C (run MVST 3B) to determine if the properties of the slurry were changed by heating. After run MVST 3B, the slurry was passed through the IKA grinder 10 times to reduce the particle size (and run as MVST 3C). Pressure drop vs flow rate curves and rheograms for these runs are shown in Figs. B.5 through B.12 in Appendix B. The data on the rheograms are represented by a straight line indicating Bingham plastic behavior. The plastic viscosity and yield stress for run MVST 3 (made at 25°C) were $7.9 \text{ mPa} \cdot \text{s}$ and 1.6 Pa, respectively. Measurements of the same slurry at 55°C resulted in a reduction in plastic viscosity to $3.7 \text{ mPa} \cdot \text{s}$ and an increase in yield stress to 3.9 Pa (data from the 1-in. viscometer were not used). No significant change in the density of the slurry occurred from heating the slurry from 25 to 55°C . The plastic viscosity and yield stress of slurry after cooldown to 25°C were $8.9 \text{ mPa} \cdot \text{s}$ and 1.9 Pa, which are near the values measured before heatup, indicating that the changes in plastic viscosity and yield stress at the higher temperature were likely a result of temperature effects rather than chemical changes in the slurry.

After run MVST 3B was completed, the particle size of the slurry was reduced by making 10 passes through the three-stage IKA grinder at a nominal flow rate of 14 gal/min. Grinding of the slurry resulted in an obvious increase in settling time. Particle size measurements with a Northrup Microtrac laser scanner showed a reduction in the

maximum particle size of the slurry from 42 μm to 30 μm after two passes and a reduction to 15 μm after 10 passes through the grinder. After grinding (run MVST 3C) the plastic viscosity of the slurry remained approximately the same at 8.2 to 8.9 $\text{mPa}\cdot\text{s}$ while the yield stress increased from 1.9 Pa to 3.8 Pa. This is the same general type of response observed in the laboratory grinding test shown in Table 5. The rheological measurements for all of the runs with MVST simulated waste are summarized in Table 10.

Average values of yield stress and plastic viscosity results obtained experimentally in the laminar flow region were used to calculate the transition region from laminar to turbulent flow and the pressure drop in the turbulent flow region using the YPLPIPE computer program. The calculated pressure drop vs flow rate values for run MVST 1 give good agreement with experimental values as shown in Fig. 11. A comparison of the calculated and measured pressure drop curves for runs MVST 2 through MVST 3C is shown in Figs. B.3, B.5, B.7, B.9, and B.11 in Appendix B.

8.2 Rheological Measurements of Simulated Hanford Single-Shell Tank Waste

Rheological measurements were made in the slurry test loop using simulated Hanford single-shell tank waste prepared by recipe F5 (described in Appendix A) that has rheological properties similar to single-shell tank sample 241-B-110. The apparent viscosity of the larger batch of simulant was lower than that of material prepared in small batches; however, the viscosity was in the range expected for pipeline transport. The first series of rheological measurements (runs H-1, H-2, H-3, and H-4) was made in the slurry test loop with simulant containing approximately 42 wt % total solids and 25 wt % undissolved solids and a density of about 1.36 g/cm^3 . The second series of measurements (runs H-5, H-6, and H-7) was made with slurry from the first series of runs that had been diluted with supernatant to give a total solids content of about 42 wt %, an undissolved solids content of 23 wt %, and a density of about 1.36 g/cm^3 . Pressure drop vs flow rate measurements were made in both laminar and turbulent flow using the three horizontal pipeline viscometers.

The first measurements with concentrated slurry (run H-1) were made at ambient temperature 25°C. This was followed by measurement (run H-2) made at 50°C, which is approximately the temperature at which pipelines for Hanford single-shell waste will operate (because of the heat generated by radioactive decay). This run was followed by two additional runs (H-3 and H-4) made primarily to determine if the properties of the simulant were changed by heating or due to aging.

To obtain information about the effect of solids concentration on the rheological properties, the simulant used for runs H-1 through H-4 was diluted with supernatant. Run H-5 was made at 25°C with the diluted slurry. Run H-6 was made with the same slurry at 50°C. This was followed by run H-7 at 25°C made with the same slurry to determine if the rheological properties of the slurry were changed by heating.

Data from the pipeline viscometers were analyzed by the Rabinowitsch-Mooney relationship previously described. Typical pressure drop vs flow rate curves and rheograms

Table 10. Summary of rheological measurements with Melton Valley Storage Tank simulant in the slurry test loop

Run number	Temperature (°C)	Density (g/cm ³)	Total solids (wt %)	Undissolved solids (wt %)	Plastic viscosity	Yield stress (Pa)
MVST 1	25	1.63	65	39	25	9.2
MVST 2	25	1.49	54	26	7.8	0.9
MVST 3	25	1.54	57	29	7.9	1.6
MVST 3A	55	1.51	57	29	3.7	3.9
MVST 3B	25	1.5	57	29	8.9	1.9
MVST 3C	25	1.5	57	29	8.2	3.8

(for run H-2) are shown in Figs. 14 and 15. Pressure drop vs flow rate curves, rheograms, and a tabulation of the data for all runs are given in Figs. B.13 through B.26 in Appendix B.

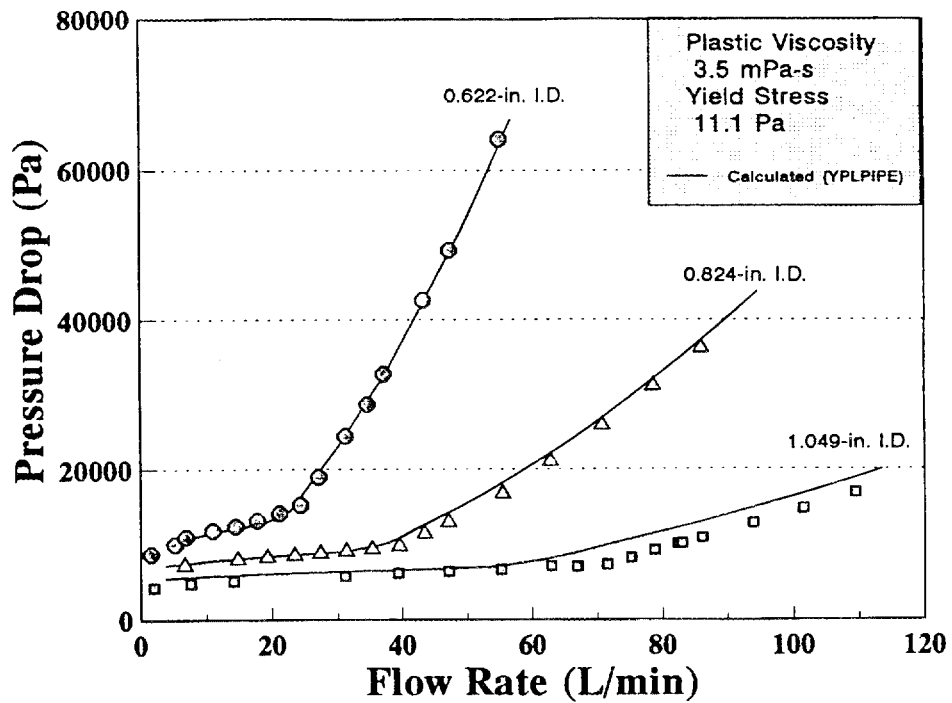
Evaluation of the shear rate vs shear stress data indicated that the slurry at all of the conditions studied could adequately be represented by a Bingham plastic model. Under the conditions studied, the slurry appeared to behave as a homogeneous slurry, and no minimum transport velocity was observed. The rheological measurements for the runs are summarized in Table 11.

As shown in Table 11, the values obtained from the different viscometers are generally consistent. The variation between viscometers is generally within the accuracy of the equipment. Wall slip was not detected within the scatter of the data after analysis using the method outlined by Brown.³¹

Average values of the plastic viscosity and yield stress obtained in laminar flow from all viscometers were used in the YPLPIPE computer program to calculate pressure drop in turbulent flow and the critical Reynolds number for transition from laminar to turbulent flow. The calculated result shown as solid lines on the pressure drop vs flow rate curves indicates good agreement with measured values for all runs. Calculated and measured friction factors and critical Reynolds numbers are shown in Fig. 16.

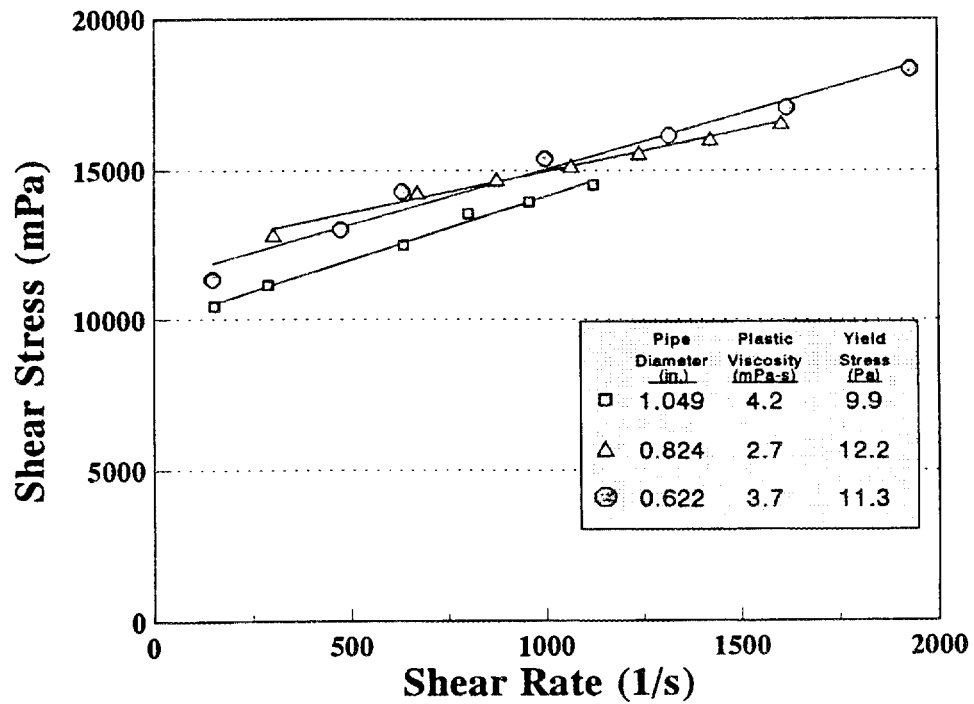
Increasing the slurry temperature from 25°C to 50°C resulted in a decrease in the plastic viscosity (average for the three viscometers ranged from about 5.4 mPa · s to 3.5 mPa · s and from 4.1 mPa · s to 2.9 mPa · s) and essentially no change in the yield stress in the two runs. Dilution of the slurry with 20 L of supernatant after run H-4 resulted in only a small change in undissolved solids (from 25 wt % to 23 wt %). The dilution resulted in a decrease in both the plastic viscosity and yield stress of the slurry, as shown in Table 11. However, the limited range of temperature and concentration covered is not sufficient to draw general conclusions on the effect of temperature and concentration.

The slurry appeared to be relatively stable over the period that the runs were made and as a result of heating the slurry to 50°C. Only small changes in properties were observed between the initial and final runs at the same concentration. Particle size analysis by a Leeds and Northrup Microtrac analyzer indicated a decrease in the size of the large particles (from 90 wt % less than 25 μm to 90 wt % less than 14.3 μm) but only a small decrease in the mean particle diameter (from 50 wt % less than 5 μm to 50 wt % less than 4.3 μm) between the initial and final runs.



H-2

Figure 14. Pressure drop versus flow rate curves for run H-2.



H-2

Figure 15. Rheograms for run H-2.

Table 11. Summary of rheological measurements with Hanford simulated waste

Run number	Temp. °C	Density (g/cm ³)	Total solids (wt %)	Plastic viscosity (mPa · s)				Yield stress (Pa)			
				PLV-1 ^a	PLV-2 ^b	PLV-3 ^c	Fann ^d	PLV-1	PLV-2	PLV-3	Fann
H-1	25	1.36	42.0	5.2	5.1	6.0	6.7	11.9	13.4	13.6	12.8
H-2	50	1.35	42.3	4.2	2.7	3.7		9.9	12.2	11.3	
H-3	25	1.36	42.4	8.1	6.0	6.1		7.2	9.8	8.7	
H-4	25	1.37	43.5	7.7	4.1	4.7		8.8	12.4	11.0	
Run H-4 slurry diluted with 20 L of supernatant											
H-5	25	1.36	41.7	3.6	3.9	4.7	4.6	5.9	8.2	8.3	6.8
H-6	50	1.36	42.7	2.1	2.1	4.4		6.6	8.4	7.9	
H-7	25	1.37	43.5	5.4	6.3	5.5		5.8	7.8	8.3	

^a1.049-in. ID by 10-ft.-long horizontal pipeline viscometer.

^b0.824-in. ID with 10-ft.-long horizontal pipeline viscometer.

^c0.622-in. ID with 10-ft.-long horizontal pipeline viscometer.

^dModel 35A viscometer.

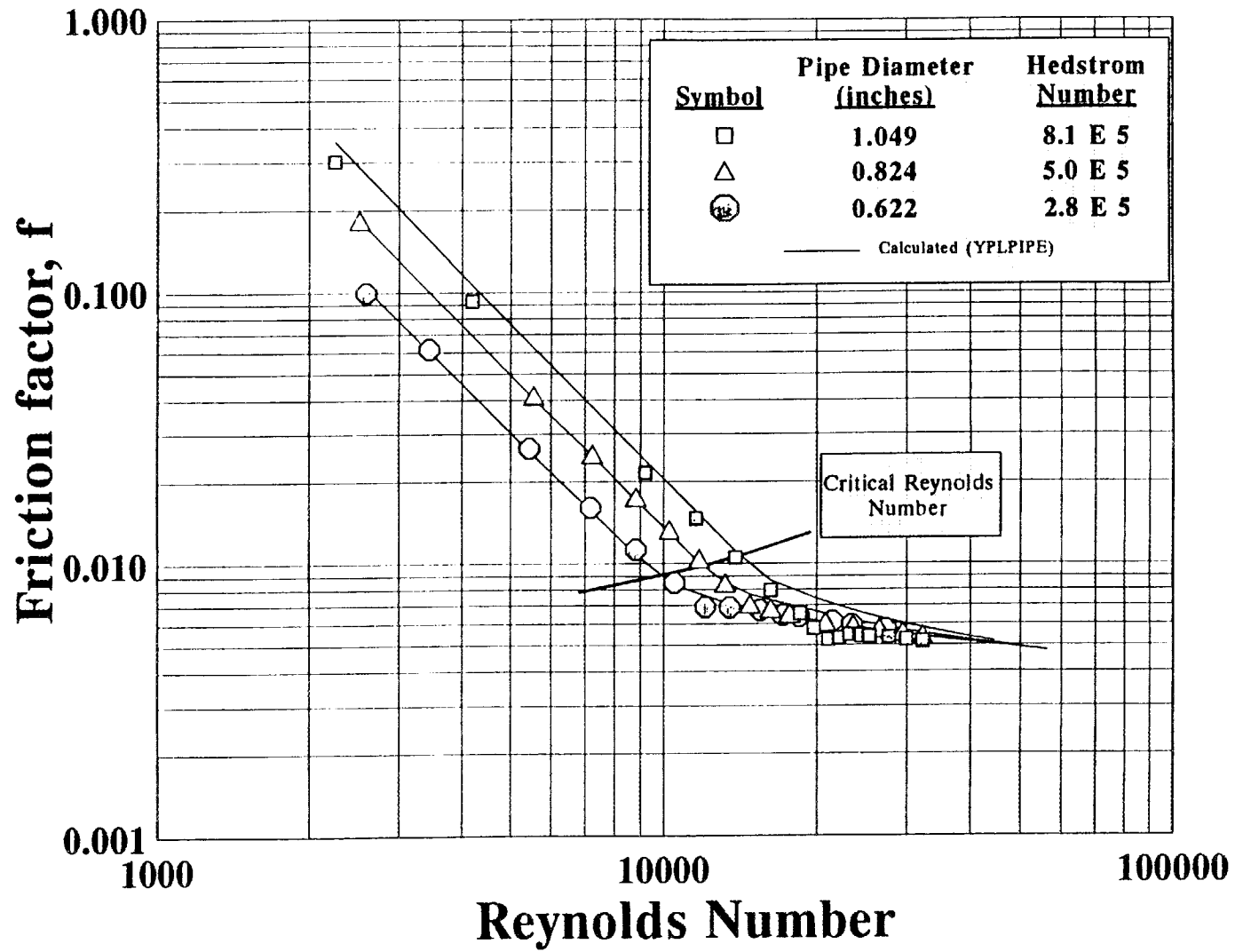


Fig. 16. Measured and calculated friction factors and critical Reynolds numbers for run H-2.

9. PERFORMANCE OF EQUIPMENT AND INSTRUMENTATION

The equipment and instrumentation in the slurry test loop performed essentially as designed. No major equipment or operational difficulties such as plugging were experienced. Measurement of the flow rate by use of the weigh table (WT-205) confirmed that the magnetic flowmeter (FE-125) gave results that were in agreement within about 5% at flow rates above 1 gal/min. Slurry density measurements by the Micromotion mass flowmeter (FE-130) were in agreement with density results by pycnometer measurement. The Moyno and centrifugal pumps performed satisfactorily. The differential pressure instrument with diaphragm seals performed satisfactorily; however, some difficulties were encountered in balancing the zero reading for measurements at low differential pressures. Also, temperature control was difficult to maintain when the loop was operated near ambient temperature because of the heat input of the pumps and the small temperature difference between the loop and the cooling water. This was corrected by the installation of a small surplus refrigerated cooling unit. The data-collection system (Genesis™ software) worked well. The data collected in files were easily transferred to floppy disks for analysis by standard spreadsheets on a personal computer.

10. SUMMARY AND CONCLUSIONS

The objective of the fluid dynamic studies was to identify or develop correlations for predicting the flow parameters needed for the design and operation of slurry pipeline transport systems for the radioactive waste slurry stored in the Hanford single-shell tanks and the ORNL MVSTs. Nonradioactive simulated waste with chemical compositions and rheological properties similar to the Hanford single-shell tank waste was developed by PNL, and simulated waste with properties similar to the MVST waste was developed at ORNL for use in the study.

A slurry test loop was constructed to study the flow properties of the simulated slurry and to evaluate equipment and instrument performance for handling slurry. Rheological properties of slurry were studied by circulating the slurry through three sizes of pipeline viscometers (constructed 1/2-, 3/4-, and 1-in. schedule 40 pipe) at rates up to 35 gal/min. Runs were made with ORNL simulated waste at concentrations of 54 wt %, 57 wt %, and 65 wt % total solids and at temperatures of 25°C and 55°C. Grinding was done before one run to study the effect of reduced particle size. Runs were made with Hanford simulated waste at 42 wt % to 43 wt % total solids and at temperatures of 25°C and 50°C. The rheology of simulated Hanford and ORNL waste supernatant solution was also measured at 4 M and 6 M nitrate concentrations.

Data from the studies in the test loop indicated that the slurry for both the ORNL and Hanford simulated slurry was non-Newtonian and could be represented by the Bingham plastic model. At the conditions studied, the yield stress of the ORNL waste ranged from 0.9 Pa to 9.2 Pa, and the plastic viscosity ranged from 4 mPa · s to

25 mPa · s. The yield stress of the Hanford simulated waste ranged from 7 Pa to 13 Pa, and the plastic viscosity ranged from 3 mPa · s to 7 mPa · s. The waste behaved as homogeneous slurry under all of the conditions studied. The supernatant solution (at concentrations of 4 M and 6 M nitrate) was Newtonian as expected, with viscosities ranging from 1.3 mPa · s to 2.7 mPa · s.

Mathematical models and commercially available computer programs for calculating pressure drop, critical Reynolds numbers, and minimum transport velocities were identified and described by a slurry transport consultant (Richard W. Hanks Associates). Measured values of pressure drop and critical Reynolds numbers showed good agreement with values calculated using a commercially available computer program (YPLPIPE).

Based on the limited range of variables studied, existing non-Newtonian models and correlations for predicting pressure drop and the region of transition from laminar to turbulent flow appear to be good for modeling the type of waste stored at Hanford and ORNL; however, additional studies over a wider range of compositions, particle sizes, and concentrations are recommended. Additional work is needed to develop computer programs for analysis of data from pipeline viscometers and to modify existing programs for calculating deposition velocity for non-Newtonian fluids and fluids that contain particles of more than one density. Although the slurries used in these tests behaved as homogeneous slurries and no information on minimum transport velocity was obtained, the actual waste may contain larger particles that will have minimum transport velocities.

The use of chemical surrogates appears to be a promising way to simulate the rheological properties of the actual waste. However, only a limited amount of rheological data is currently available for the actual waste for comparison. The rheological properties of material prepared in larger batches did not always duplicate that prepared on a small scale. Additional work is recommended on chemical simulant development to identify the variables that are important in determining rheological properties over a wide range of compositions. The equipment and instruments used in the slurry test loop operated satisfactorily. Additional testing with larger pipe sizes and longer runs is recommended to evaluate flow correlations for scale-up.

ACKNOWLEDGEMENTS

The authors wish to express their appreciation to summer participants Seann M. Reed and Christopher E. Lockwood for their assistance in simulant development, operation of the slurry test loop, and computer programming for data analysis. The authors also wish to express their appreciation to M. D. Boring, J. J. Perona, and J. L. Snyder for their helpful comments in reviewing the report and to Roger L. Gilchrist, Manager, Underground Storage Tank-Integrated Demonstration for his leadership and support of the project.

REFERENCES

1. T. D. Hylton, Personal Communication, August 31, 1992.
2. F. R. Ruppel, Personal Communication, September 1992.
3. A. H. P. Skelland, *Non-Newtonian Flow and Heat Transfer*, J. Wiley, New York, 1967.
4. B. Rabinowitsch, *Zeit. Physik. Chem.* A145 (1) (1929).
5. M. Mooney, *J. Rheol.* 2 (210) (1930).
6. V. L. Streeter, *Fluid Mechanics, 5th Ed.*, McGraw-Hill, New York, 1971, p. 292.
7. R. W. Hanks and D. G. Sloan, *Proc. 6th Int'l Tech. Conf. on Slurry Transp.*, Las Vegas, March 26-28, 1981, pp. 107-120, Slurry Transport Association, Washington, D.C.
8. E. J. Wasp, et al., *Pipeline News*, July 1963, p. 20.
9. R. W. Hanks, *AIChE Journal* 9, 306-309 (1963).
10. R. W. Hanks and B. H. Dadia, *AIChE Journal* 17, 554-557 (1971).
11. D. G. Thomas, *AIChE Journal* 6, 631-639 (1960).
12. R. W. Hanks, "Principles of Slurry Pipeline Hydraulics," in *Encyclopedia of Fluid Mechanics*, Vol. V (Slurry Flow Technology), N. P. Cheremisinoff, Ed., Gulf Publishing Co, Houston, 1986, pp. 213-276.
13. A. B. Metzner and J. C. Reed, *AIChE Journal* 1, 434 (1955).
14. R. W. Hanks, *Proc. 4th Int'l Tech. Conf. on Slurry Transp.*, Las Vegas, March 28-30, 1979, pp. 91-101, Slurry Transport Association, Washington, D.C.
15. N. W. Ryan and M. M. Johnson, *AIChE Journal* 5, 433 (1959).
16. R. W. Hanks, *AIChE Journal* 9, 45-48 (1963).
17. R. W. Hanks and B. L. Ricks, *J. Hydraulics*, 9, 39-44 (1975).
18. R. W. Hanks, *Proc. 5th Int'l Conf. on Hydraulic Transp. of Solids in Pipes*, Hannover, Germany, May 8-11, 1978, Pub. by BHRA Fluid Engineering, Cranfield, U.K., pp. C2-C25 (1978).
19. R. Durand, *Proc. Minnesota Int'l Hydraulics Convention*, September 1-4, 1953, p. 89, University of Minnesota.

20. R. W. Hanks, "Development of Slurry Viscometry Data Analysis Procedure," Richard W. Hanks Associates Consulting Report to Battelle PNL, Contract No. B-R6822-A-U, April 22, 1987.
21. M. B. Sears, J. L. Botts, R. N. Ceo, J. J. Ferrada, W. H. Griest, J. M. Keller, and R. L. Schenley, *Sampling and Analysis of Radioactive Liquid and Waste Sludges in the Melton Valley and Evaporator Facility Storage Tanks at ORNL*, ORNL/TM-11652, Oak Ridge National Laboratory, Oak Ridge, Tenn., September 1990.
22. R. N. Ceo, M. B. Sears and J. T. Shor, *Physical Characterization of Radioactive Waste Tank Sludges*, ORNL/TM-11653, Oak Ridge National Laboratory, Oak Ridge, Tenn., October 1990.
23. D. W. Turner, J. B. Berry, and J. W. Moore, "An Overview of the ORNL Waste Handling and Packaging Plant," *Waste Management '90*, February 1990.
24. H. O. Weeren, *Sluicing Operations at Gunite Waste Storage Tanks*, FW-84142, September, 1984
25. A. J. Mattus, Oak Ridge National Laboratory, Personal Communication to J. B. Berry, August 13, 1990.
26. M. R. Elmore, E. O. Jones, and N. G. Colton, *Underground Storage Tank-Integrated Demonstration, 1st-Quarter FY92 Status Report for Tank Waste Simulant Development Task*, TTP#RL-8529-PT, Pacific Northwest Laboratories, January 1992.
27. Personal communication from E.O. Jones to J.B. Berry, Oak Ridge National Laboratory, October 21, 1991.
28. N. G. Colton and M. R. Elmore, Pacific Northwest Laboratories, Letter Report to E. L. Youngblood, Oak Ridge National Laboratory, October 15, 1992.
29. *Chemical Engineers' Handbook*, Fourth Edition, John H. Perry Ed., McGraw Hill Book Company, p. 3-201.
30. Personal communication with G. J. Rust and D. C. Bjorklund, Westinghouse Hanford Co., February 1992.
31. *Slurry Handling Design of Solid-Liquid Systems*, N. P. Brown and N. I. Heywood, Eds., Elsevier Science Publishers LTD, 1991, pp. 71-73.

APPENDIX A

Development of Simulants for Hanford Single-Shell Waste Tanks

Report prepared by

Battelle Pacific Northwest Laboratories

P. O. Box 999

Richland, Washington 99352

under

Subcontract No. 10XSL613V

for

OAK RIDGE NATIONAL LABORATORY

Oak Ridge, Tenn.

Managed by

Martin Marietta Energy Systems, Inc.



Pacific Northwest Laboratories
P.O. Box 999
Richland, Washington U.S.A. 99352
Telephone (509)376-4252

October 15, 1992

Mr. Lloyd Youngblood
Oak Ridge National
Laboratory MSIN 6330
P.O. Box 2008
Oak Ridge, TN 37831-6330

Dear Mr. Youngblood:

The objective for Development of Simulants for Hanford Single-shell Waste Tanks was to develop non-hazardous simulants that have the following characteristics: (a) have apparent viscosity versus shear rate characteristics similar to those measured for actual waste samples, (b) are based on formulations that can be extrapolated to simulate the rheological properties of the range of waste compositions contained in the single-shell tanks, and (c) are suitable for use in a slurry test loop (approximately 50 gallon capacity) to study the pipeline transport of waste slurries.

With the above-stated objectives in mind, recipes for Hanford single-shell tank (SST) physical simulants were derived, and simulants were prepared. The rheological characteristics of the simulants were compared with Hanford SST 241-B-110, and the recipes were adjusted until the simulant displayed apparent viscosity versus shear rate characteristics similar to the waste sample.

Four recipes for simulants that exhibited similar rheological characteristics to 241-B-110 are outlined in Attachment 1. The estimated compositions of the simulants, along with the composition of 241-B-110 and an average SST sludge waste (based on the analyses of 18 SSTs), are listed in Attachment 2.1. Note that recipe "G" contains the bulk constituents found in sludge while recipes "F-3" through "F-5" contain the bulk constituents with the exception of bismuth and phosphate. Kaolin was substituted for bismuth phosphate in the "F" series simulants due to the high cost of the chemical (\$150/100g). For your information, the range of major constituents found in the 18 analyzed SST wastes is also provided in Attachment 3.

The simulants are prepared from five starting materials plus water, and scale-up of the recipe to prepare 50 gallons of simulated sludge should be fairly straight forward. Two points to note in the preparation of the simulant: (1) Good dissolution and mixing should be maintained to keep particle sizes as small as possible, and (2) sodium hydroxide and the iron nitrate solution should be added to the mixture slowly, as heat is generated with the additions. The chemical constituents in the sludge are not federally regulated to the best of my knowledge (sodium nitrate is <40 wt% wet sludge, and at this concentration is not considered an oxidizer); however, the pH of the sludge is ≥ 12.5 , and the simulant is thereby considered hazardous due to its corrosive nature.

Mr. Lloyd Youngblood
October 15, 1992
Page 2

Apparent viscosity versus shear rheograms for "F"-series and "G" simulants (~40 wt% solid) are contained in Attachments 2.2 and 2.3, and may be compared with the rheogram for a composite of waste from 241-B-110 in Attachment 2.4. Rheological characteristics of the simulants are similar to the actual waste sample: The shape of the rheograms imply the simulants and waste sample are yield-pseudoplastic materials, and simulant data lie within the same apparent viscosity versus shear rate region as the waste sample data. The "F"-series simulants were also diluted, and rheograms for the diluted samples are contained in Attachments 2.5 through 2.7. The increased noise in these rheograms is due to the fact some of the data from the diluted samples lie at the very low end of the working range for the viscometer used for these analyses.

Particle size volume density graphs for the simulants are provided in Attachments 2.8 through 2.11 and may be compared with the particle size graphs for various segments from Core 2, 241-B-110 waste in Attachments 2.12 through 2.15. (No particle size analysis was performed on a composite sample). Note particle size distribution in the simulants is similar to particle size distribution in Segment 1 (Attachment 2.12), which is the top layer of waste in the tank; however, average particle size in subsequent waste segments decreases as sampling depth increases. Note as well that simulant particles in the 2 to 10 μm range are mainly due to kaolin.

The recipe for simulant "F-5" could be used as a base simulant, and one component could be varied to see what effect that component might have on the rheological behavior of the simulant. For example, a 10-fold increase in aluminum hydroxide would yield a simulant with the following dry weight percent composition:

25.0% Gibbsite
1.5% Kaolin
0.7% Si
2.9% Fe
13.0% NaNO_3

However, the rheological characteristics of the simulant would probably be controlled by the particle size of the gibbsite, and the particle size would not necessarily be representative of particle sizes of aluminum hydroxides formed and kept in solution in the tanks.

Viscosity versus shear rate behavior in the simulant could be varied further by:

1. Increasing kaolin and water by 4.2 g and 5 g respectively (or multiples thereof) in simulant recipe "F-3". Addition of the kaolin should reduce the average particle size, while the increase in water should keep the simulant at 40 wt% solids.

Mr. Lloyd Youngblood
October 15, 1992
Page 3

2. Increasing the percent solids concentration to >40 wt% solids.
Based on the analyses of 18 SST wastes, solids in sludge generally
range from 40 to 60 wt%.

Within reason, we believe simulants prepared from the recipes provided, along with the above-mentioned variations, are representative of a range of existing Hanford tank wastes. However, because of very limited rheological characterization data for tank wastes, we are unable to quantify the extent of this range. Additionally, we would like to point out that since these simulants were developed to model the properties of wastes as they exist in the tanks, the component concentrations and rheological behavior do not necessarily reflect the properties of "retrieved" waste that would then be transported through pipelines. The method of retrieval (especially the amount of dilution necessary) will undoubtedly impact the waste composition and behavior. This uncertainty would need to be factored into your testing.

We have appreciated the opportunity to work with you on this effort, and we hope our input will be helpful to your research. If we may be of further assistance, please contact us.

Very truly yours,


N. G. Colton
Research Scientist


M. R. Elmore
Project Manager

Attachments: 17

SST PHYSICAL SIMULANT RECIPES

SST Simulant F-3

To 30 mL H₂O add in the following order while stirring:

8.38 g Kaolin
10.65 g Gibbsite (Al(OH)₃)
10.01 g Na₂SiO₃·9 H₂O
8.60 g NaOH

Dissolve 28.96 g Fe(NO₃)₃·9 H₂O in 20 mL H₂O and add to above.

SST Simulant F-4

To 25 mL H₂O add in the following order while stirring:

4.19 g Kaolin
10.65 g Gibbsite (Al(OH)₃)
10.01 g Na₂SiO₃·9 H₂O
8.60 g NaOH

Dissolve 28.96 g Fe(NO₃)₃·9 H₂O in 20 mL H₂O and add to above.

SST Simulant F-5

To 22.5 mL H₂O add in the following order while stirring:

2.10 g Kaolin
10.65 g Gibbsite (Al(OH)₃)
10.01 g Na₂SiO₃·9 H₂O
8.60 g NaOH

Dissolve 28.96 g Fe(NO₃)₃·9 H₂O in 20 mL H₂O and add to above.

SST Simulant G

To ~40¹ mL H₂O add in the following order while stirring:

2.80 g BiPO₄
10.65 g Gibbsite (Al(OH)₃)
10.01 g Na₂SiO₃·9 H₂O
8.60 g NaOH
28.96 g Fe(NO₃)₃·9 H₂O

¹ Amount of water approximated; further work on simulant discontinued due to high price of BiPO₄ (\$150/100g).

Attachment 2.1: Estimated Compositions and Physical Properties (Simulants and SST 241-B-110)

Estimated Compositions (dry weight %)

<u>F-3</u>	<u>F-4</u>	<u>F-5</u>	<u>G</u>	<u>B-110 SST</u>	<u>"Avg" SST</u>
16.0% Kaolin ¹	9.5% Kaolin ¹	5.0% Kaolin ¹	6.1% BiPO ₄	6.3% BiPO ₄	6.2% BiPO ₄
6.7% Al ²	7.9% Al ²	8.3% Al ²	7.5% Al	0.1% Al	6.8% Al
1.9% Si ³	2.3% Si ³	2.4% Si ³	2.0% Si	2.3% Si	5.4% Si
7.7% Fe	9.1% Fe	9.6% Fe	8.7% Fe	4.8% Fe	4.9% Fe
35.0% NaNO ₃	42.0% NaNO ₃	44.0% NaNO ₃	40.0% NaNO ₃	54.0% NaNO ₃	45.0% Soluble Salts ⁴

¹Kaolin substituted for BiPO₄ due to high cost of BiPO₄ (\$150/100 g)

²Al from kaolin not included⁴ in %

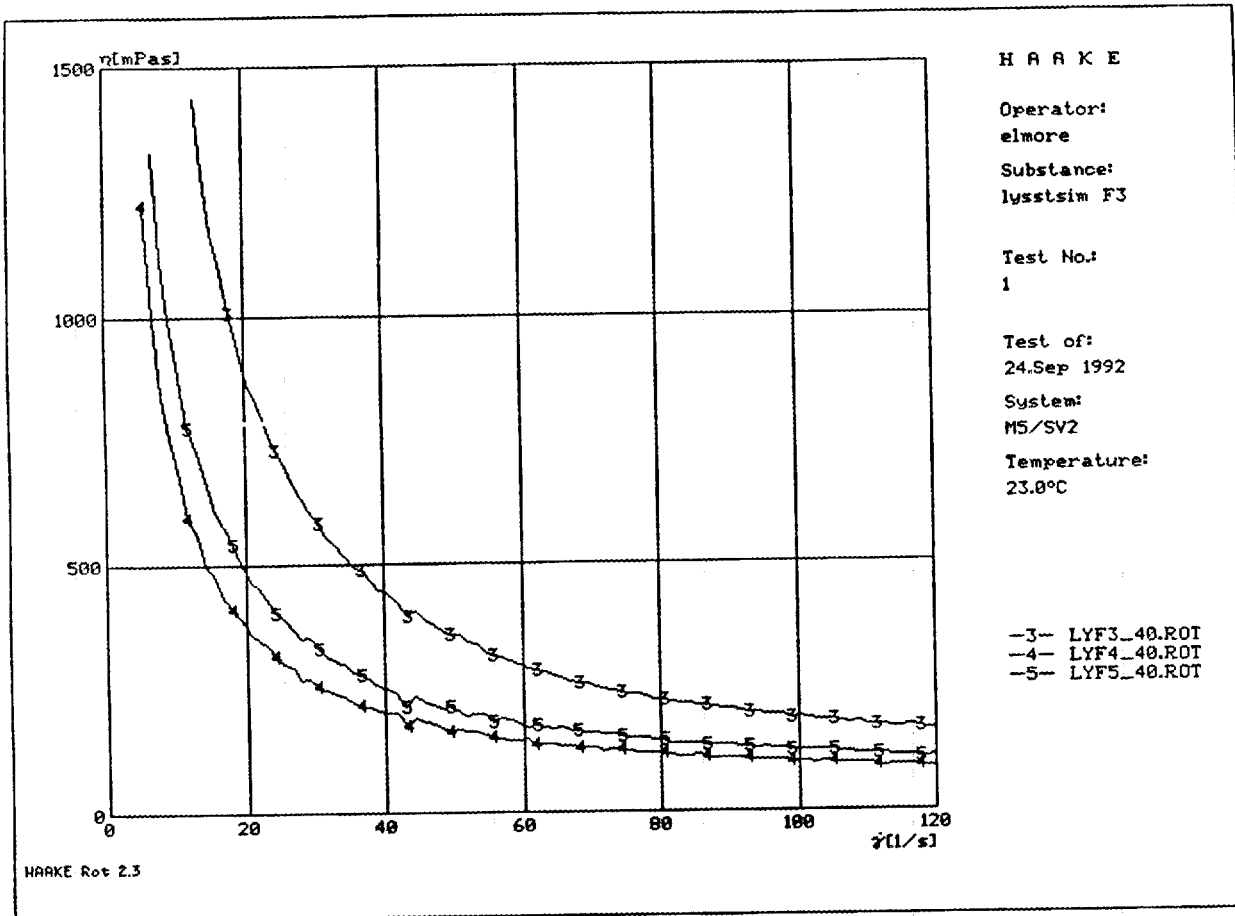
³Si from kaolin not included in %

⁴Includes sodium nitrate, nitrite, sulfate, carbonate, phosphate; note simulant samples contain only sodium nitrate for simplicity.

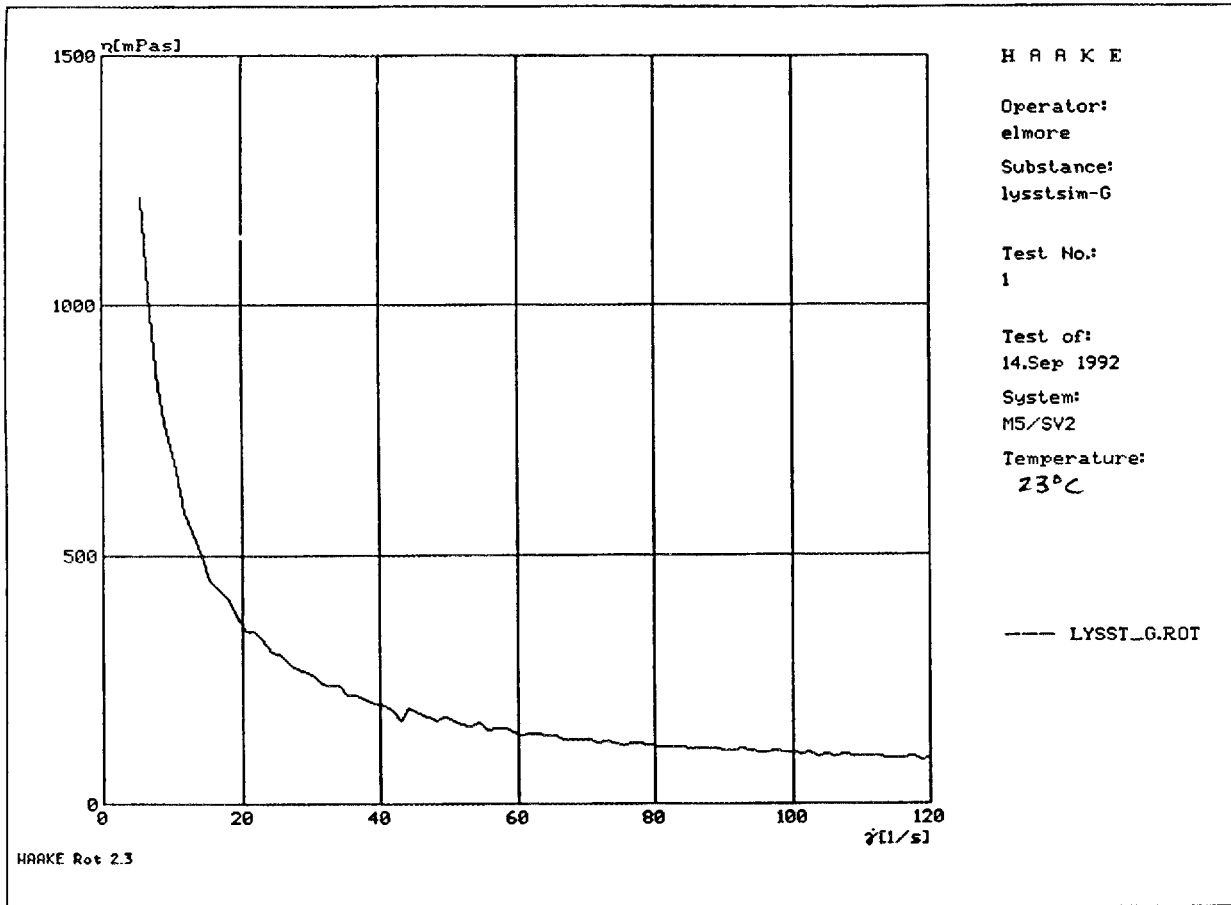
58

Physical Properties

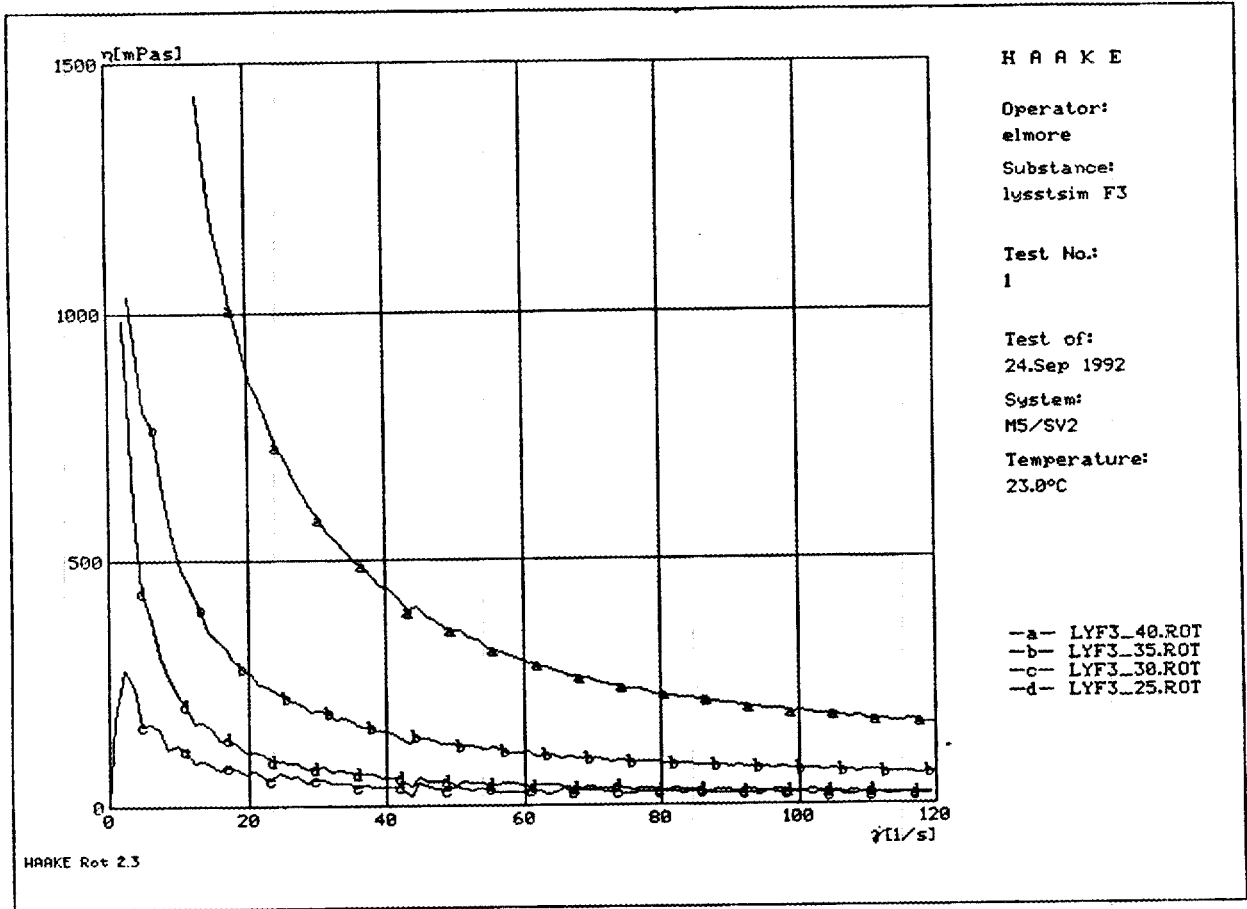
	<u>F-3</u>	<u>F-4</u>	<u>F-5</u>	<u>G</u>	<u>B-110 SST</u>
Centrifuged Solids	~65 vol%	~60 vol%	~60 vol%	~65 vol%	44 vol%
Dried Solids	40 wt%	39 wt%	39 wt%	42 wt%	40 wt%
Density	1.4 g/mL	1.3 g/mL	1.3 g/mL	1.4 g/mL	1.33 g/mL
Viscosity vs. Shear	-----Refer Attachments 2.2 - 2.7-----				
Particle Size	-----Refer Attachments 2.8 - 2.15-----				



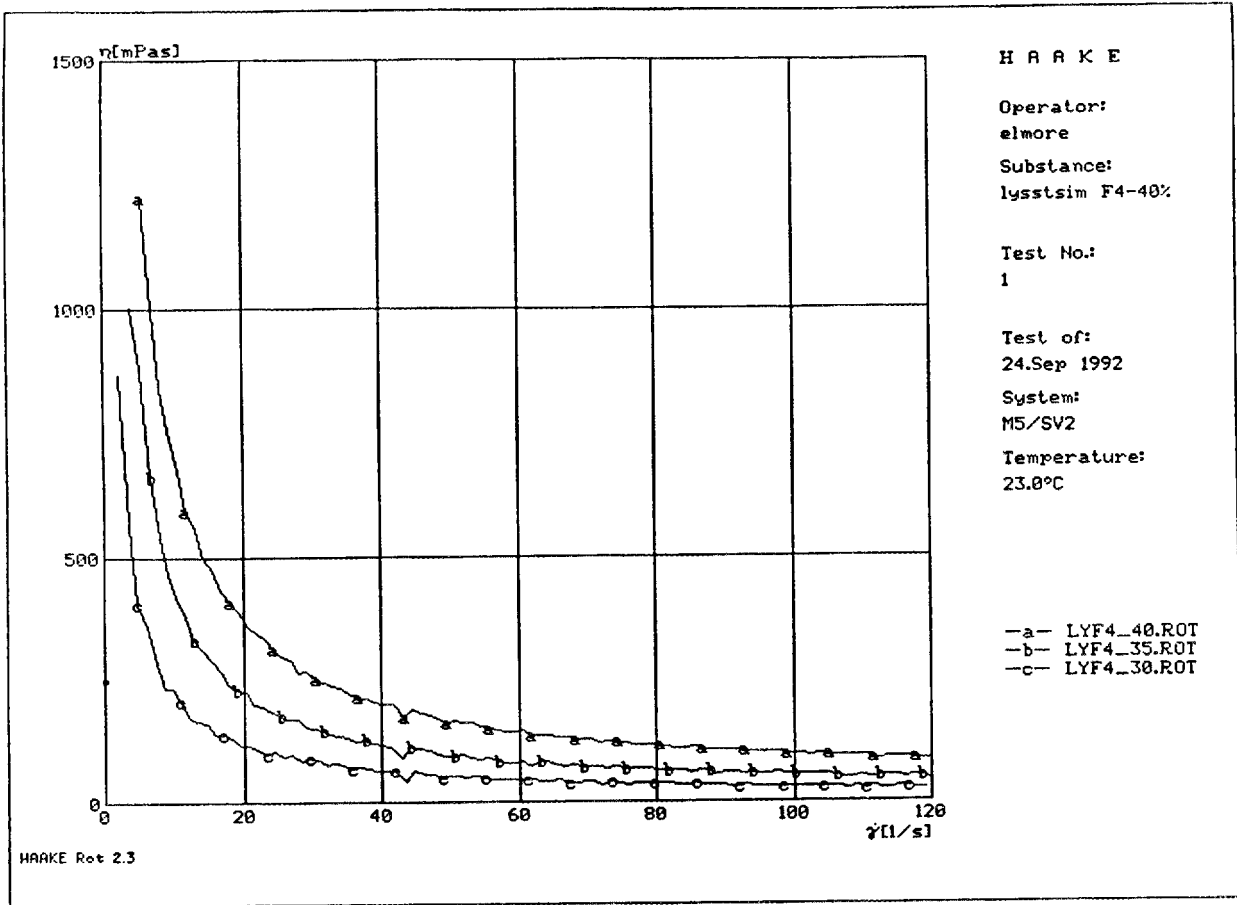
Attachment 2.2: Apparent Viscosity vs. Shear Rate
 Simulants F-3, F-4, and F-5 (at 40 wt% solids)



Attachment 2.3: Apparent Viscosity vs. Shear Rate
Simulant G (40 wt% solids)

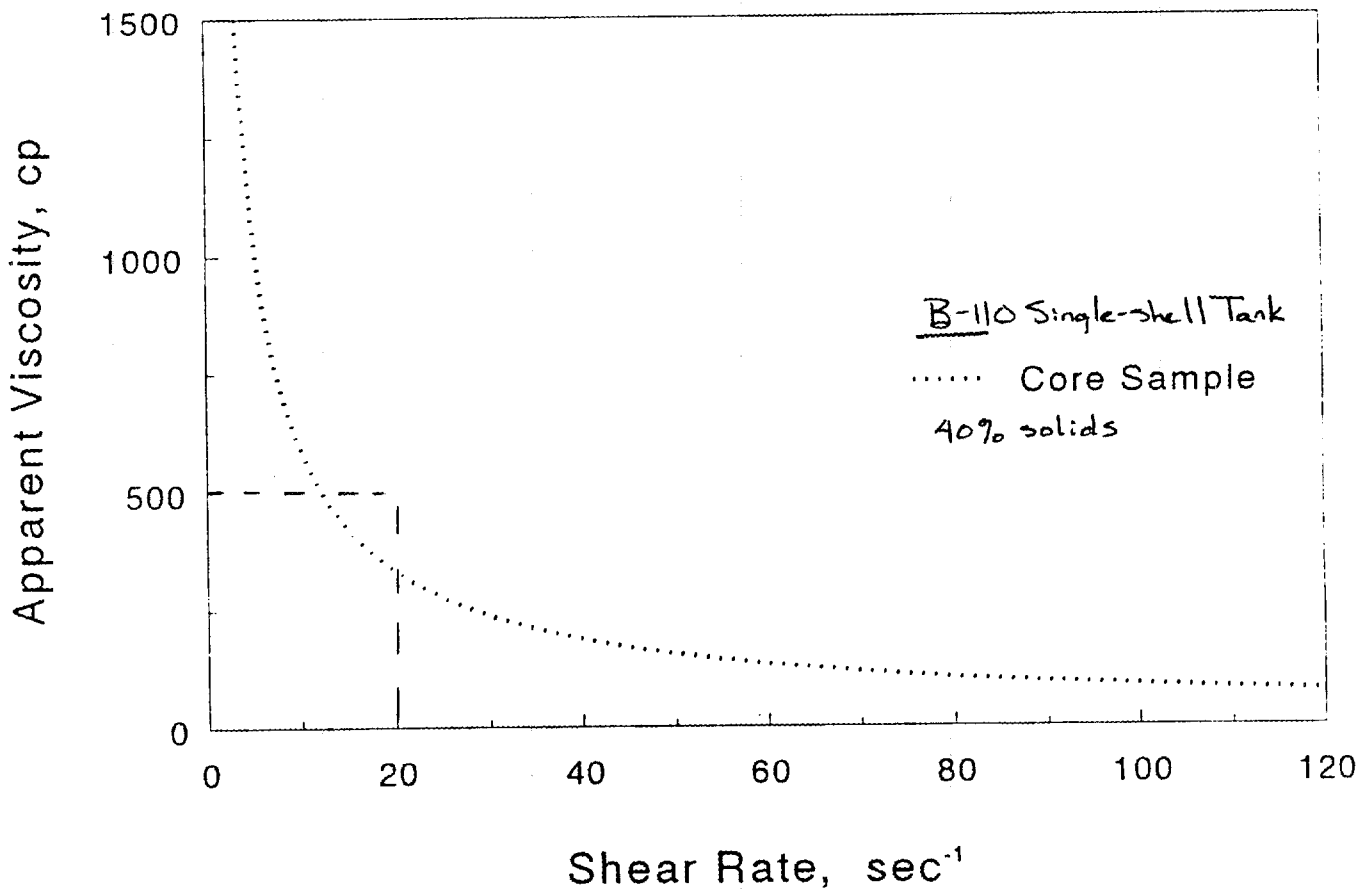


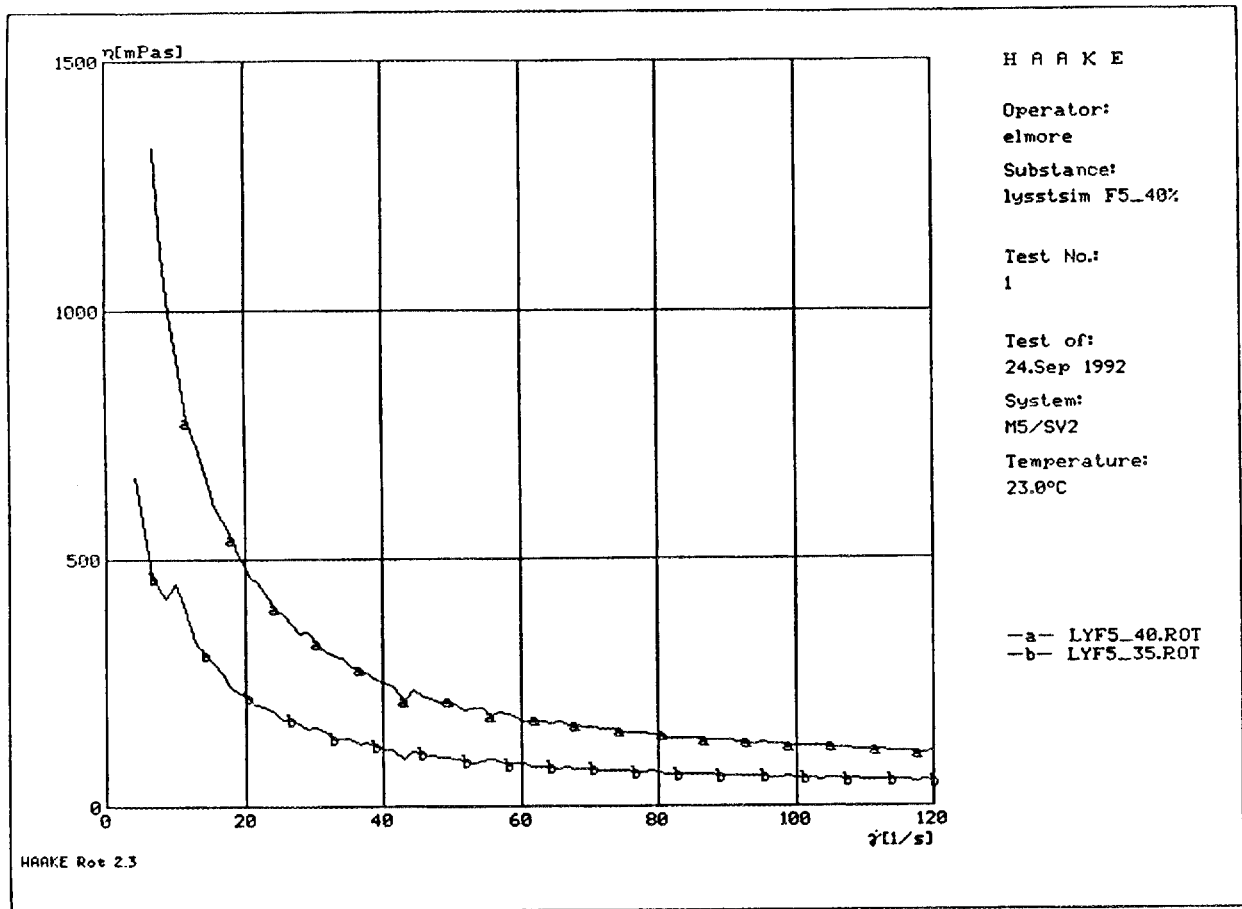
Attachment 2.5: Apparent Viscosity vs. Shear Rate
 Simulant F-3 at 40, 35, 30, 25 wt% solids



Attachment 2.6: Apparent Viscosity vs. Shear Rate
Simulant F-4 at 40, 35, 30 wt% solids

Attachment 2.4: Apparent Viscosity vs. Shear Rate
Single-shell Tank 241-B-110, Composite





Attachment 2.7: Apparent Viscosity vs. Shear Rate
Simulant F-5 at 40, 35 wt% solids

Attachment 2.8: Particle Size Distribution
 Simulants F-2 and F-3 (simulants differ only in water content)

B r i n k m a n n
Particle Size Analyzer

FILE NAME : 92-11143/ F2+F3
 E NAME : 9211143.001

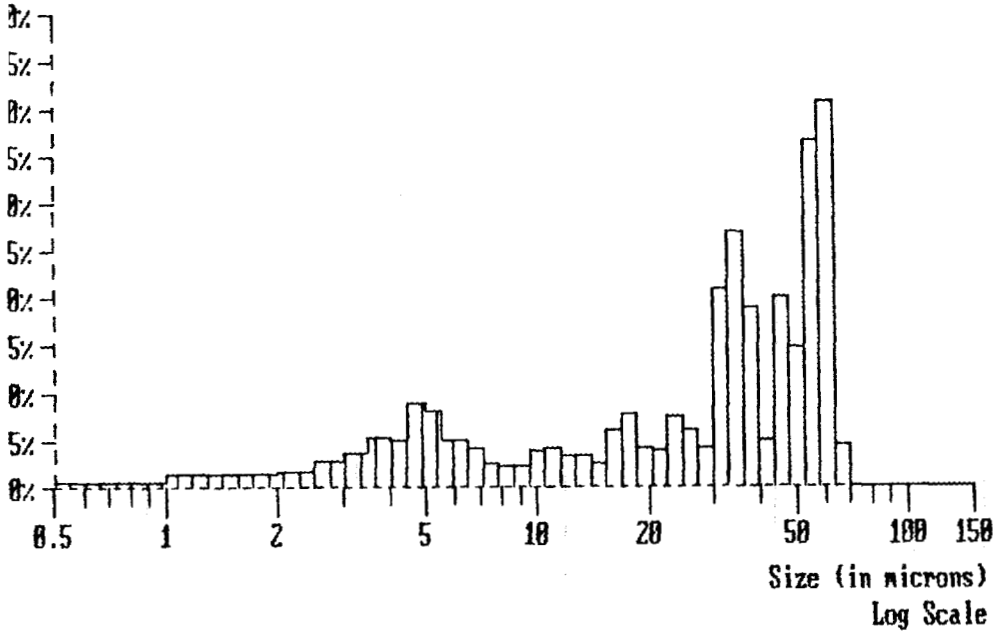
McBurt

DATE	: 25/07/1992	ACQ. RANGE	: 0.5-150	COUNTS	: 77086
TIME	: 11:31	ACQ. MODE	: SAMPLE	S.N.F.	: 0.76
FIG.	: 1 (0.7 S1)	ACQ. TIME	: 237 SEC	S.D.U.	: 3432
CELL TYPE	: MAGNETIC (2)	SAMPLE SIZE	: 4	CONCENTR.	: 5.3E+06 #/ml
FILE TYPE	: REGULAR	REQ. CONF.	: 95.00%(V)	SOLIDS	: 6.0E-03 %

PROBABILITY VOLUME DENSITY GRAPH

FILE: 92-11143/ F2	Mean(nv): 2.79µm	Median : 33.22µm
IE-05 cc/ml(100.0%)	S.D.(nv): 1.93µm	Mean(vm): 31.46µm
at 60.87 µm		S.D.(vm): 21.19µm
<< SCALE RANGE (µm): ADJUSTED >>		Conf(vm): 99.87 %

MATE WLO2018
MW 9/25/92



Attachment 2.9: Particle Size Analysis
 Simulant F-4

B r i n k m a n n
 Particle Size Analyzer

SAMPLE NAME : 92-11283/ F-4
 FILE NAME : 9211283.001

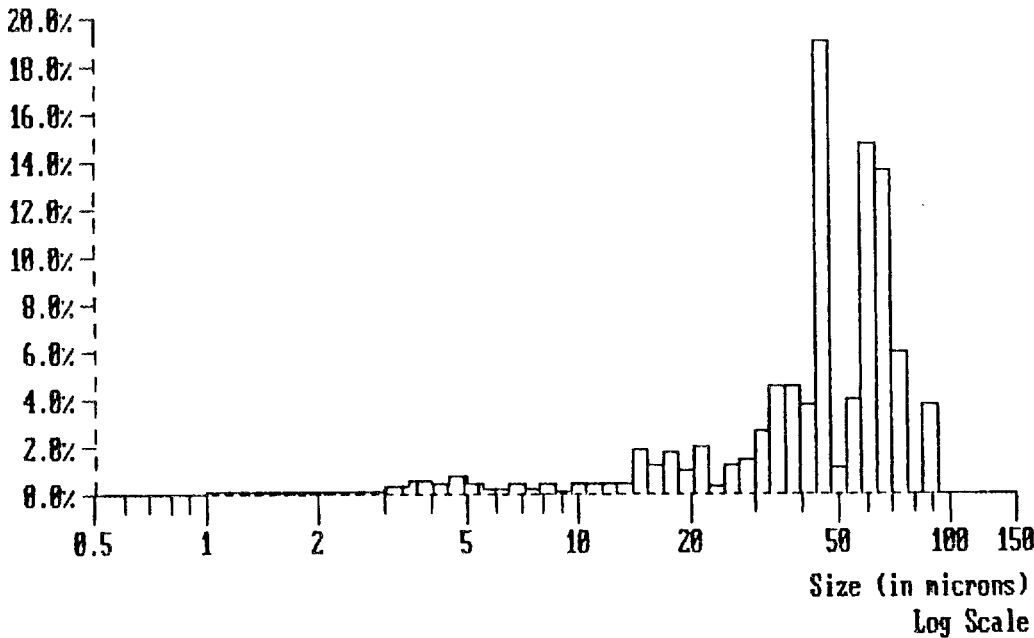
McBent

DATE	: 25/09/1992	ACQ. RANGE	: 0.5-150	COUNTS	: 29567
TIME	: 13:13	ACQ. MODE	: SAMPLE	S.N.F.	: 0.80
CONFIG.	: 1 (0.7 S1)	ACQ. TIME	: 139 SEC	S.D.U.	: 2290
CELL TYPE	: MAGNETIC (2)	SAMPLE SIZE	: 3	CONCENTR.	: 2.4E+06 #/ml
SAMPLE TYPE	: REGULAR	REQ. CONF.	: 95.00%(V)	SOLIDS	: 8.4E-03 %

PROBABILITY VOLUME DENSITY GRAPH

*MATE WCO2018
 MWLhu 9/25/92*

Name: 92-11283/ F-4	Mean(nv): 4.85µm	Median : 46.12µm
8.4E-05 cc/ml(100.0%)	S.D.(nv): 3.22µm	Mean(vn): 46.35µm
Mode at 45.76 µm		S.D.(vn): 21.71µm
<< SCALE RANGE (µm): ADJUSTED >>		Conf(vn): 98.86 %



Attachment 2.10: Particle Size Analysis
 Simulant F-5

B r i n k m a n n
Particle Size Analyzer

PLE NAME : 92-11284/ F-5
 E NAME : 9211284.001

McBent

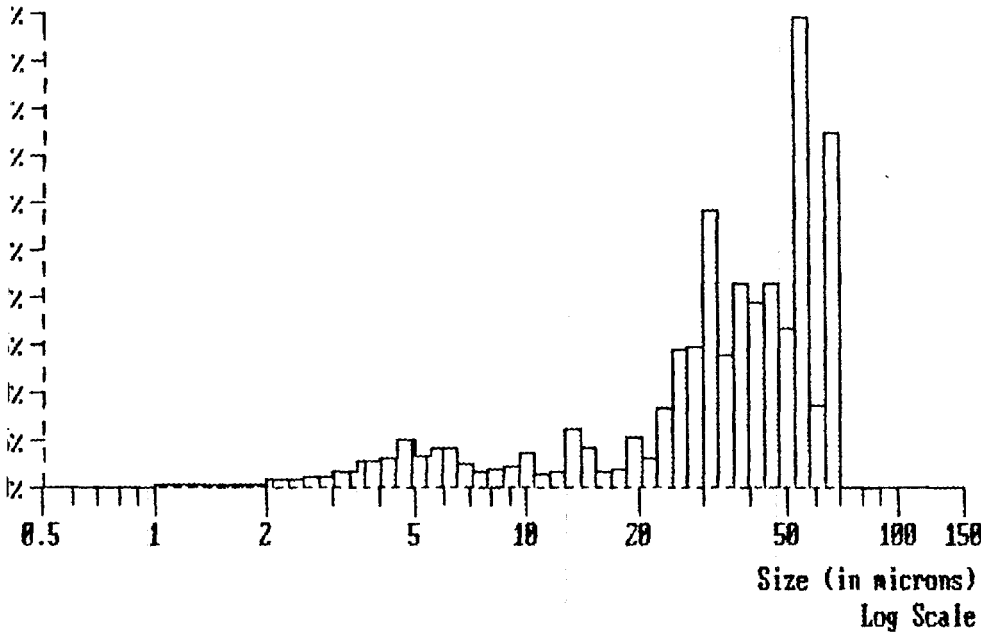
E : 25/09/1992 | ACQ. RANGE : 0.5-150 | COUNTS : 32181
 E : 13:21 | ACQ. MODE : SAMPLE | S.N.F. : 0.65
 FIG. : 1 (0.7 S1) | ACQ. TIME : 137 SEC | S.D.U. : 2523
 L TYPE : MAGNETIC (2) | SAMPLE SIZE : 3 | CONCENTR.: 2.3E+06 #/ml
 PLE TYPE : REGULAR | REQ. CONF. : 95.00%(V) | SOLIDS : 8.6E-03 %

PROBABILITY VOLUME DENSITY GRAPH

M+TE WCO2018
MWCh
9/25/92

: 92-11284/ F-5
 85 cc/ml (100.0%)
 at 55.35 μ m
 Mean(nv): 4.12 μ m
 S.D.(nv): 3.21 μ m
 Median : 37.37 μ m
 Mean(vn): 36.85 μ m
 S.D.(vn): 19.57 μ m
 Conf(vn): 97.44 %

<< SCALE RANGE (μ m): ADJUSTED >>



Attachment 2.11: Particle Size Distribution
 Simulant G

B r i n k m a n n
Particle Size Analyzer

SAMPLE NAME : 92-11144/ G
 FILE NAME : 9211144.001

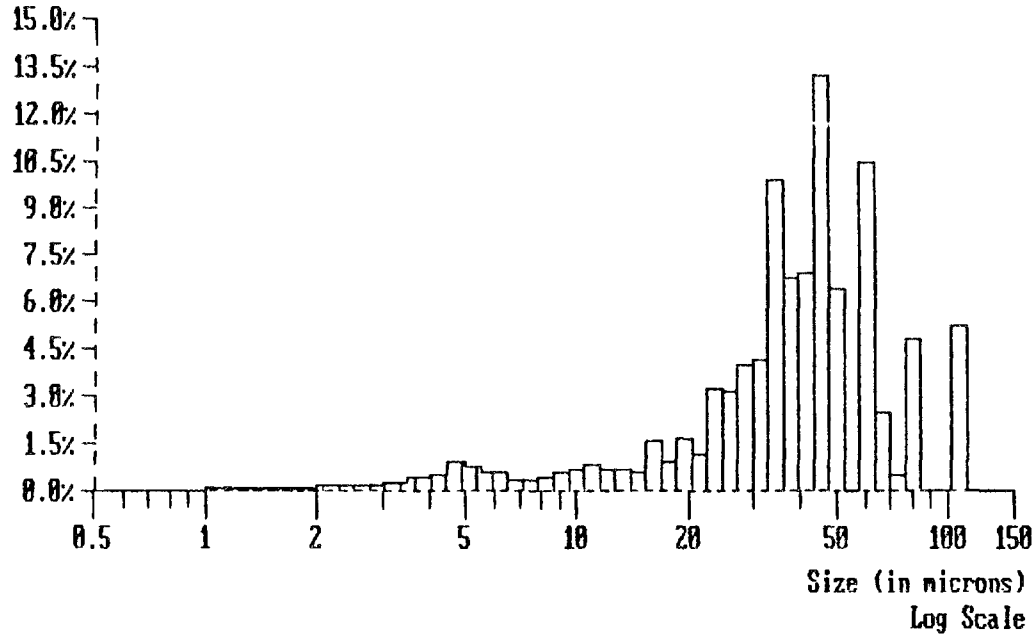
McBurt

DATE : 25/09/1992 | ACC. RANGE : 0.5-150 | COUNTS : 27165
 TIME : 11:40 | ACC. MODE : SAMPLE | S.N.F. : 0.76
 CONFIG. : 1 (0.7 S1) | ACC. TIME : 104 SEC | S.D.U. : 2751
 CELL TYPE : MAGNETIC (2) | SAMPLE SIZE : 2 | CONCENTR.: 3.3E+06 #/ml
 SAMPLE TYPE : REGULAR | REQ. CONF. : 95.00%(V) | SOLIDS : 1.4E-02 %

PROBABILITY VOLUME DENSITY GRAPH

*MATE WCO2018
 MW then 9/25/92*

Name: 92-11144/ G
 1.4E-04 cc/ml(100.0%)
 Mode at 45.76 μ m
 Mean(nv): 4.32 μ m
 S.D.(nv): 3.51 μ m
 Median : 39.83 μ m
 Mean(vm): 42.55 μ m
 S.D.(vm): 24.63 μ m
 Conf(vm): 95.95 %



SST Core 2, Segment 1 Particle Size Analysis
 Sample # 89-0410

PROBABILITY NUMBER DENSITY GRAPH

Name: 118B-CORE 2-SEG 1

1.7E+06 #/ml(100.0μ)

Mode at 0.75 μ

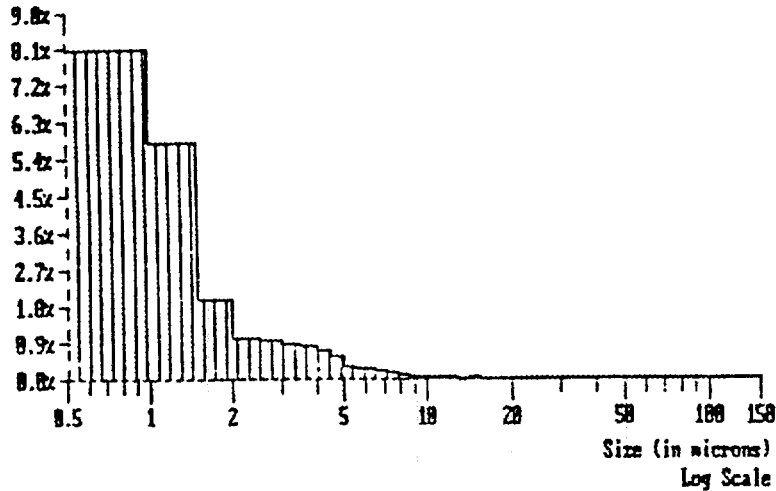
<< SCALE RANGE (μ): ADJUSTED >>

Median : 0.92μ

Mean(n): 1.30μ

S.D.(n): 1.60μ

Conf(n): 100.00 %



PROBABILITY VOLUME DENSITY GRAPH

Name: 118B-CORE 2-SEG 1

5.2E+05 cc/ml(100.0μ)

Mode at 37.04 μ

<< SCALE RANGE (μ): ADJUSTED >>

Mean(nv): 3.91μ

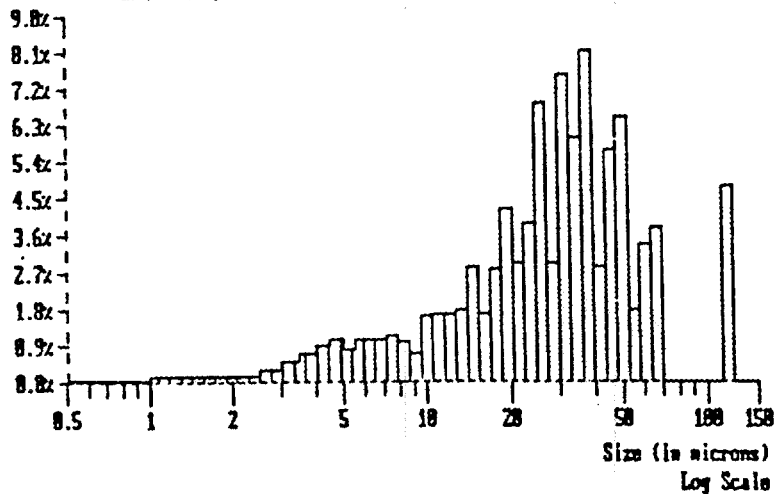
S.D.(nv): 3.86μ

Median : 30.34μ

Mean(vv): 33.50μ

S.D.(vv): 25.23μ

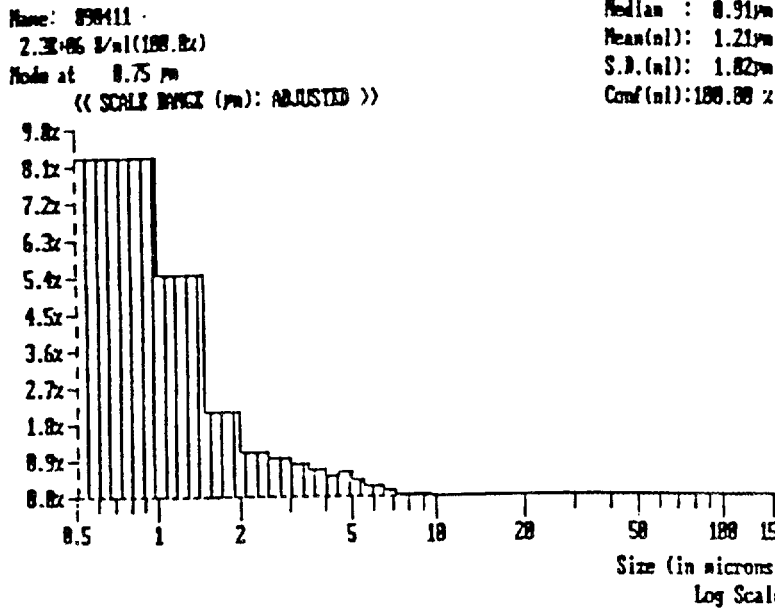
Conf(vv): 96.65 %



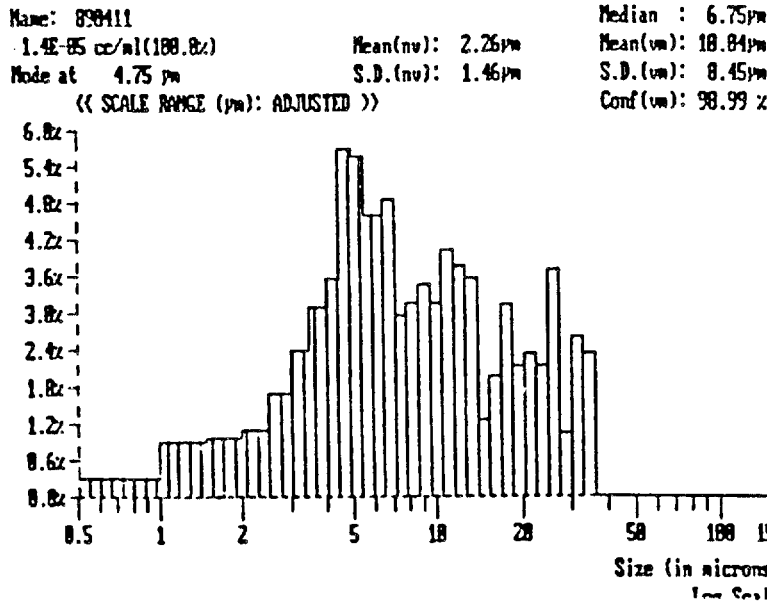
Attachment 2.12: Particle Size Analysis
 SST 241-B-110, Core 2, Segment 1

SST Core 2, Segment 2 Particle Size Analysis
 Sample # 89-0411

PROBABILITY NUMBER DENSITY GRAPH



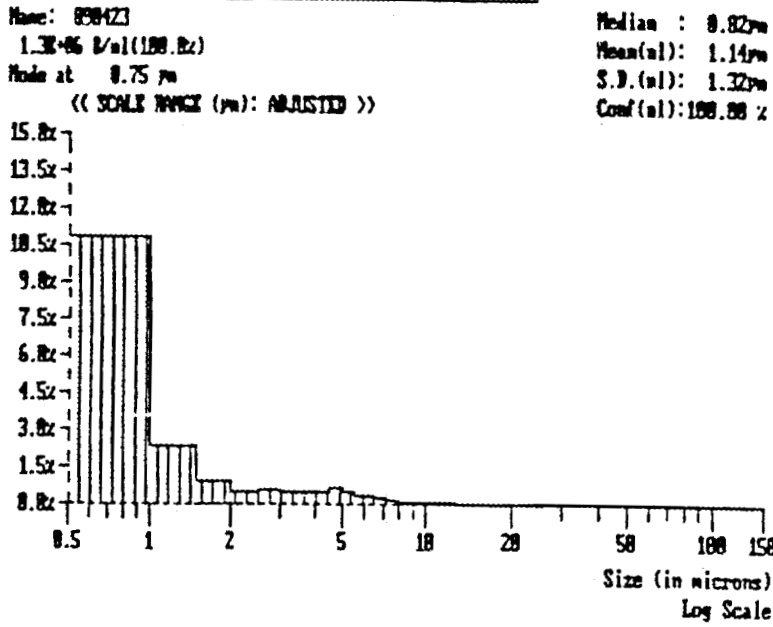
PROBABILITY VOLUME DENSITY GRAPH



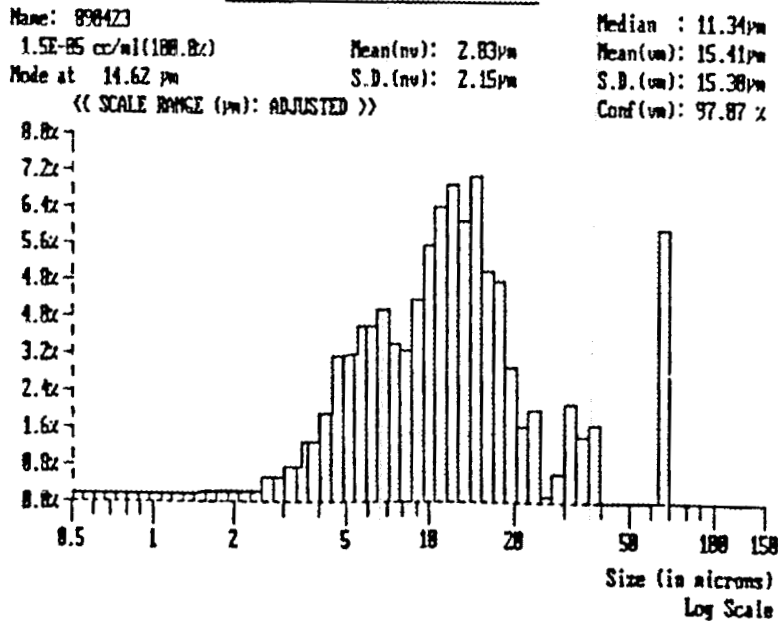
Attachment 2.13: Particle Size Analysis
 SST 241-B-110, Core 2, Segment 2

SST Core 2, Segment 4 Particle Size Analysis
 Sample # 89-0423

PROBABILITY NUMBER DENSITY GRAPH



PROBABILITY VOLUME DENSITY GRAPH



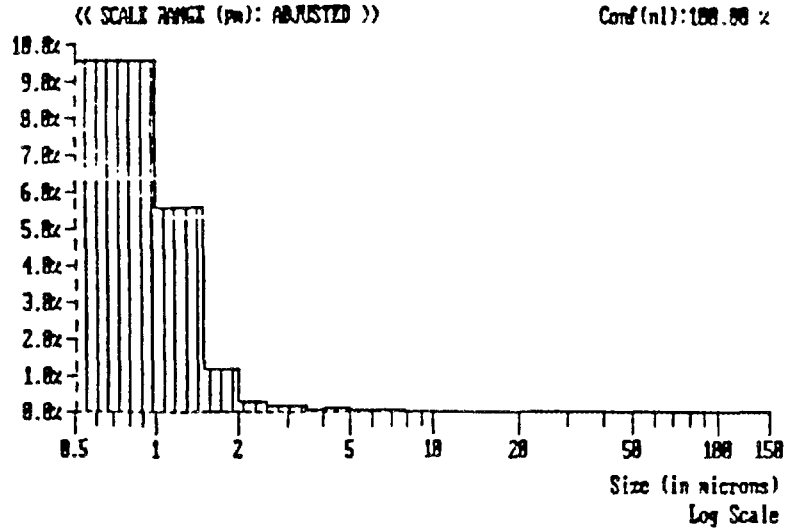
Attachment 2.14: Particle Size Analysis
 SST 241-B-110, Core 2, Segment 4

SST Core 2, Segment 5 Particle Size Analysis
 Sample # 89-0424

PROBABILITY NUMBER DENSITY GRAPH

Name: 890424
 1.7E-06 1/nl(100.0%)
 Mode at 0.75 μm

Median : 0.86 μm
 Mean(nl): 0.99 μm
 S.D.(nl): 0.69 μm
 Conf(nl): 100.00 %

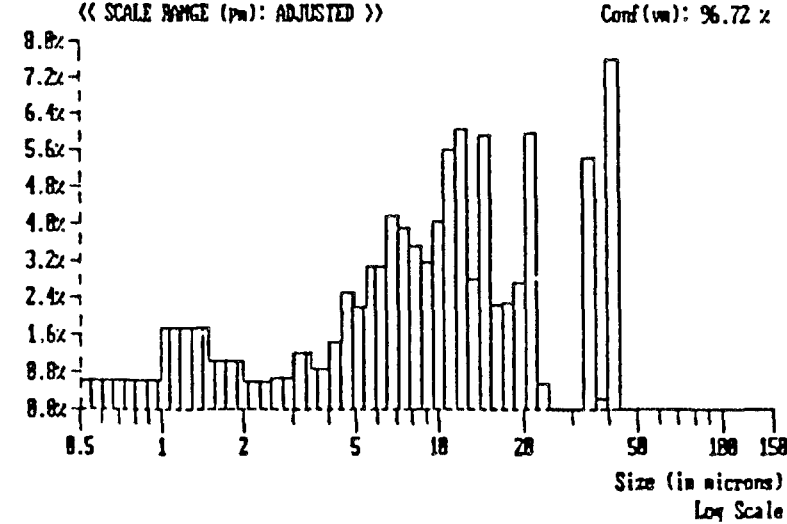


PROBABILITY VOLUME DENSITY GRAPH

Name: 890424
 5.4E-06 cc/nl(100.0%)
 Mode at 41.61 μm

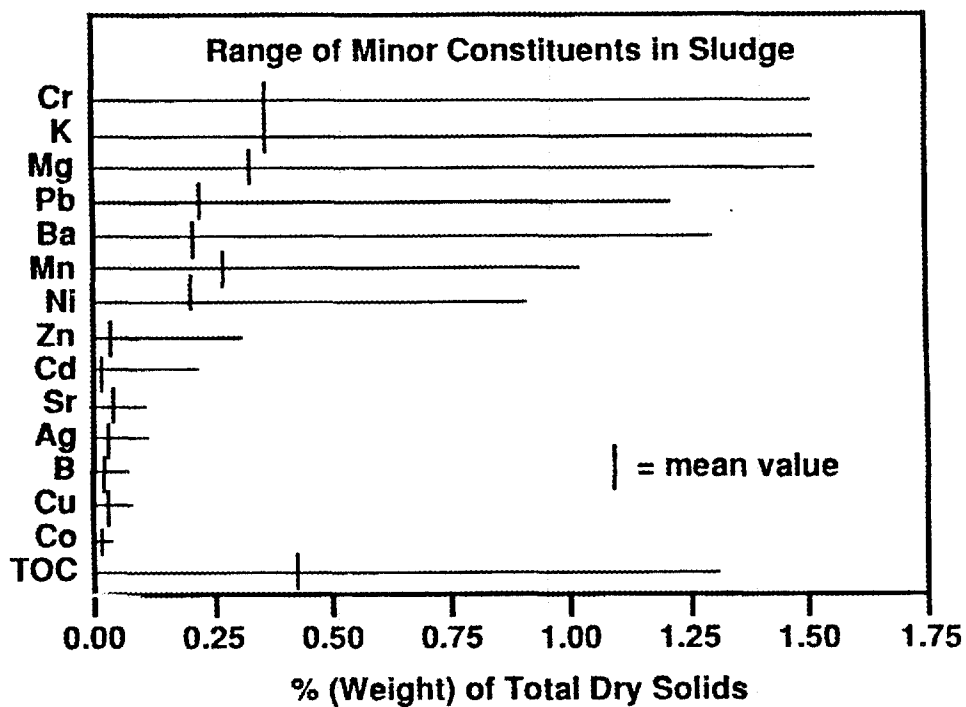
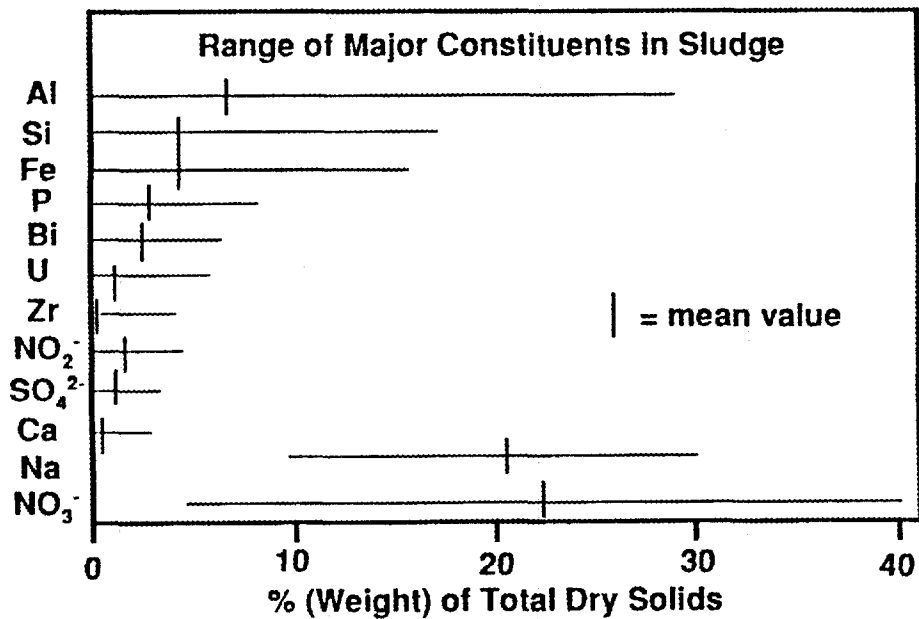
Mean(nv): 1.84 μm
 S.D.(nv): 1.18 μm

Median : 10.86 μm
 Mean(vn): 13.12 μm
 S.D.(vn): 11.79 μm
 Conf(vn): 96.72 %



Attachment 2.15: Particle Size Analysis
 SST 241-B-110, Core 2, Segment 5

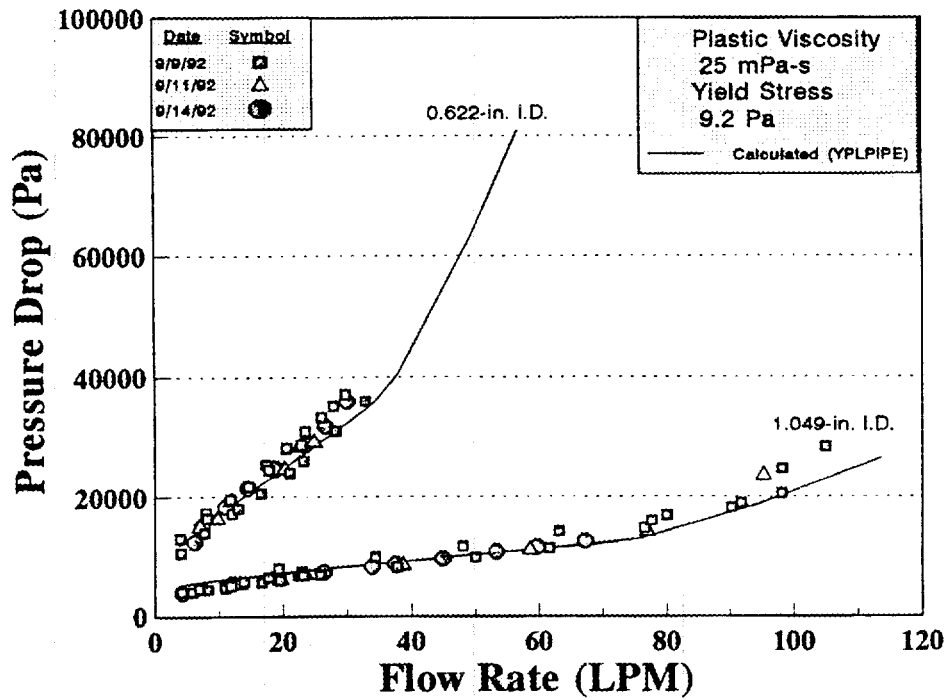
Attachment 3: Range of Constituents in SSTs
 (Based on the Analyses of 18 SSTs)



(EO Jones, NG Colton, and GR Bloom, "Hanford Single-Shell Tank Waste: Preliminary Pretreatment Testing of Simulated Waste," presented at the 7th Annual DOE Model Conference, Oak Ridge, TN, October, 1991)

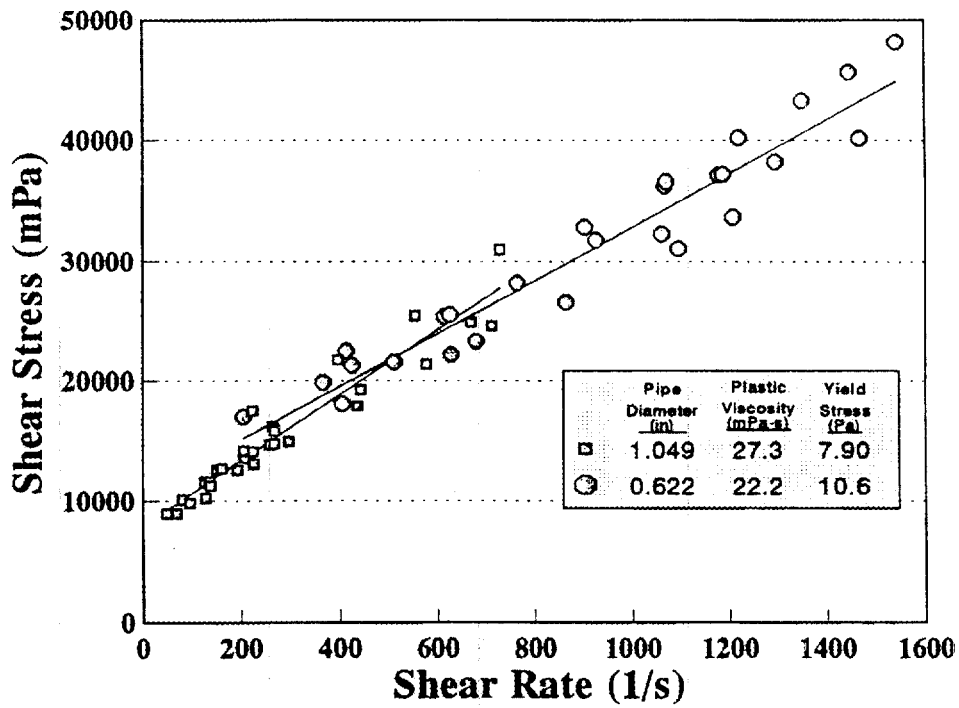
APPENDIX B

**Pressure Drop versus Flow Rate Curves for MVST Runs MVST 2, 3, 3A, 3B, and 3C and
Hanford Single-Shell Tank Simulated Waste Runs H-1 through H-7 , and
Tabulated Rheology Data for Hanford Single-Shell Waste Runs H-1 through H-7**



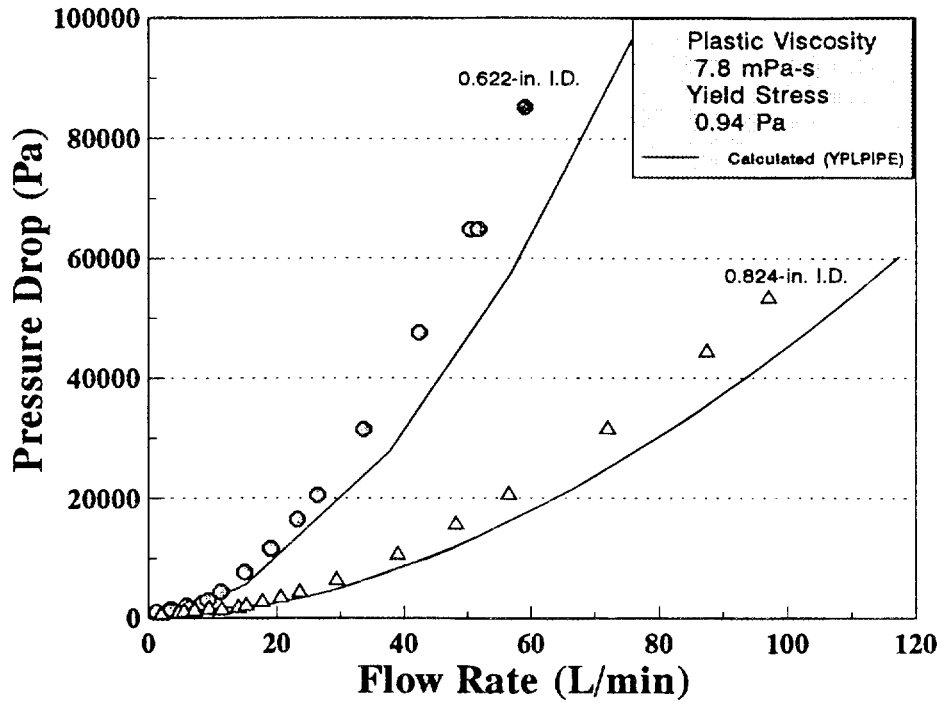
M-1

Figure B.1 Pressure drop versus flow rate for run MVST-1.



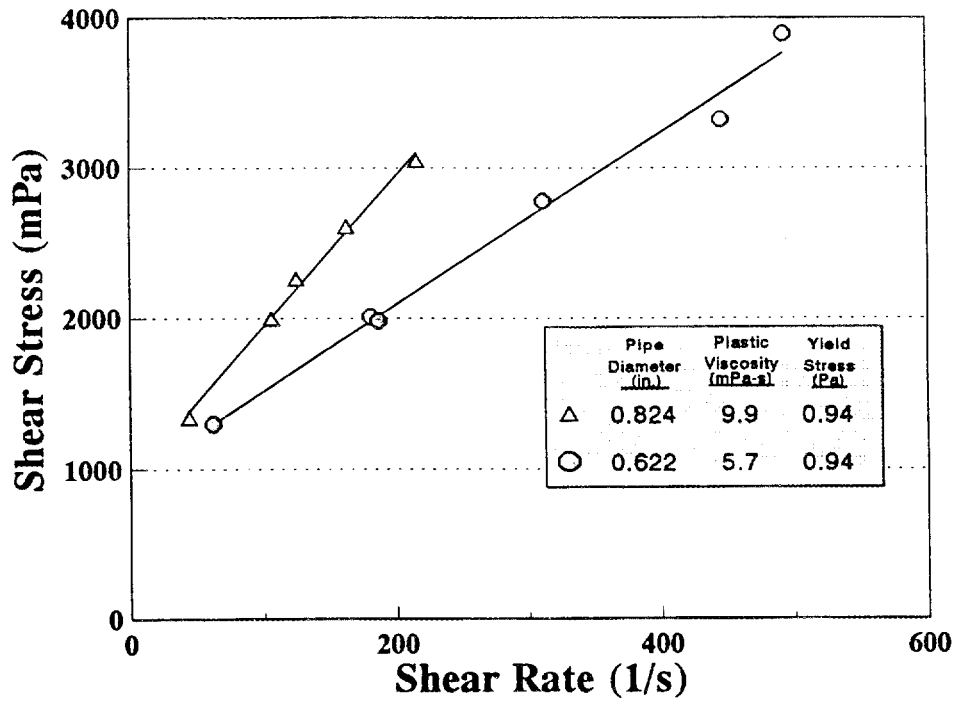
M-1

Figure B.2 Rheograms for run MVST-1.



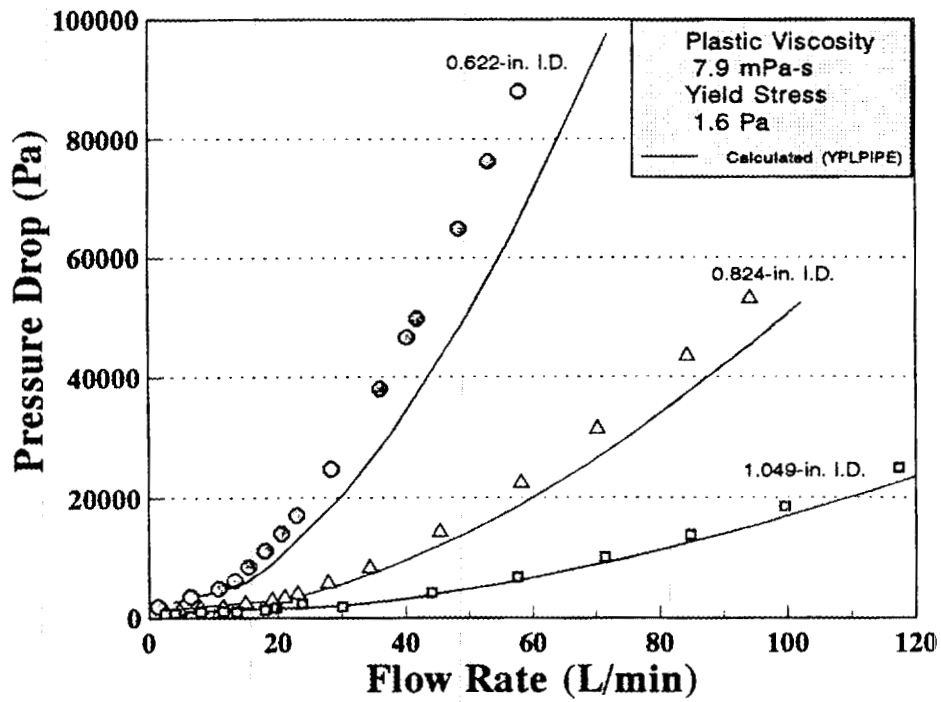
M-2b

Figure B.3 Pressure drop versus flow rate for run MVST-2.



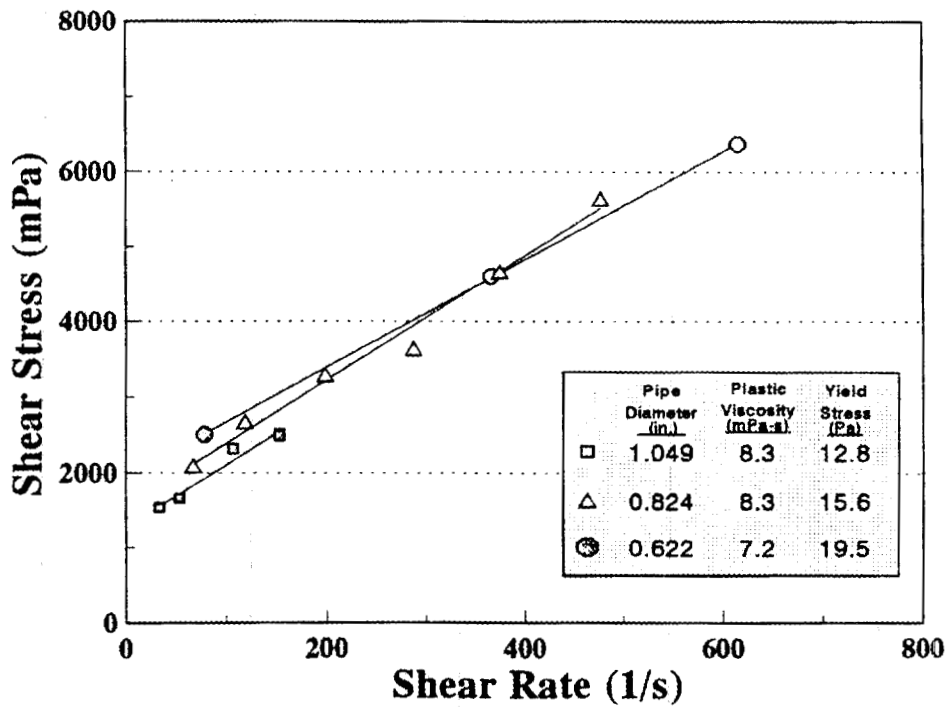
M-2b

Figure B.4 Rheograms for run MVST-2.



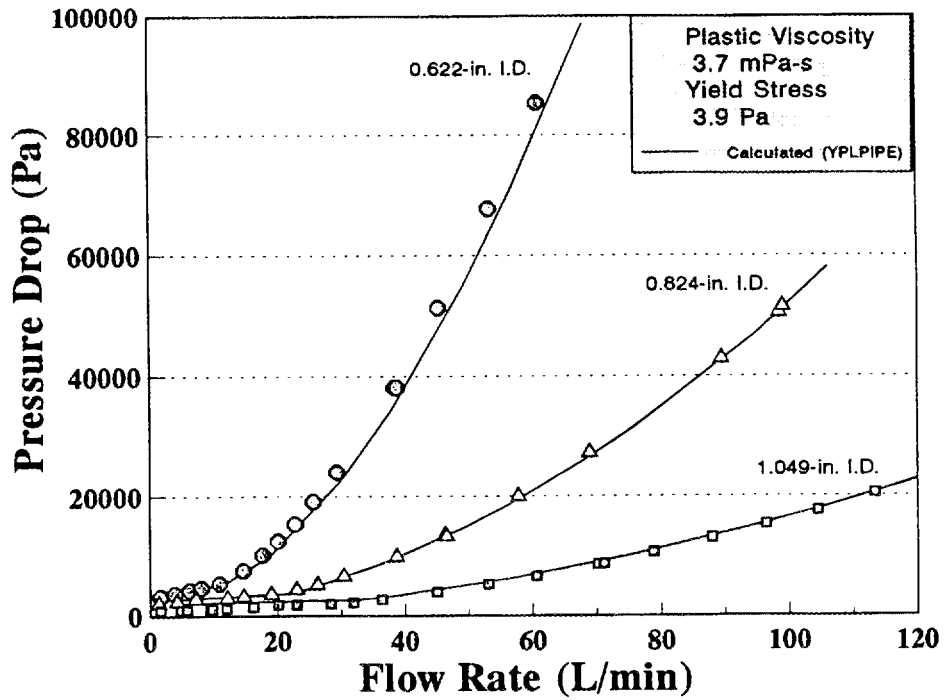
M-3

Figure B.5 Pressure drop versus flow rate for run MVST-3.



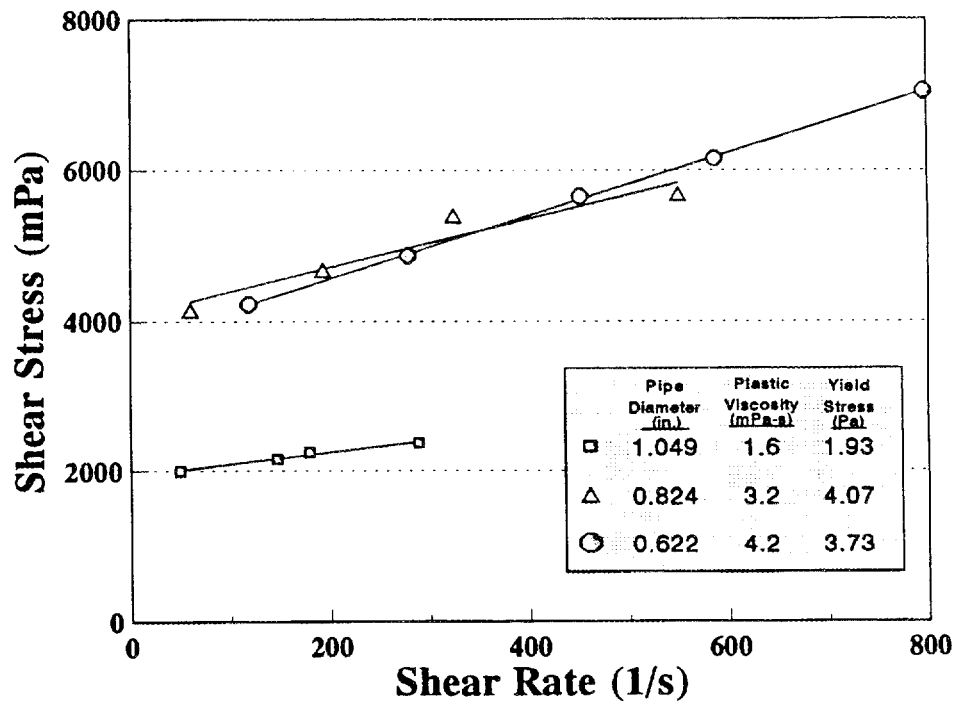
M-3

Figure B.6 Rheograms for run MVST-3.



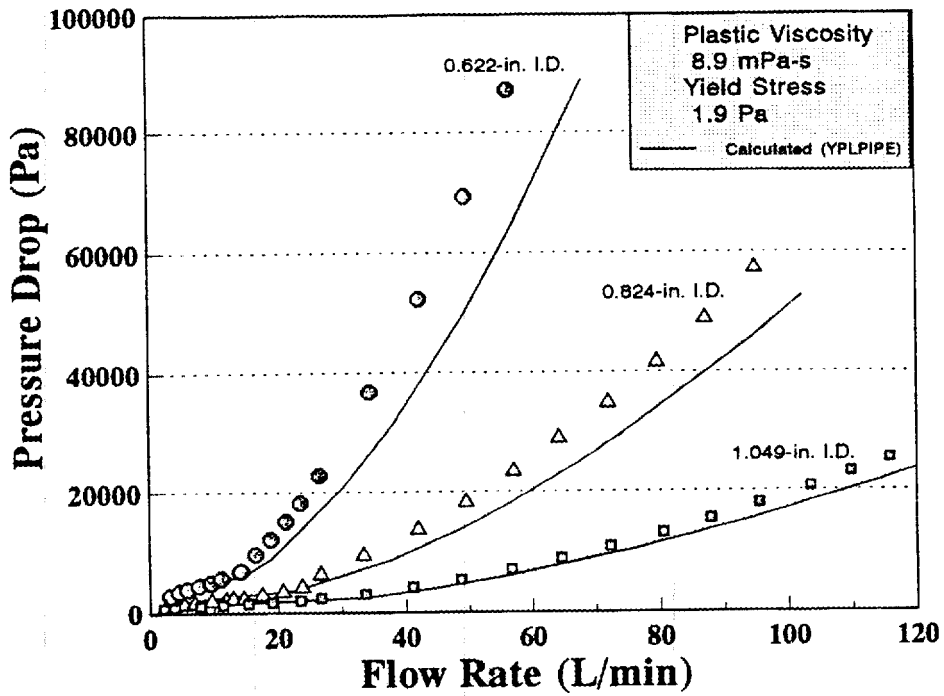
M-3a

Figure B.7 Pressure drop versus flow rate for run MVST-3A.



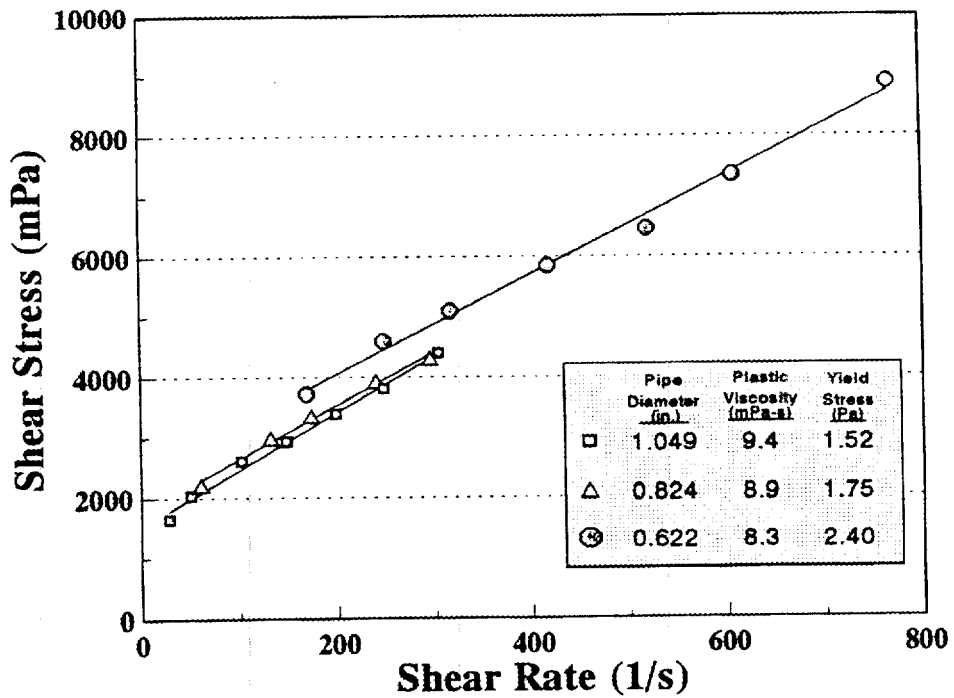
M-3a

Figure B.8 Rheograms for run MVST-3A.



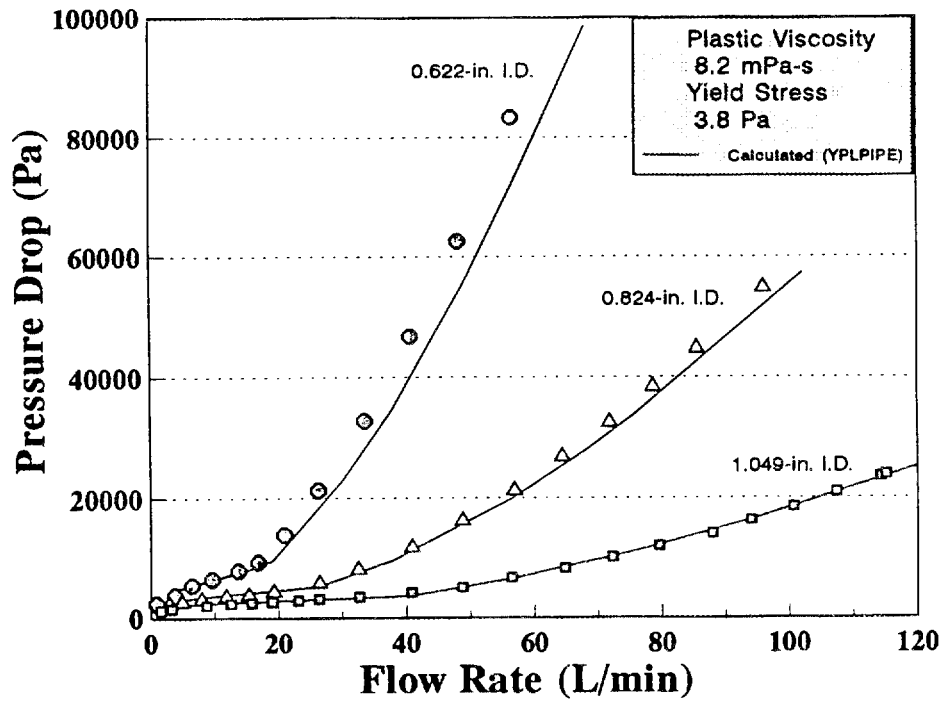
M-3b

Figure B.9 Pressure drop versus flow rate for run MVST-3B.



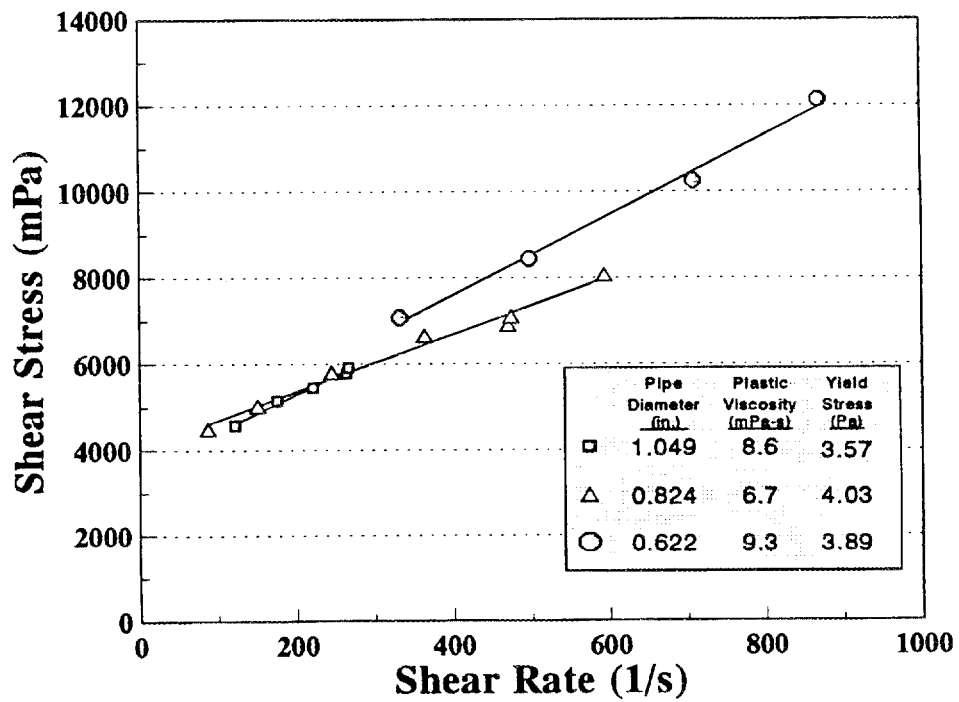
M-3b

Figure B.10 Rheograms for run MVST-3B.



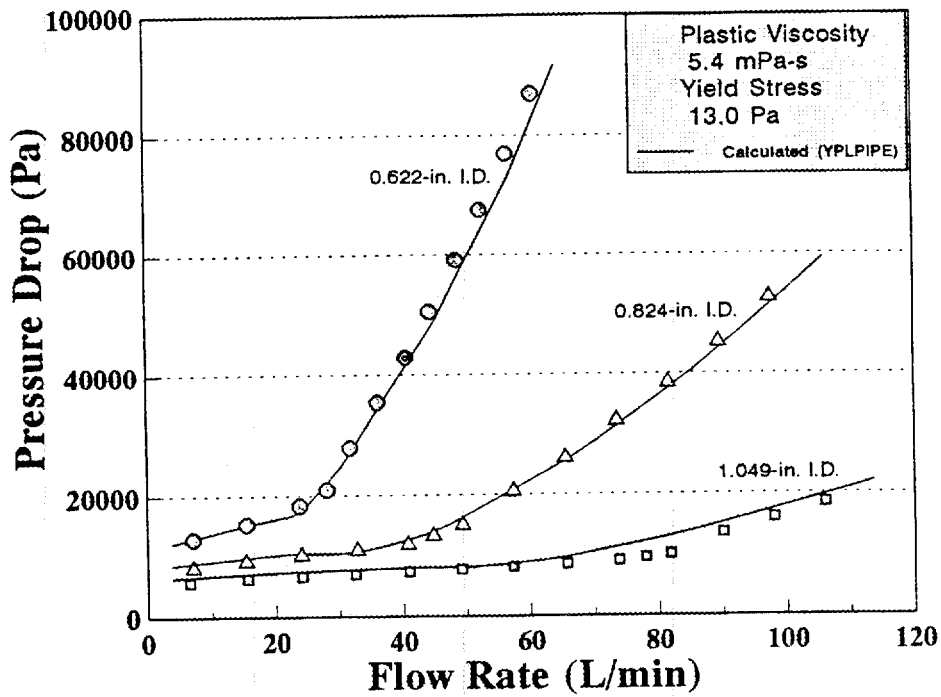
M-3c

Figure B.11 Pressure drop versus flow rate for run MVST-3C.



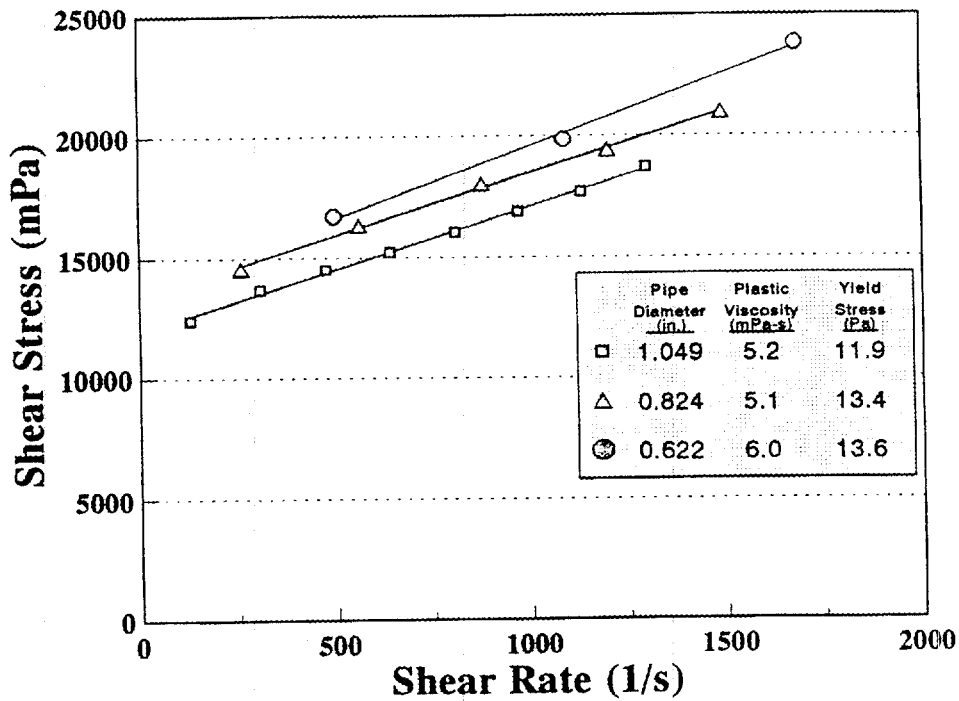
M-3c

Figure B.12 Rheograms for run MVST-3C.



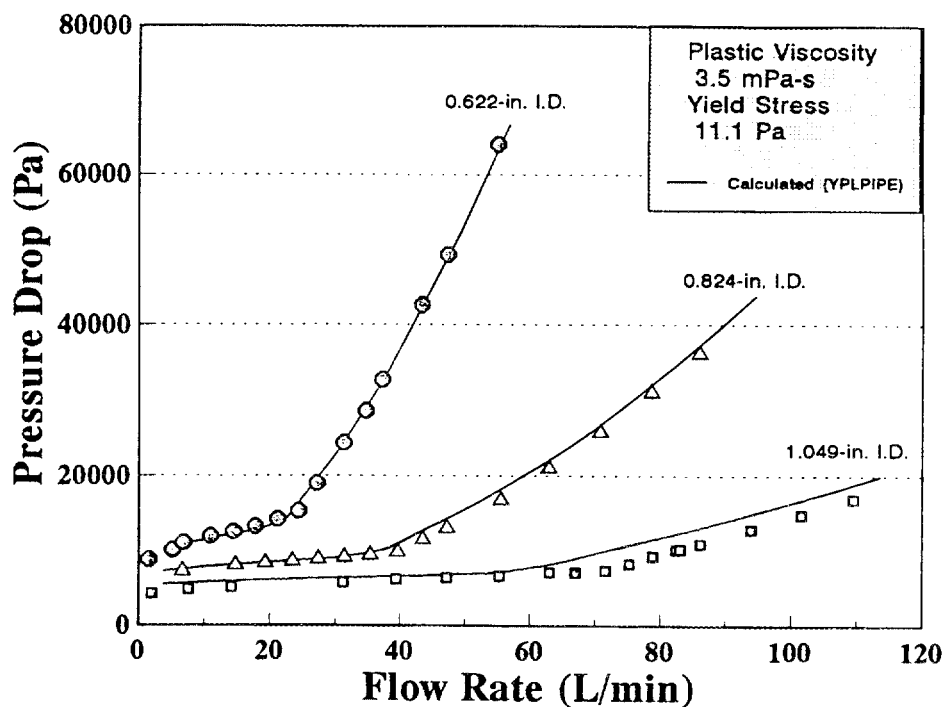
H-1

Figure B.13 Pressure drop versus flow rate for run H-1.



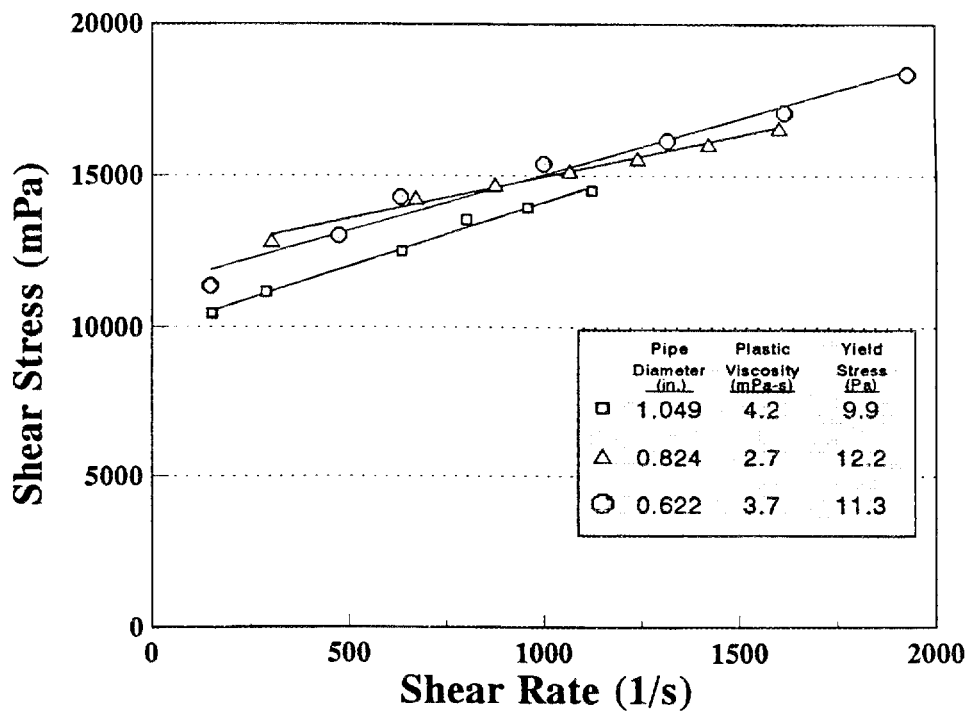
H-1

Figure B.14 Rheograms for run H-1.



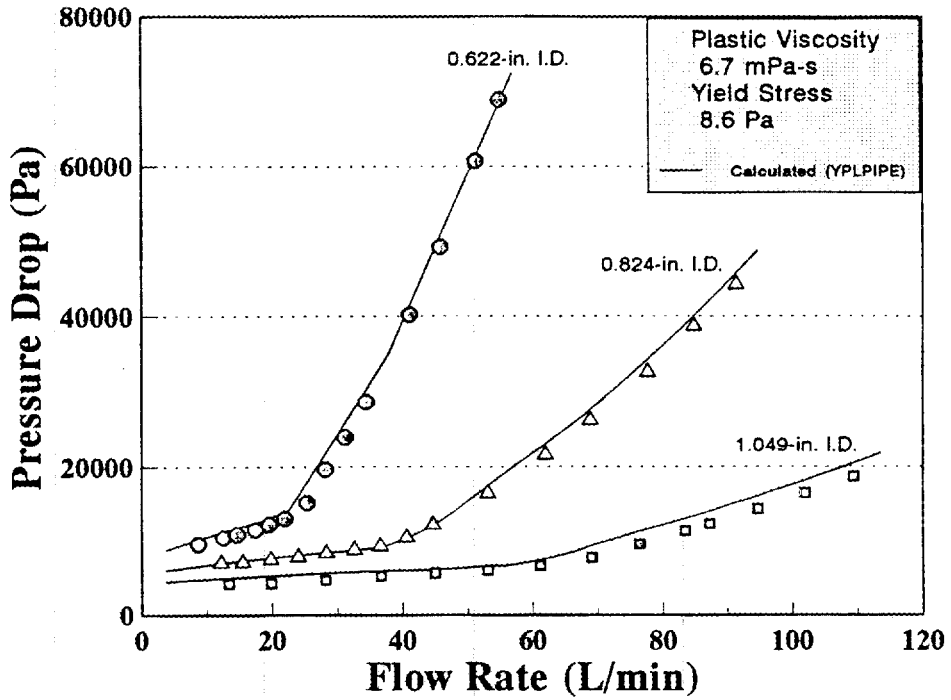
H-2

Figure B.15 Pressure drop versus flow rate for run H-2.



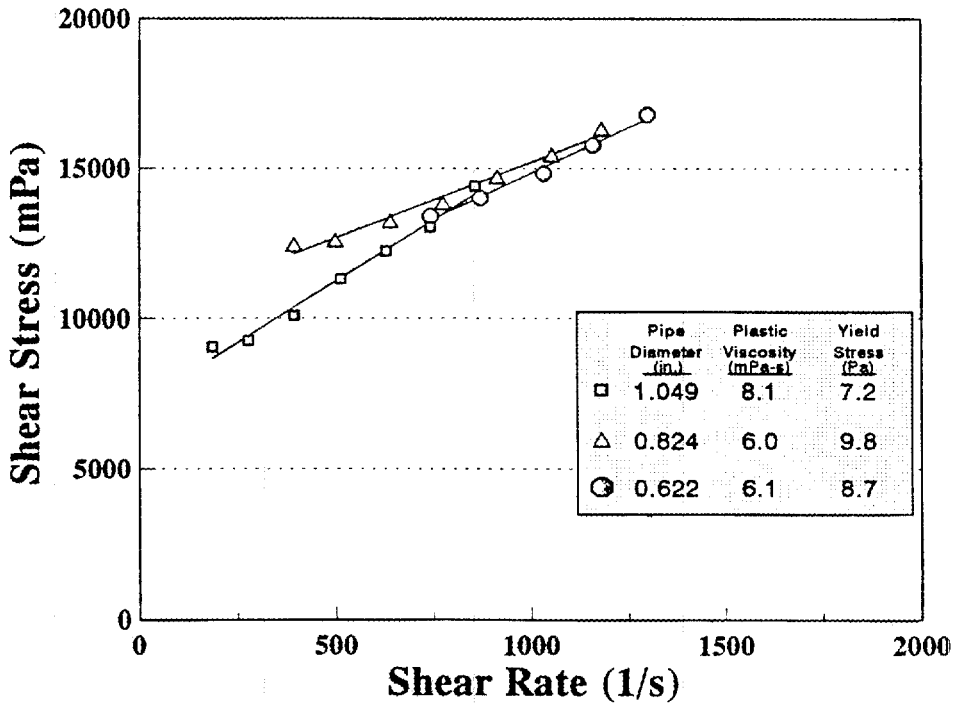
H-2

Figure B.16 Rheograms for run H-2.



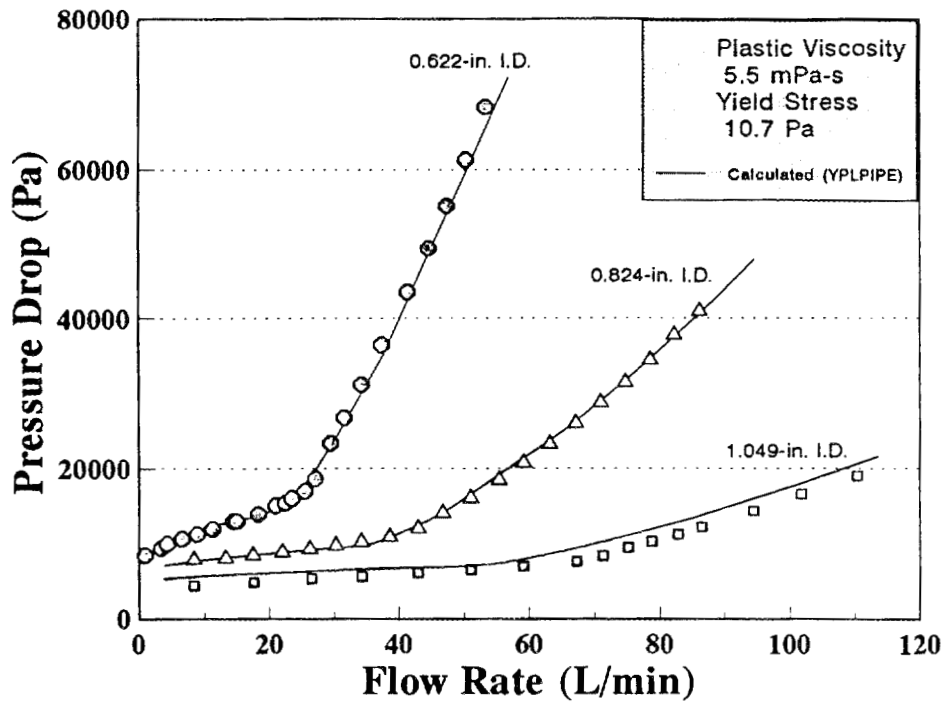
H-3

Figure B.17 Pressure drop versus flow rate for run H-3.



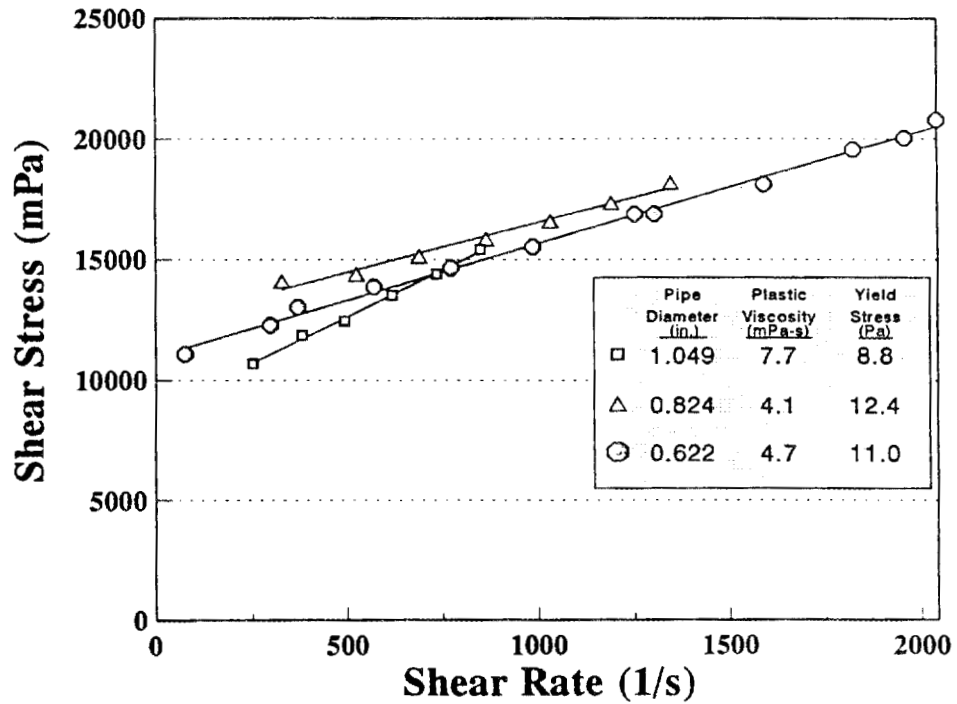
H-3

Figure B.18 Rheograms for run H-3.



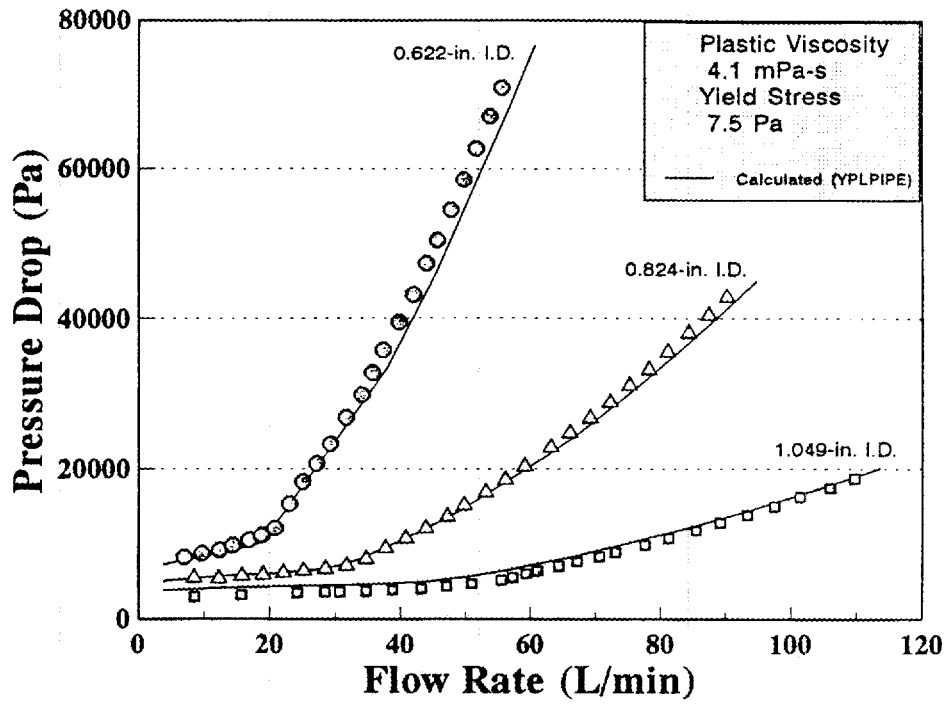
H-4

Figure B.19 Pressure drop versus flow rate for run H-4.



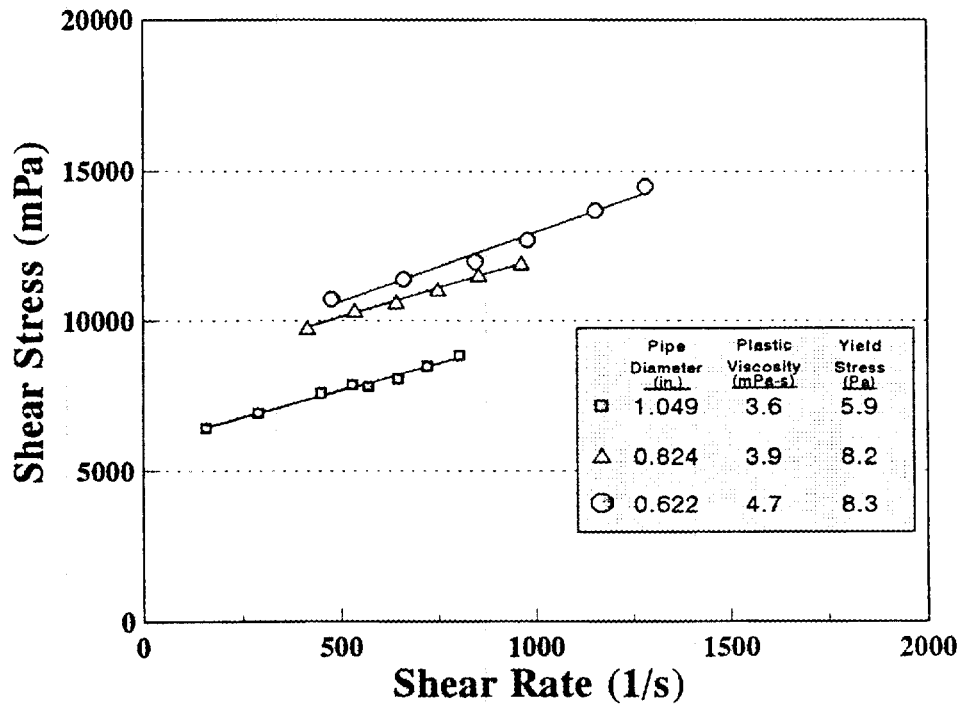
H-4

Figure B.20 Rheogram for run H-4.



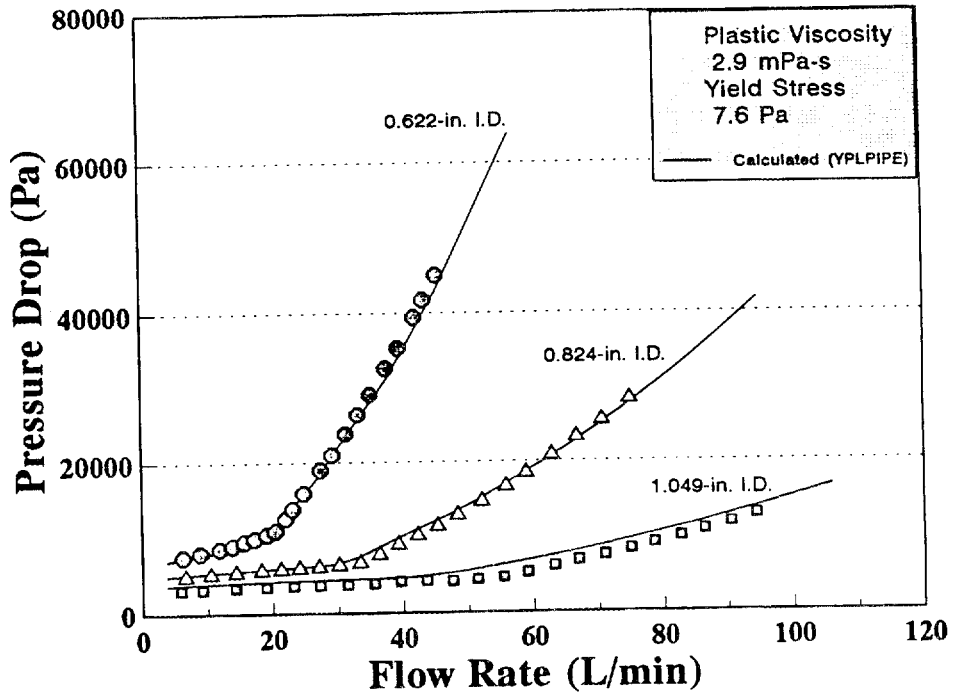
H-5

Figure B.21 Pressure drop versus flow rate for run H-5.



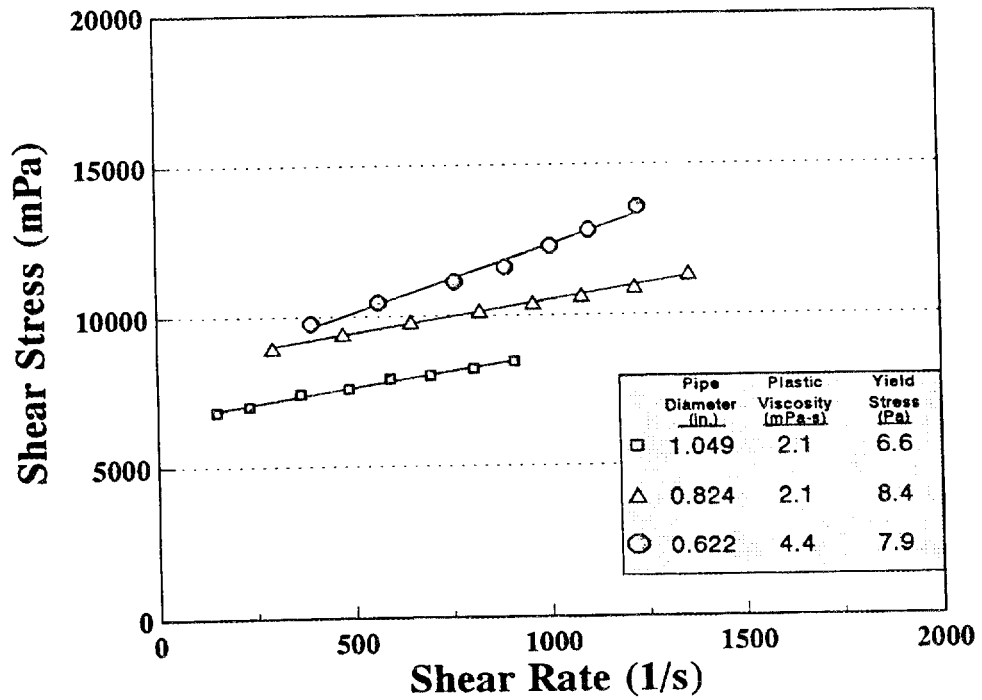
H-5

Figure B.22 Rheograms for run H-5.



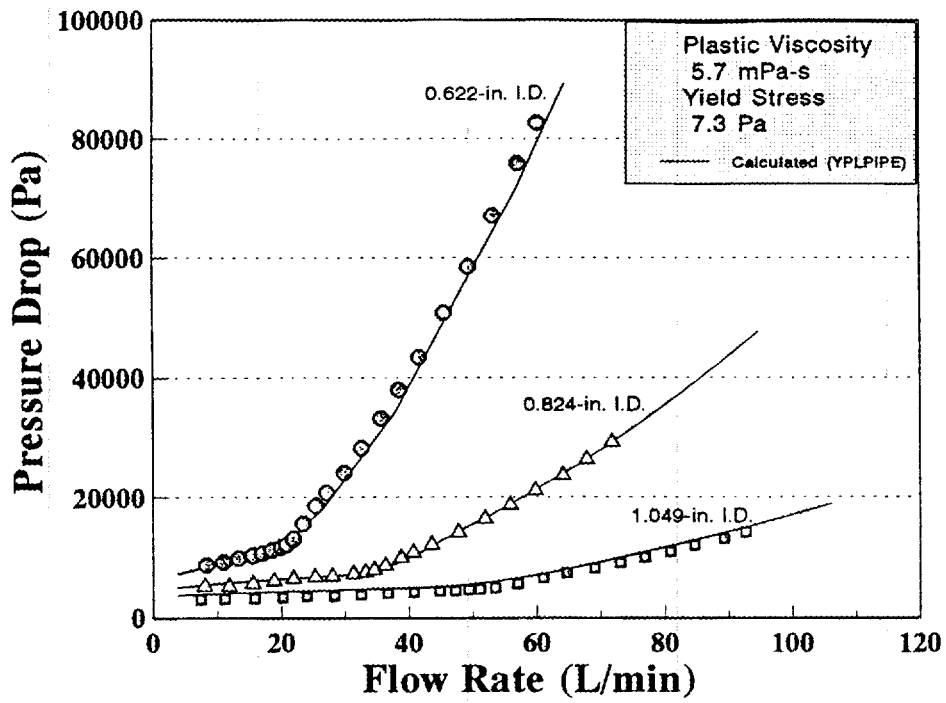
H-6

Figure B.23 Pressure drop versus flow rate for run H-6.



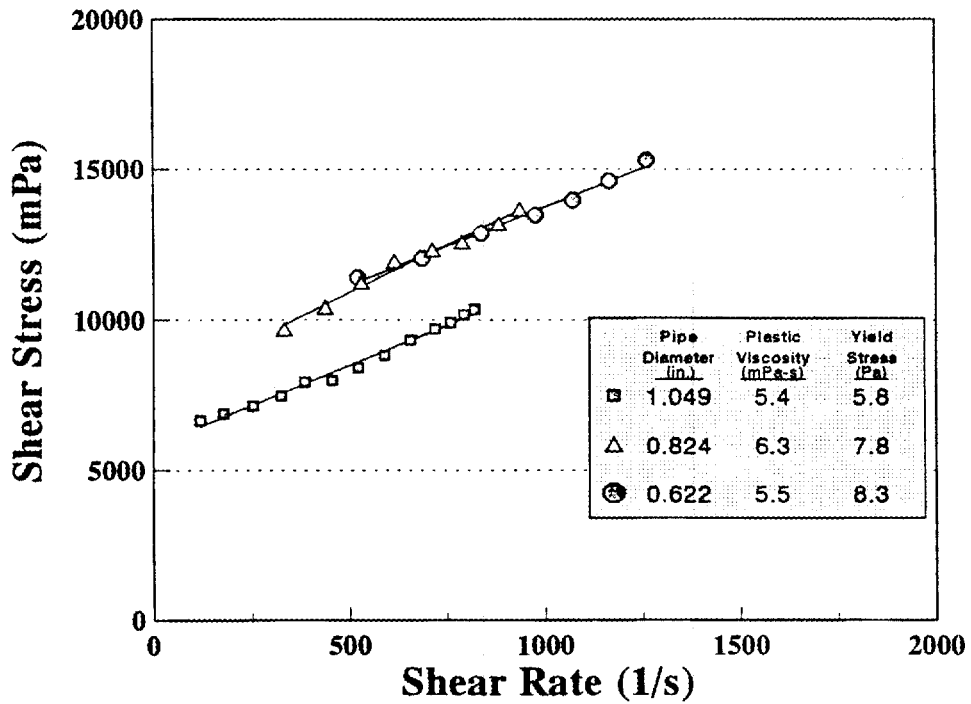
H-6

Figure B.24 Rheograms for run H-6.



H-7

Figure B.25 Pressure drop versus flow rate for run H-7.



H-7

Figure B.26 Rheogram for run H-7.

Run Number	H-1		<u>Diameter (in.)</u>
Temperature	25 °C	PLV-1	1.049
Density	1.36 g/mL	PLV-2	0.824
Total Solids Content	42.0 wt %	PLV-3	0.622

PLV-1				PLV-3			
Flow Rate (L/min)	Press. Drop (Pa)	8V/D (1/s)	Tau (mPa)	Flow Rate (L/min)	Press. Drop (Pa)	8V/D (1/s)	Tau (mPa)
6.56	5677	58.9	12407	7.07	12906	304.3	16724
15.60	6266	140.1	13694	15.47	15329	666.1	19864
24.10	6640	216.4	14512	23.85	18366	1027.0	23799
32.47	6967	291.5	15226	28.09	20970		
41.01	7338	368.2	16037	31.82	27943		
49.20	7723	441.7	16878	36.21	35458		
57.33	8093	514.8	17688	40.65	42921		
65.75	8562	590.3	18711	44.51	50561		
73.80	9087			48.66	59124		
78.01	9565			52.48	67696		
81.92	10096			56.63	77038		
90.13	13564			60.71	86949		
98.12	16002						
106.06	18489						

PLV-2			
Flow Rate (L/min)	Press. Drop (Pa)	8V/D (1/s)	Tau (mPa)
7.09	8485	131.4	14565
15.36	9510	284.5	16326
24.03	10497	445.1	18020
32.83	11312	608.2	19419
40.75	12216		
44.83	13608		
49.37	15381		
57.43	20945		
65.59	26410		
73.63	32515		
81.69	38769		
89.64	45561		
97.54	52883		

Run Number	H-2		<u>Diameter (in.)</u>
Temperature	50 °C	PLV-1	1.049
Density	1.35 g/mL	PLV-2	0.824
Total Solids Content	42.3 wt %	PLV-3	0.622

PLV-1				PLV-3			
Flow Rate (L/min)	Press. Drop (Pa)	8V/D (1/s)	Tau (mPa)	Flow Rate (L/min)	Press. Drop (Pa)	8V/D (1/s)	Tau (mPa)
2.05	4257	18.4	9302	1.64	8760	70.5	11352
7.64	4799	68.6	10489	5.21	10044	224.3	13015
14.22	5111	127.7	11169	6.94	11027	298.9	14289
31.22	5727	280.4	12516	10.97	11875	472.5	15388
39.42	6183	353.9	13513	14.46	12462	622.8	16149
47.19	6380	423.7	13944	17.75	13177	764.5	17075
55.31	6633	496.6	14495	21.19	14153	912.5	18340
63.03	7086			24.38	15244		
67.02	7045			27.25	18969		
71.57	7307			31.28	24406		
75.25	8191			34.65	28660		
78.89	9248			37.21	32760		
83.09	10150			43.32	42608		
82.46	10101			47.26	49223		
86.19	10854			55.01	64071		
93.99	12797						
101.64	14735						
109.48	16842						

PLV-2			
Flow Rate (L/min)	Press. Drop (Pa)	8V/D (1/s)	Tau (mPa)
6.70	7485	124.1	12849
14.82	8307	274.5	14260
19.31	8564	357.8	14702
23.52	8826	435.7	15151
27.38	9070	507.2	15571
31.39	9346	581.5	16044
35.38	9654	655.4	16574
39.58	10078		
43.49	11715		
47.23	13246		
55.52	17006		
62.95	21313		
70.80	26128		
78.69	31384		
86.03	36460		

Run Number	H-3		<u>Diameter (in.)</u>
Temperature	25 °C	PLV-1	1.049
Density	1.36 g/mL	PLV-2	0.824
Total Solids Content	42.4 wt %	PLV-3	0.622

PLV-1				PLV-3			
Flow Rate (L/min)	Press. Drop (Pa)	8V/D (1/s)	Tau (mPa)	Flow Rate (L/min)	Press. Drop (Pa)	8V/D (1/s)	Tau (mPa)
13.38	4151			8.69	9509	374.4	12322
19.93	4245	178.9	9277	12.59	10337	542.0	13394
28.20	4616	253.2	10087	14.75	10813	635.1	14012
36.73	5179	329.8	11318	17.51	11441	754.0	14826
44.97	5599	403.8	12237	19.64	12177	845.7	15780
53.06	5965	476.4	13036	22.00	12966	947.6	16802
61.21	6597			25.36	15119		
69.09	7668			28.19	19635		
76.45	9492			31.18	23977		
83.53	11302			34.40	28672		
87.27	12229			41.14	40221		
94.80	14280			45.82	49178		
102.01	16425			51.22	60768		
109.40	18694			54.83	68974		

PLV-2			
Flow Rate (L/min)	Press. Drop (Pa)	8V/D (1/s)	Tau (mPa)
12.22	7251		
15.48	7335	286.7	12591
19.78	7715	366.4	13244
23.98	8063	444.3	13842
28.25	8573	523.3	14718
32.61	9003	604.1	15455
36.55	9511		
40.58	10689		
44.66	12400		
53.07	16687		
62.04	21906		
68.93	26528		
77.70	32935		
84.82	39016		
91.37	44547		

Run Number	H-4		<u>Diameter (in.)</u>
Temperature	25 °C	PLV-1	1.049
Density	1.37 g/mL	PLV-2	0.824
Total Solids Content	43.5 wt %	PLV-3	0.622

PLV-1				PLV-3			
Flow Rate (L/min)	Press. Drop (Pa)	8V/D (1/s)	Tau (mPa)	Flow Rate (L/min)	Press. Drop (Pa)	8V/D (1/s)	Tau (mPa)
8.36	4449	75.0	9723	0.87	8556	37.5	11087
17.58	4890	157.8	10687	3.43	9479	147.9	12283
26.54	5429	238.3	11865	4.26	10056	183.5	13030
34.29	5697	307.9	12450	6.56	10700	282.4	13865
43.03	6183	386.4	13512	8.89	11304	382.7	14647
51.15	6585	459.2	14391	11.34	11972	488.2	15514
59.15	7047	531.1	15402	14.98	13018	645.3	16869
67.30	7661			18.28	13976	787.3	18111
71.31	8427			22.50	15461	969.1	20035
75.23	9497			14.39	13014	619.6	16864
78.80	10319			20.96	15093	902.6	19558
82.86	11272			23.47	16048	1010.7	20795
86.50	12231			25.49	16974		
94.51	14359			27.12	18652		
101.84	16604			29.47	23420		
110.38	19013			31.62	26819		
				34.34	31258		
				37.40	36496		
				41.40	43478		
				44.64	49293		
				47.38	55059		
				50.30	61297		
				53.35	68281		

PLV-2			
Flow Rate (L/min)	Press. Drop (Pa)	8V/D (1/s)	Tau (mPa)
8.36	8212	154.9	14098
13.31	8379	246.6	14384
17.52	8805	324.5	15115
21.98	9220	407.2	15828
26.23	9647	485.9	16560
30.26	10097	560.5	17333
34.23	10580	634.1	18163
38.59	11237		
43.00	12339		
46.82	14368		
51.08	16362		
55.37	18738		
59.20	21045		
82.33	38056		
86.19	41278		

Run Number	H-5		<u>Diameter (in.)</u>
Temperature	25 °C	PLV-1	1.049
Density	1.36 g/mL	PLV-2	0.824
Total Solids Content	41.7 wt %	PLV-3	0.622

PLV-1				PLV-3			
Flow Rate (L/min)	Press. Drop (Pa)	8V/D (1/s)	Tau (mPa)	Flow Rate (L/min)	Press. Drop (Pa)	8V/D (1/s)	Tau (mPa)
8.57	2947	76.9	6441	7.00	8266	301.6	10711
15.69	3177	140.9	6943	9.71	8778	418.3	11375
24.17	3480	217.0	7606	12.41	9237	534.5	11970
28.43	3604	255.2	7876	14.38	9799	619.2	12698
30.67	3582	275.4	7827	16.92	10556	728.8	13679
34.73	3698	311.8	8081	18.81	11181		
38.76	3888	348.0	8497	20.82	12122		
43.21	4055	388.0	8861	23.04	15351		
47.12	4367	423.0	9544	25.03	18274		
50.97	4682			27.09	20725		
55.55	5190			29.22	23350		
57.35	5566			31.63	26896		
59.36	6058			33.98	29939		
61.05	6419			35.60	32884		
64.43	7061			37.28	35855		
67.18	7668			39.66	39547		
70.58	8288			41.85	43175		
73.05	8914			43.91	47276		
77.62	9879			45.59	50399		
81.33	10787			47.67	54496		
85.55	11836			49.69	58544		
89.18	12880			51.61	62750		
93.42	13884			53.72	67122		
97.53	15039			55.52	70975		
101.39	16281						
106.04	17438						
109.75	18731						

PLV-2			
Flow Rate (L/min)	Press. Drop (Pa)	8V/D (1/s)	Tau (mPa)
8.51	5782		
12.30	5698	227.8	9782
15.84	6025	293.5	10342
18.97	6191	351.4	10628
22.12	6431	409.7	11040
25.24	6709	467.6	11518
28.46	6944	527.1	11921
31.74	7406		
34.68	8274		
37.69	9723		
40.80	11039		
43.91	12398		
47.16	13951		
49.80	15461		
53.11	17166		
56.08	18847		
59.13	20629		
63.09	23168		
65.97	25089		
69.14	27059		
72.22	29143		
75.18	31396		
78.19	33512		
81.10	35866		
84.30	38366		
87.40	40749		
90.17	43197		

Run Number	H-6		<u>Diameter (in.)</u>
Temperature	50 °C	PLV-1	1.049
Density	1.36 g/mL	PLV-2	0.824
Total Solids Content	42.7 wt %	PLV-3	0.622

PLV-1			
Flow Rate (L/min)	Press. Drop (Pa)	8V/D (1/s)	Tau (mPa)
5.90	3125	53.0	6829
9.18	3203	82.4	7000
14.26	3391	128.0	7411
19.04	3463	170.9	7569
23.19	3617	208.2	7905
27.24	3663	244.6	8005
31.53	3762	283.1	8222
35.61	3871	319.7	8460
39.60	4168		
43.59	4215		
47.60	4170		
51.39	4356		
55.41	4619		
59.11	5273		
63.17	6108		
66.86	6825		
70.98	7528		
75.00	8302		
78.58	9077		
82.73	9922		
86.42	10812		
90.52	11744		
94.41	12818		

PLV-3			
Flow Rate (L/min)	Press. Drop (Pa)	8V/D (1/s)	Tau (mPa)
6.16	7550	265.3	9783
8.86	8076	381.4	10465
11.91	8594	512.9	11137
13.94	8952	600.3	11601
15.74	9489	677.9	12296
17.28	9881	744.3	12804
19.25	10470		
20.46	10931		
22.14	12600		
23.19	13853		
24.86	15952		
27.50	18992		
29.31	21012		
31.36	23812		
33.29	26488		
35.21	29204		
37.56	32758		
39.53	35419		
41.98	39456		
43.44	41720		
45.35	44959		

PLV-2			
Flow Rate (L/min)	Press. Drop (Pa)	8V/D (1/s)	Tau (mPa)
6.56	5222	121.6	8965
10.54	5490	195.3	9425
14.40	5714	266.8	9809
18.31	5918	339.2	10160
21.34	6067	395.3	10415
24.10	6204	446.4	10651
27.11	6365	502.3	10926
30.19	6616	559.3	11357
33.38	6931		
36.42	7999		
39.32	9277		
42.26	10483		
45.36	11733		
48.48	13179		
52.23	14994		
55.86	16946		
58.95	18701		
62.97	21005		
66.77	23450		
70.73	25761		
75.01	28646		

Run Number	H-7		<u>Diameter (in.)</u>
Temperature	25 °C	PLV-1	1.049
Density	1.37 g/mL	PLV-2	0.824
Total Solids Content	43.5 wt %	PLV-3	0.622

PLV-1				PLV-3			
Flow Rate (L/min)	Press. Drop (Pa)	8V/D (1/s)	Tau (mPa)	Flow Rate (L/min)	Press. Drop (Pa)	8V/D (1/s)	Tau (mPa)
7.38	3039	66.2	6641	8.28	8790	356.5	11390
11.09	3145	99.6	6874	10.90	9272	469.4	12015
15.78	3265	141.7	7135	13.31	9925	573.1	12862
20.22	3418	181.5	7470	15.50	10394	667.8	13469
23.98	3632	215.3	7938	17.02	10773	733.2	13960
28.33	3654	254.4	7985	18.50	11273	796.6	14607
32.52	3847	292.0	8407	20.01	11807		
36.71	4038	329.6	8825	20.77	12180		
40.85	4272	366.8	9336	21.87	13151		
44.80	4446	402.2	9715	23.39	15664		
47.29	4539	424.6	9921	25.35	18562		
49.42	4659	443.7	10181	27.12	20814		
51.11	4735			29.86	24079		
53.48	4999			32.58	28226		
56.99	5737			35.68	33178		
60.97	6647			38.46	37942		
64.70	7467			41.67	43426		
68.97	8280			45.55	50792		
72.96	9149			49.43	58474		
76.95	10066			53.24	67127		
80.94	11051			57.10	75948		
84.71	12066			60.09	82691		
89.28	13136						
92.72	14233						

PLV-2			
Flow Rate (L/min)	Press. Drop (Pa)	8V/D (1/s)	Tau (mPa)
8.01	5655		
11.78	5652	218.3	9703
15.54	6066	287.8	10414
18.84	6539	349.0	11225
21.86	6949	404.9	11930
25.30	7163	468.8	12296
28.01	7316	518.8	12559
31.30	7679		
33.23	7960		
34.57	8403		
36.28	9092		
38.84	10339		
40.67	11256		
43.58	12557		
47.77	14579		
51.89	16768		
55.85	19051		
59.85	21501		
64.10	24024		
67.83	26669		
71.79	29534		

INTERNAL DISTRIBUTION

- | | | |
|----------------------|------------------------|-----------------------------------|
| 1. M. R. Ally | 36. R. K. Genung | 70. T. F. Scanlan |
| 2. W. D. Arnold | 37. J. R. Hightower | 71. C. B. Scott |
| 3. P. L. Askew | 38. R. D. Hunt | 72. J. A. Setaro |
| 4. T. J. Abraham | 39-43. T. D. Hylton | 73. R. B. Shelton |
| 5. P. E. Arakawa | 44. L. L. Jacobs | 74. J. L. Snyder |
| 6. J. W. Autry | 45. L. L. Kaiser | 75. R. C. Stewart |
| 7. J. M. Begovich | 46. C. M. Kendrick | 76. L. E. Stratton |
| 8. J. T. Bell | 47. T. E. Kent | 77. W. T. Thompson |
| 9-13. J. B. Berry | 48. J. R. Lawson | 78. J. R. Trabalka |
| 14. M. D. Boring | 49. R. Macon | 79. J. R. Travis |
| 15. C. H. Brown | 50. J. D. Maddox | 80. M. W. Tull |
| 16. C. H. Byers | 51. C. P. Manrod | 81. D. W. Turner |
| 17. C. Clark, Jr. | 52. R. C. Mason | 82. R. I. Van Hook |
| 18. D. A. Conatser | 53. A. J. Mattus | 83. J. F. Walker |
| 19. A. G. Croff | 54. E. W. McDaniel | 84. J. H. Wilson |
| 20-24. R. L. Cummins | 55. C. P. McGinnis | 85-89. E. L. Youngblood |
| 25. S. J. Davidson | 56. B. C. McClelland | 90. Central Research
Library |
| 26. D. L. Daugherty | 57. L. E. McNeese | 91. Document Reference
Section |
| 27. S. M. DePaoli | 58. R. C. Orrin | 92-93. Laboratory Records |
| 28. J. R. DeVore | 59. J. R. Parrott, Jr. | 94. Laboratory Records,
R.C. |
| 29. T. L. Donaldson | 60. B. D. Patton | 95. ORNL Patent Section |
| 30. J. T. Etheridge | 61. J. J. Perona | |
| 31. J. R. Forgy, Jr. | 62. J. G. Pruett | |
| 32. V. L. Fowler | 63. S. M. Robbinson | |
| 33. C. E. Frye | 64. S. T. Rudell | |
| 34. H. R. Gaddis | 65-69. F. R. Ruppel | |
| 35. S. B. Garland | | |

EXTERNAL DISTRIBUTION

96. Office of Assistant Manager, Energy Research and Development, DOE-OR, P.O. Box 2001, Oak Ridge, TN 37831
- 97-98. Office of Scientific and Technical Information, P. O. Box 62, Oak Ridge, TN 37831
99. Sherry Gibson, DOE Headquarters, 12800 Middlebrook Road, Germantown, MD 20874.
100. J. O. Moore, Division of Waste Management and Technology Development, DOE-OR, P.O. Box 2001, Oak Ridge, TN 37831
101. Dr. R. W. Hanks, Slurry Transport Consultant, 495 East 1010 South, Orem, Utah 84058.
102. M. R. Elmore, Pacific Northwest Laboratories, Battelle Boulevard, P.O. Box 999, Richland, WA 99352
103. N. G. Colton, Pacific Northwest Laboratories, Battelle Boulevard, P.O. Box 999, Richland, WA 99352

104. P. A. Scott, Pacific Northwest Laboratories, Battelle Boulevard, P.O. Box 999, Richland, WA 99352
105. Roger L. Gilchrist, Manager, UST-ID, Westinghouse Hanford Company, P.O. Box 1970, MSIN: L5-63, Richland, WA 99352
106. J. A. Bamberger, Pacific Northwest Laboratories, Battelle Boulevard, P.O. Box 999, Richland, WA 99352
107. E. O. Jones, Pacific Northwest Laboratories, Battelle Boulevard, P.O. Box 999, Richland, WA 99352
108. Dr. Inn Choi, Pacific Northwest Laboratories, Battelle Boulevard, P.O. Box 999, Richland, WA 99352
109. Mark A. Schiffhauer, West Valley Nuclear Services Co., Inc., P.O. Box 191, West Valley, NY 14171-0191.
110. Dale Waters, Westinghouse Hanford Company, P.O. Box 1970, MS S4-58, Richland, WA 99352
111. Stephen D. Riesenweber, Westinghouse Hanford Company, RI-30, P.O. Box 1970, Richland WA 99352
112. Brian Koons, Kaiser Engineers, 1200 Jadwin Avenue, MS E6-21, Richland, WA 99352
113. Robert F. Eggers, Westinghouse Hanford Company, Retrieval Development, P.O. Box 1970, MSIN S4-54, Richland, WA 99352
114. Walter Knecht, Westinghouse Hanford Company, P.O. Box 1970, MISN HO-34, Richland, WA 99352
115. Dr. H. K. Hepworth, Box 15600, Northern Arizona University, Flagstaff, AZ 86011-1560